Published for SISSA by Springer

Received: *August 10, 2020*
Accepted: *October 7, 2020*
Published: *November 16, 2020*

Single particle operators and their correlators in free $\mathcal{N} = 4$ SYM

F. Aprile,[a,b] **J.M. Drummond,**[c] **P. Heslop,**[d] **H. Paul,**[c] **F. Sanfilippo,**[e] **M. Santagata**[c] **and A. Stewart**[d]

[a] *Dipartimento di Fisica, Università di Milano-Bicocca, Piazza della Scienza, U2, I-20126 Milano, Italy*
[b] *INFN — Sezione di Milano-Bicocca, Piazza della Scienza, U2, I-20126 Milano, Italy*
[c] *School of Physics and Astronomy and STAG Research Centre, University of Southampton, Highfield, SO17 1BJ, U.K.*
[d] *Mathematics Department, Durham University, Science Laboratories, South Rd, Durham DH1 3LE, U.K.*
[e] *INFN — Sezione di Roma 3, Via della Vasca Navale 84, I-00146 Roma, Italy*

E-mail: francesco.aprile1@unimib.it, J.M.Drummond@soton.ac.uk, paul.heslop@durham.ac.uk, H.Paul@soton.ac.uk, fr.sanfilippo@gmail.com, M.Santagata@soton.ac.uk, alastair.j.stewart@durham.ac.uk

Abstract: We consider a set of half-BPS operators in $\mathcal{N} = 4$ super Yang-Mills theory which are appropriate for describing single-particle states of superstring theory on $AdS_5 \times S^5$. These single-particle operators are defined to have vanishing two-point functions with all multi-trace operators and therefore correspond to admixtures of single- and multi-traces. We find explicit formulae for all single-particle operators and for their two-point function normalisation. We show that single-particle $U(N)$ operators belong to the $SU(N)$ subspace, thus for length greater than one they are simply the $SU(N)$ single-particle operators. Then, we point out that at large N, as the length of the operator increases, the single-particle operator naturally interpolates between the single-trace and the S^3 giant graviton. At finite N, the multi-particle basis, obtained by taking products of the single-particle operators, gives a new basis for all half-BPS states, and this new basis naturally cuts off when the length of any of the single-particle operators exceeds the number of colours. From the two-point function orthogonality we prove a multipoint orthogonality theorem which implies vanishing of all near-extremal correlators. We then compute all maximally and next-to-maximally extremal free correlators, and we discuss features of the correlators when the extremality is lowered. Finally, we describe a half-BPS projection of the operator product

https://doi.org/10.1007/JHEP11(2020)072

JHEP11(2020)072

expansion on the multi-particle basis which provides an alternative construction of four- and higher-point functions in the free theory.

Keywords: $1/N$ Expansion, AdS-CFT Correspondence, Supersymmetric Gauge Theory

ArXiv ePrint: 2007.09395

JHEP11(2020)072

Contents

JHEP11(2020)072

1 Introduction

As the most symmetric QFT in four dimensions, and at the same time the paradigmatic example of the AdS/CFT correspondence, $\mathcal{N}$=4 super Yang-Mills (SYM) has been the subject of a huge amount of interest. The expected flow of information usually uses semi-classical physics in AdS to reconstruct strong 't Hooft coupling phenomena in the gauge theory, but this flow can also be reversed, and recently, vey precise and concrete investigations of perturbative quantum gravity have been undertaken by means of analytic bootstrap techniques at strong coupling. For example, one-loop quantum gravity amplitudes in AdS have been obtained by computing $O(1/N^4)$ corrections to strong coupling correlators in SYM [1–5].

One aspect of these investigations was the need to be very careful about the precise definition of the gauge theory operators dual to single-particle supergravity states, in order to properly account for the OPE at tree level and one loop. These single-particle operators are protected half-BPS operators, but the space of half-BPS operators of given charge is degenerate, and only in the planar limit can the single-particle operators be identified with the single-trace half-BPS operators $\mathrm{Tr}(\phi^p)$. This identification indeed was known to receive $O(1/N)$ multi-trace corrections (see eg [6–8]), and the first order double trace corrections have recently been fully worked out directly from supergravity in [9, 10]. On the other hand, the non-perturbative nature of the AdS/CFT correspondence strongly points towards a non-perturbative (i.e. valid to all orders in N) definition of the single-particle states. In fact, a deceptively simple non-perturbative definition was formulated in [11]:

> Single-particle operators are half-BPS operators which have vanishing two-point functions with all multi-trace operators, i.e. they are orthogonal to all multi-trace operators w.r.t. the metric defined by the two point function.

The definition above fixes the single-particle operators uniquely, up to normalisation, in terms of a certain admixture of single- and multi-trace operators. In particular, the leading operator in the planar limit is the single-trace operator, but the admixture is new. Our definition has been already used, and indeed is crucial in correctly determining one-loop $O(1/N^4)$ SUGRA correlators of operators with charges higher than four, for example, arbitrary charge correlators in position space [4], where a number of subtle features have been solved, and 22pp correlators in Mellin space [5].

The first result in this paper is to obtain explicit formulae for the multi-trace components of the single-particle operators and examine some of their nice properties. Then, we will study some of their correlators and show that compared to the single-trace cousins,

JHEP11(2020)072

the single-particle operators have a number of very surprising and nice properties. This is slightly counter-intuitive at first, because now we have to deal with an admixture of single and multi-trace operators, but nevertheless it is true in many ways, as we will demonstrate.

One of the nice properties is that the operators in the U(N) theory and the SU(N) theory are the same. Indeed, in the U(N) theory the single-particle operators of charge greater equal than two must be orthogonal to all multi-trace operators involving also Tr(ϕ), and this automatically makes them the SU(N) operators. To formalise this statement we introduce the SU(N) projection on the space of the U(N) operators, and show that the U(N) single-particle operators belong to the SU(N) subspace, which is orthogonal to the span of multi-trace operators in which at least one trace is Tr(ϕ). It follows that correlators of U(N) single-particle operators are equal to correlators of SU(N) single-particle operators.

Another nice property of the single-particle operators is that they automatically vanish if the charge of the operators exceeds the number of colours N. This should be contrasted for example with the single trace basis which does not vanish, but rather decomposes into complicated linear combinations of products of lower trace operators. The cut-off with N of the operators dual to single-particle states has long been expected from AdS/CFT, and it follows from the string exclusion principle [12]. In the large N limit, with gravity being a valid description of $\mathcal{N} = 4$ SYM, the idea is simply that as the angular momentum of the type-IIB graviton on $AdS_5 \times S^5$ increases, it becomes less and less pointlike on the sphere, eventually growing into a D3 brane wrapping an $S^3 \subset S^5$. As shown in [13], the charge of this D3 brane, p, is bounded by N, thus proving the cut-off with N on the gravity side. In [14] these D3 branes were identified with the (sub)-determinant half-BPS operators of dimension $p \sim N$, or equivalently with the completely antisymmetric (single column Young tableau) Schur polynomials [15]. Very beautifully, we find that in the large N limit, as we vary the charge p, our single-particle operators interpolate between the single trace operator, for fixed p, and the D3 brane operator, for values of $p \sim N$. Thus our single-particle operator precisely becomes the sphere giant predicted in [13].

In fact, the single-particle operators have appeared before in the literature, and not identified as operators dual to single-particle states. A beautiful orthogonal basis for all half-BPS operators in the U(N) theory was given in [15] in terms of Schur polynomials, labelled by Young tableaux. These also automatically truncate with N since a U(N) Young tableau with height larger than N vanishes. However this basis does not project onto an orthogonal basis for SU(N) (and indeed the operators are not even linearly independent in the SU(N) theory). In [16] a non-orthogonal but linearly independent basis of all SU(N) half-BPS operators was defined. This basis was later identified as the dual (via the metric defined by the two point function) to the trace basis in [17] and a group theoretic expression for this dual basis was given. The single particle operators we discuss here are a subset of the dual basis: the operators dual to single trace operators.

It is the purpose of this paper to unpack the definition of single-particle operators, turn it into an explicit formula, and investigate its properties. The outline will be as follows.

In section 2 we discuss the details of the multi-trace admixture which defines the single-particle operators. We first give explicit examples at low charge, and then we use group theory techniques to obtain a general formula, *valid for any single-particle operator of any*

JHEP11(2020)072

charge p. Our formulae allows us to study the 'shape' of the operator in the large N limit, and in particular to see explicitly the interpolation between the single-trace and the sphere giant, as function of p (see section 2.3). Moreover, we will be able to compute the two-point function normalisation exactly.

In section 3 we uplift the defining two-point function orthogonality to a multi-point orthogonality theorem, which in turn implies vanishing of a large class of diagrams in correlators. We call these near-extremal n-point functions, where extremality will be defined as a measure of how much the diagram is connected w.r.t. the heaviest operator (see (3.11)). This is the first instance of hidden simplicity of multi-point single-particle correlators versus the single-trace correlators, and very interestingly, a similar feature was noticed on the (super-)gravity side in [18].

In section 4, we consider the first non vanishing correlators, and we study maximally-extremal (ME) and next-to-maximally extremal (NME) n-point functions. Both are simple. The ME correlators are computed by trees and two point functions. The NME are mostly computed by weighted sums of ME correlators, which we know in general. When we compute these correlators by using Wick contractions techniques on the trace basis, the combinatorics is hard in the intermediate steps. Instead, the final result is way much simpler. We provide more evidence about this mechanism mentioning also the case of NNME three-point functions.

Finally, in section 5 we discuss the half-BPS OPE on the single-particle basis, and we use it as an alternative computational tool to bootstrap, and provide constraints, on the correlators of interest. We exemplify the procedure at four-points for next-to-next- and next-to-next-to-next extremal correlators.

2 Single-particle half-BPS operators (SPOs)

Half-BPS operators in $\mathcal{N}=4$ super Yang-Mills theory can be described via products of single-trace scalar operators in the symmetric traceless representations of SO(6),

$$T_p(x) = \mathrm{Tr}\,\phi(x)^p \qquad ; \qquad \phi(X,Y) = Y^R \phi_R(X) \tag{2.1}$$

Here ϕ_R is the elementary field of the $\mathcal{N}=4$ supermultiplet, and we have introduced an auxiliary SO(6) vector Y^R which is null, $Y\cdot Y=0$, to project onto the symmetric traceless representation. An insertion point x corresponds to both a space-time X_i coordinate and an SO(6) vector Y^R.

In addition to the single-trace operators T_p we obtain other half-BPS operators from taking products of the form

$$T_{p_1\dots p_m}(x) \equiv T_{p_1}(x)\dots T_{p_m}(x)\,, \qquad p_1 \geq \dots \geq p_m \geq 1\,. \tag{2.2}$$

The scaling dimension of $T_{p_1\dots p_m}$ is given by $(p_1+\dots+p_m)$. The case $m=1$ reduces obviously to the single trace operator.

We will refer to the basis of half-BPS operators made of all possible $T_{p_1\dots p_m}(x)$ as the *trace basis*, and we will denote the basis elements with the symbol $T_{\underline{p}}$, where $\underline{p}$ stands for a partition of p, so if the partition has length greater than two the operator is multi-trace.

JHEP11(2020)072

To compute correlation functions in free field theory we use elementary propagators. Here we will take the gauge group to be U(N) or SU(N) so that the propagator takes the form,

$$\left\langle \phi_r{}^s(X_1,Y_1)\phi_t{}^u(X_2,Y_2)\right\rangle = \delta_r^u\delta_t^s\, g_{12} \qquad \mathrm{U}(N) \tag{2.3}$$

$$\left\langle \phi_r{}^s(X_1,Y_1)\phi_t{}^u(X_2,Y_2)\right\rangle = \left(\delta_r^u\delta_t^s - \frac{1}{N}\delta_r^s\delta_t^u\right) g_{12} \qquad \mathrm{SU}(N) \tag{2.4}$$

where

$$g_{12} = \frac{Y_1\cdot Y_2}{(X_1-X_2)^2} \tag{2.5}$$

A correlation function of operators in the trace basis will have the schematic form

$$\langle T_{\underline{p_1}}(x_1)\dots T_{\underline{p_n}}(x_n)\rangle = \sum_{\{b_{ij}\}}\prod_{i,j} g_{ij}^{b_{ij}}\; \mathcal{C}_{\{b_{ij}\},\underline{p_1}\dots\underline{p_n}}(N) \tag{2.6}$$

where b_{ij} counts the number of propagators from insertion point i to j. The collection of these bridges, $\{b_{ij}\}_{i<j}$, labels the propagator structure. With $\mathcal{C}_{\{b_{ij}\}}(N)$ we denote the corresponding color factor.

2.1 Definition and low charge examples

The AdS/CFT correspondence maps the spectrum of operators in $\mathcal{N}=4$ super Yang-Mills theory to the spectrum of IIB superstring theory on the $\mathrm{AdS}_5\times S^5$ background. The superstring can be found in unexcited states (giving the IIB supergravity multiplet) or excited states. The half-BPS operators correspond to the supergravity states (and their multi-particle products).

In the natural basis of scattering states, the multi-particle states should be orthogonal to single-particle ones. A key point of our discussion is that the trace basis of half-BPS operators is not an orthogonal basis with respect to the inner product given by the two-point functions. In general

$$\langle T_p(x_1)\, T_{q_1\dots q_n}(x_2)\rangle \neq 0 \qquad n\geq 2\ . \tag{2.7}$$

To align with the AdS/CFT intuition, in [4, 11] we gave a prescription for identifying which half-BPS operators correspond to the single-particle states. Our definition of the relevant operators $\mathcal{O}_p$ is simply to take those operators which are orthogonal to all multi-trace operators,

$$\text{Single particle operators } \equiv \{\mathcal{O}:\ \langle \mathcal{O}_p(x_1)\, T_{q_1\dots q_n}(x_2)\rangle = 0\,,\quad (n\geq 2)\}\ . \tag{2.8}$$

This in turn implies $\langle \mathcal{O}_p(x_1)[\mathcal{O}_{q_1}\dots\mathcal{O}_{q_n}](x_2)\rangle = 0$, i.e. single-particle operators are orthogonal to multi-particle states.

From the Gram-Schmidt orthogonalisation we immediately obtain a formula for $\mathcal{O}_p$ in terms of the (color factor of) two-point functions. In fact, consider the space of operators of

JHEP11(2020)072

charge p and label them by corresponding partitions $\{\lambda_i = q_1 \dots q_n\}_{i=1,\dots P}$, with $\lambda_P \equiv \{p\}$. Then,

$$\mathcal{O}_p(x) = \frac{1}{\mathcal{N}_p} \det \begin{pmatrix} \mathcal{C}_{\lambda_1|\lambda_1} & \mathcal{C}_{\lambda_2|\lambda_1} & \dots & \mathcal{C}_{p|\lambda_1} \\ \vdots & \vdots & \dots & \vdots \\ \mathcal{C}_{\lambda_1|\lambda_{P-1}} & \mathcal{C}_{\lambda_2|\lambda_{P-1}} & \dots & \mathcal{C}_{p|\lambda_{P-1}} \\ \hline T_{\lambda_1}(x) & T_{\lambda_2}(x) & \dots & T_p(x) \end{pmatrix} \tag{2.9}$$

where

$$\mathcal{N}_p = \det \left(\mathcal{C}_{\lambda_i\lambda_j}\right)_{1\le i,j\le P-1} \qquad ; \qquad \langle T_{\lambda_i}(x_1) T_{\lambda_j}(x_2)\rangle = g_{12}^p \, \mathcal{C}_{\lambda_i\lambda_j} \tag{2.10}$$

The determinant (2.9) is understood as a Laplace expansion about the last row, which contains the list of all allowed operators of charge p. Upon using the determinant for computing $\langle \mathcal{O}_p(x_1) T_{q_1\dots q_n}(x_2)\rangle$, it becomes obvious that the last row of the matrix would now coincide with another row, leading to a vanishing result.

In our normalisation $\mathcal{O}_p$ coincides with the single-trace operators T_p up to multi-trace admixtures. Each multi-trace contribution is suppressed at large N, and the single-particle operator reduces to single-trace operators in the strict large N limit. However, the novelty of our SPO is precisely the determination of the multi-trace admixture, which we will now exemplify with a number of computations, for low charge operators, before discussing our general formulae in the next section.

With SU(N) gauge group, T_p and $\mathcal{O}_p$ coincide for $p = 2, 3$ since there are no multi-trace operators for charges $p < 4$,

$$\mathcal{O}_p = T_p \qquad \text{for } p = 2, 3 \qquad\qquad \text{SU}(N)\,. \tag{2.11}$$

In terms of supergravity states the $p = 2$ case corresponds to the superconformal primary for the energy-momentum multiplet which is dual to the graviton multiplet in AdS_5. The $p = 3$ case is the first Kaluza-Klein mode arising from reduction of the IIB graviton supermultiplet on S^5.

For gauge group U(N) on the other hand there exists a $p = 1$ operator, since the trace of the fundamental scalar no longer vanishes. At weight 1 there is only one operator and thus $\mathcal{O}_1 = T_1$. However using Wick contractions with the U(N) propagator (2.3) one can easily verify that for $p > 1$, as well as the single-trace contributions, we have non-trivial multi-trace admixtures. At weight 2 there are two operators, T_2 and T_{11} with the single particle operator defined to be orthogonal to the double-trace T_{11}. Similarly for $p = 3$ the single particle operators is defined to be orthogonal to both the double-trace T_{21} and the triple trace T_{111}. Explicitly we obtain

$$\begin{aligned} \mathcal{O}_2 &= T_2 - \frac{1}{N} T_{11} \\ \mathcal{O}_3 &= T_3 - \frac{3}{N} T_{21} + \frac{2}{N^2} T_{111} \end{aligned} \qquad\qquad \text{U}(N)\,. \tag{2.12}$$

where for example the coefficient of the double-trace contribution to $\mathcal{O}_2$ is determined from the orthogonality condition $\langle \mathcal{O}_2(x_1) T_{11}(x_2)\rangle = 0$. The additional terms compared to the

JHEP11(2020)072

SU(N) operators (2.11) in fact simply project out the trace part of the fundamental scalar ϕ and so the SU(N) and U(N) operators in fact coincide.

For $p > 3$ we have non-trivial multi-trace admixtures even in the SU(N) case as can be easily verified using SU(N) Wick contractions (i.e. with propagator (2.11)). This was discussed in [11] (see also previous discussions in [6, 8, 19]). For example, the single-particle operator for $p = 4$ is given by

$$\mathcal{O}_4 = T_4 - \frac{2N^2-3}{N(N^2+1)}T_{22} \qquad \text{SU}(N)\,, \tag{2.13}$$

where the coefficient of the double-trace contribution determined from the orthogonality condition $\langle \mathcal{O}_4 T_{22}\rangle = 0$.[1] It is now interesting to consider the single particle operator in the U(N) theory. It is given by

$$\mathcal{O}_4 = T_4 - \frac{(2N^2-3)}{N\,(N^2+1)}T_{22} + \frac{10}{N^2+1}T_{211} - \frac{4}{N}T_{13} - \frac{5}{N\,(N^2+1)}T_{1111} \qquad \text{U}(N)\,, \tag{2.14}$$

where the coeffcients are determined by demanding orthogonality with all higher trace operators $T_{22}, T_{211}, T_{13}, T_{1111}$.

We see that the U(N) operators given above, explicitly reduce to the SU(N) operators upon imposing $T_1 = 0$. This pattern goes on, and for illustration we give the next few higher weight examples,

$$\begin{aligned}
\mathcal{O}_5 &= T_5 - \frac{5\,(N^2-2)\,T_{32}}{N\,(N^2+5)} + \mathcal{U}_5 \\
\mathcal{O}_6 &= T_6 - \frac{(3N^4-11N^2+80)\,T_{33}}{N\,(N^4+15N^2+8)} - \frac{6(N-2)(N+2)\,(N^2+5)\,T_{42}}{N\,(N^4+15N^2+8)} \\
&\quad + \frac{7\,(N^2-7)\,T_{222}}{N^4+15N^2+8} + \mathcal{U}_6
\end{aligned} \tag{2.15}$$

where

$$\mathcal{U}_5 = \frac{15\,(N^2-2)\,T_{221}}{N^2\,(N^2+5)} + \frac{5\,(3N^2+8)\,T_{311}}{N^2\,(N^2+5)} - \frac{35T_{2111}}{N\,(N^2+5)} + \frac{14T_{11111}}{N^2\,(N^2+5)} - \frac{5T_{41}}{N} \tag{2.16}$$

$$\begin{aligned}
\mathcal{U}_6 &= \frac{42(N-1)(N+1)T_{321}}{N^4+15N^2+8} + \frac{21\,(N^2+11)\,T_{411}}{N^4+15N^2+8} - \frac{42\,(2N^2-5)\,T_{2211}}{N\,(N^4+15N^2+8)} \\
&\quad - \frac{56\,(N^2+5)\,T_{3111}}{N\,(N^4+15N^2+8)} + \frac{126T_{21111}}{N^4+15N^2+8} - \frac{42T_{111111}}{N\,(N^4+15N^2+8)} - \frac{6T_{51}}{N}
\end{aligned} \tag{2.17}$$

For SU(N) the contributions denoted by $\mathcal{U}$ vanish in each case.

The statement that U(N) single particle operators reduce to the SU(N) single particle operator upon imposing $T_1 = 0$ is true in general, as we will prove in section 2.4, and it has very nice consequences. The correlators of U(N) operators are much simpler to compute, and can be directly related to group theoretic quantities, essentially since the propagator (2.3) is so simple. For this reason, there is a long history of studying half-BPS operators in the U(N) theory, eg [15]. Here we see that although correlators in the

[1] Other attempts at finding this combination can be found in [26].

JHEP11(2020)072

U(N) theory are simpler to compute, the trade-off is that the SPOs themselves are more complicated. In the end the computation of a correlator involving SPOs is equivalent whether using the U(N) or SU(N) theory.

2.2 General formulae for SPOs

So far we have uniquely defined SPOs (up to normalisation) as operators orthogonal to all multi-trace operators, and showed some examples at low charges. We will now give three different formulae for the single particle operators, which explicitly compute the multi-trace admixture. The plan will be the following.

In section 2.2.1 we will give a formula in the trace basis, see (2.33), which is perhaps the most familiar basis. This formula is equivalent to (2.9) but uses more powerful group theory techniques to resolve for the expansion of the SPO in terms of multi-traces. We quote it here

$$\mathcal{O}_p(x) = \sum_{\{q_1,\ldots,q_m\}\vdash p} C_{q_1,\ldots,q_m} T_{q_1,\ldots,q_m}(x) \tag{2.18}$$

$$C_{q_1,\ldots,q_m} = \frac{|[\sigma_{q_1\ldots q_m}]|}{(p-1)!} \sum_{s\in\mathcal{P}(\{q_1,\ldots,q_m\})} \frac{(-1)^{|s|+1}(N+1-p)_{p-\Sigma(s)}(N+p-\Sigma(s))_{\Sigma(s)}}{(N)_p-(N+1-p)_p}$$

It is very non trivial. The group theory data consists of $\mathcal{P}(\{q_1,\ldots,q_m\})$, the powerset of the traces $T_{q_1,\ldots,q_m}$, then $|s|$ is the cardinality of s and $\Sigma(s)=\sum_{s_i\in s} s_i$. Finally, $|[\sigma_{q_1\ldots q_m}]|$ is the size of the conjugacy classes of σ with length cycles $q_1\ldots q_m$.

In section 2.2.2 we give a much simpler formula, see (2.39), directly in terms of the eigenvalues $E_k(z_i)$ of the elementary fields ϕ,

$$\mathcal{O}_p(x) = \sum_{k=1}^{p} d_k(p,N) E_k(z_i)(x) \tag{2.19}$$

$$d_k(p,N) = \frac{(-1)^{k+1} p\,(N-p+1)_{p-k}(p-1)_k}{(N)_p-(N-p+1)_p} \tag{2.20}$$

In section 2.2.3 we give another simple formula in terms of the Schur polynomial basis (for operators), see (2.42), where we note that only hook representations appear.

If we think that half-BPS operators are symmetric functions of the eigenvalues of the scalar matrix ϕ_r^s, the three basis for gauge invariant operators, that we used to expand the SPOs above, correspond to three well-known bases for symmetric polynomials: 1) The trace basis corresponds to the power sum symmetric polynomials. 2) The explicit eigenvalue monomials (after summing over permutations) are called the monomial symmetric polynomials. 3) The Schur polynomials are named directly in terms of the corresponding symmetric polynomial basis of the same name.

There are a number of well known formulae relating 1), 2) and 3) to each other, known as Newton identities, and it would be interesting to explore these relations further in this context.

JHEP11(2020)072

2.2.1 Formula in terms of products of traces

We first observe that the single-particle operators $\mathcal{O}_p$ must be proportional to the dual ξ_p field of the single-trace operators T_p

$$\langle \xi_p(x_1)\, T_{q_1\dots q_n}(x_2)\rangle = 0\,, \qquad n \geq 2 \tag{2.21}$$

where the dual fields ξ_p were introduced by Tom Brown in [17].

Indeed, group theoretic formulae for SPOs were given in [17] (albeit without the explicit physical description as single-particle operators). He defined a more general basis of operators: the dual of the trace basis. This is given by operators $\xi_{p_1\dots p_n}$ (with $p_1 \geq \dots \geq p_n$) which obey[2]

$$\langle \xi_{p_1\dots p_m}(x_1) T_{q_1\dots q_n}(x_2)\rangle = \begin{cases} 1 & \text{if } (p_1,\dots,p_m) = (q_1,\dots,q_n)\,, \\ 0 & \text{otherwise.} \end{cases} \tag{2.22}$$

In other words each element of the dual to the trace basis is orthogonal to (i.e. it has vanishing two-point function with) all elements of the trace basis but one, and we then normalise it to have unit two-point coefficient with this element. Note that an orthogonal basis is its own dual. We will refer to the basis given by the $\xi_{p_1,\dots,p_n}$ as the *dual basis*.

For a single index (i.e. $m = 1$) the definition of the dual basis (2.22) reduces to (2.21), which is the defining property of single particle operators (2.8). So the ξ_p are orthogonal to all multi-trace operators and thus equal to $\mathcal{O}_p$ up to normalisation. The normalisation can then be determined from (2.9), i.e. $\mathcal{O}_p = T_p +$ multi-traces, which implies

$$\langle \xi_p \mathcal{O}_p\rangle = 1 \tag{2.23}$$

and hence

$$\xi_p(x) = \frac{\mathcal{O}_p(x)}{\langle \mathcal{O}_p \mathcal{O}_p\rangle} \qquad \text{and} \qquad \mathcal{O}_p(x) = \frac{\xi_p(x)}{\langle \xi_p \xi_p\rangle}\,. \tag{2.24}$$

By definition (as the dual basis with respect to the inner product defined by the two-point function) the change of basis matrix from the dual to the trace basis is simply the two point function:

$$\xi_{p_1\dots p_n}(x) = \sum_{\{q_1,\dots q_m\}\vdash p} \langle \xi_{p_1\dots p_n} \xi_{q_1\dots q_m}\rangle T_{q_1\dots q_m}(x) \tag{2.25}$$

where the sum is over all partitions of p, that is all sets of integers $q_1 \geq \dots \geq q_m$ such that $q_1 + \dots + q_m = p$. Brown in [17] gives group theoretic expressions for these two-point functions as

$$\begin{aligned} \langle \xi_{p_1\dots p_n} \xi_{q_1\dots q_m}\rangle &= \frac{|[\sigma_{p_1\dots p_n}]|}{p!}\frac{|[\sigma_{q_1\dots q_m}]|}{p!} \sum_{R\vdash p} \frac{1}{f_R} \chi_R(\sigma_{p_1\dots p_n})\chi_R(\sigma_{q_1\dots q_m}) \\ p &= p_1 + \dots + p_n = q_1 + \dots + q_m\,. \end{aligned} \tag{2.26}$$

where

[2] In this section we will focus only on two-point functions and we will always drop the trivial space-time dependent part, $(g_{12})^p$, referring the discussion to the normalisation/color factor.

JHEP11(2020)072

- $\sigma_{p_1 \ldots p_n} \in S_p$ is a permutation[3] made of disjoint cycles of lengths $p_1, p_2, \ldots$ and $||[\sigma_{p_1 \ldots p_n}]||$ is the size of the corresponding conjugacy class of the permutation (i.e. the number of permutations with that disjoint cycle structure). Similarly for $\sigma_{q_1 \ldots q_m}$.

- the sum is over all partitions R of p. One can view R as a Young diagram with p boxes, labelling a representation of the permutation group S_p.

- the expression $\chi_R(\sigma)$ is the character for this S_p representation.

- the sum is weighted by

$$f_R = \prod_{(r,c)\in R} (N - r + c) \tag{2.27}$$

  where (row, cln) are the coordinates of the boxes of the Young diagram.[4]

Since we are focusing on single particle operators we can assume $n = 1$ in (2.25) so $\xi_{p_1 \ldots p_n} = \xi_p$ and the permutation $\sigma_{p_1 \ldots p_n}$ consists of a single cycle of length p of which there are $(p-1)!$ possibilities, so $||[\sigma_p]|| = (p-1)!$. Furthermore we observe that for such a permutation, only Hook reprentations have a non vanishing S_p. Indeed we note that:

$$\chi_R(\sigma_p) = \begin{cases} (-1)^{h_R - 1} & R = \text{ hook YT of height } h_R \\ 0 & \text{otherwise} \end{cases} \tag{2.28}$$

where "hook YT" means that R has a hook-shaped diagram: all non-zero rows but the first have length 1 and all non-zero columns but the first have height 1. Thus the coefficient of a given multi-trace operator in ξ_p is

$$\langle \xi_p \, \xi_{q_1 \ldots q_m} \rangle = \frac{1}{p} \frac{||[\sigma_{q_1 \ldots q_m}]||}{p!} \sum_{R \in \text{ hooks}} \frac{1}{f_R} (-1)^{1+h_R} \chi_R(\sigma_{q_1 \ldots q_m}) \ . \tag{2.29}$$

We have found that this sum over hook representations is always given by the following explicit formula[5]

$$\langle \xi_p \, \xi_{q_1 \ldots q_m} \rangle = \frac{1}{p} \frac{||[\sigma_{q_1 \ldots q_m}]||}{p!} \frac{1}{p-1} \sum_{s \in \mathcal{P}(\{q_1, \ldots, q_m\})} \frac{(-1)^{|s|+1}}{(N + 1 - \Sigma(s))_{p-1}} \, . \tag{2.30}$$

The sum $s \in \mathcal{P}(\{q_1, \ldots, q_m\})$ is over all subsets s of the set $\{q_1, \ldots, q_m\}$ including the empty set and the full set $\{q_1, \ldots, q_m\}$. Note that the set of all subsets of a set S is known as the powerset of S and denoted $\mathcal{P}(S)$.[6] Then $|s|$ denotes the number of elements of the subset s and $\Sigma(s)$ the total of all the elements in subset s, $\Sigma(s) = \sum_{s_i \in s} s_i$.

[3] For example the one given by $(1, \ldots, p_1)(p_1 + 1, \ldots p_1 + p_2) \ldots (p_1 + \ldots + p_{n-1} + 1, \ldots, p)$.

[4] Group theoretically f_R is proportional to the ratio between the dimensions of R as a rep of $\mathrm{U}(N)$ and the dimension of R as a rep of S_p, i.e. $f_R = p! d_R[\mathrm{U}(N)]/d_R[S_p]$.

[5] More precisely, in all of the many cases we explored, we always find that (2.29) agrees with (2.30).

[6] For example $\mathcal{P}(\{3,2,1\}) = \{\{\}, \{1\}, \{2\}, \{3\}, \{2,1\}, \{3,1\}, \{3,2\}, \{3,2,1\}\}$.

JHEP11(2020)072

An important special case of (2.30) is the case $m = 1$ giving the two-point function of the dual of the single trace operator. In this case the sum is over just two elements $s = \{\}$ and $s = \{p\}$ since $\mathcal{P}(\{p\}) = \{\{\}, \{p\}\}$. The expression (2.30) thus simplifies to

$$\langle \xi_p \, \xi_p \rangle = \frac{1}{p^2} \frac{1}{p-1} \left(\frac{1}{(N+1-p)_{p-1}} - \frac{1}{(N+1)_{p-1}} \right) . \tag{2.31}$$

Finally inserting (2.30) into (2.25) and in turn into (2.24) together with (2.31) gives an explicit expression for the single particle operator as a sum of multi-trace operators

$$\mathcal{O}_p(x) = \sum_{\{q_1 \dots q_m\} \vdash p} C_{q_1,\dots,q_m} T_{q_1,\dots q_m}(x) \tag{2.32}$$

with coefficients

$$\begin{aligned} C_{q_1,\dots q_m} &= \frac{\langle \xi_p \, \xi_{q_1 \dots q_m} \rangle}{\langle \xi_p \, \xi_p \rangle} \\ &= \frac{|[\sigma_{q_1 \dots q_m}]|}{(p-1)!} \sum_{s \in \mathcal{P}(\{q_1,\dots,q_m\})} \frac{(-1)^{|s|+1}}{(N+1-\Sigma(s))_{p-1}} \left(\frac{1}{(N+1-p)_{p-1}} - \frac{1}{(N+1)_{p-1}} \right)^{-1} \\ &= \frac{|[\sigma_{q_1 \dots q_m}]|}{(p-1)!} \sum_{s \in \mathcal{P}(\{q_1,\dots,q_m\})} \frac{(-1)^{|s|+1} (N+1-p)_{p-\Sigma(s)} (N+p-\Sigma(s))_{\Sigma(s)}}{(N)_p - (N+1-p)_p} . \end{aligned} \tag{2.33}$$

The second equality is more useful computationally and is obtained by multiplying and dividing by $(N+1-p)_{2p-1}$ and using the identity

$$\frac{(N+1-p)_{2p-1}}{(N+1-\Sigma(s))_{p-1}} = (N+1-p)_{p-\Sigma(s)} (N+p-\Sigma(s))_{\Sigma(s)} . \tag{2.34}$$

The only final ingredient is the size of the conjugacy classes. If all cycle lengths are distinct, i.e. $p = q_1 + \ldots + q_m$ with $q_i \neq q_j$, the size of the conjugacy classes is simply $p! / \prod q_i$. However if there are multiple cycles of the same length, i.e. some $q_i = q_j$ in the partition of p, then these cycles are interchangeable and we have to divide by this symmetry in addition. To deal with this case, let $\lambda_1, \lambda_2, \dots, \lambda_r$ be *distinct* so that $\prod_j \lambda_j^{k_j} = \prod_i q_i$ and $\sum_j k_j \lambda_j = p$. Then

$$|[\sigma_{q_1 \dots q_m}]| = \frac{p!}{\prod_{i=1}^r k_i! \lambda_i^{k_i}} . \tag{2.35}$$

We thus have a formula for computing the coefficients $C_{q_1 \dots q_m}$ which give the representation of the SPOs in the trace basis. Very nicely, this formula is explicit in p and $\{q_1, \dots q_m\}$, and depends only on the group theory data associated to such partition.

Notice that the value of m counts the splitting of $\mathcal{O}_p$ into m traces. In appendix A we provide some extra examples for generic $q_1 \dots q_m$ when $m = 2$, i.e. double traces, and $m = 3$, i.e. triple traces.

JHEP11(2020)072

2.2.2 Formula in terms of eigenvalues

In fact the formula for the SPOs is much simpler when expressed directly in terms of the eigenvalues of the adjoint scalar ϕ_r^s which we call $z_1, z_2, \ldots, z_N$. For this purpose consider

$$m_{[\lambda_1,\ldots,\lambda_N]}(z_1,\ldots z_N) = \sum_{\sigma\in S_N} z_{\sigma(1)}^{\lambda_1} z_{\sigma(2)}^{\lambda_2}\cdots z_{\sigma(N)}^{\lambda_N} \tag{2.36}$$

$$E_{p,k}(z_1,\ldots z_N) = \sum_{\substack{q_1+\ldots+q_k=p\\ q_1\geq q_2\geq\ldots q_k>0}} m_{[q_1,\ldots,q_k,0^{N-k}]}(z_1,\ldots z_N) \tag{2.37}$$

which respectively are: $m_{\underline{\lambda}}$ the monomial symmetric polynomial indexed by $\underline{\lambda}$, and $E_{p,k}$ the sum over all monomials indexed by a partition of p in k parts.

So $E_{p,1} = T_p(x)$ is obvious. Other examples are

$$\begin{aligned} E_{p,p}(z_1\ldots z_N) &= z_1\ldots z_p + \ldots \\ E_{4,2}(z_1\ldots z_N) &= (z_1^3 z_2 + \ldots) + (z_1^2 z_2^2 + \ldots) \end{aligned} \tag{2.38}$$

We find that the single-particle operators can be written as[7]

$$\mathcal{O}_p = \sum_{k=1}^{p} d_k(p,N) E_{p,k}(z_i)\,, \tag{2.39}$$

where the coefficient $d_k(p,N)$ is

$$\begin{aligned} d_k(p,N) &= \frac{(-1)^{k+1} p\,(N-p+1)_{p-k}(p-1)_k}{(N)_p - (N-p+1)_p} \\ &= (-1)^k \frac{(p-1)_k}{(N-k+1)_k} \frac{p}{1-\frac{(N)_p}{(N-p+1)_p}} \end{aligned} \tag{2.40}$$

Note that interestingly the coefficient of a monomial in this formula only depends on the number of different eigenvalues appearing in the monomial and not on any other details of the monomial.

2.2.3 Formula in terms of Schur polynomials

Finally we consider the SPOs written in terms of the Schur polynomial formula. In [17] a group theoretic formula for the dual of the trace basis was also given in terms of the Schur polynomial basis, $\chi_R(\phi)$. The Schur polynomial basis is an orthogonal (in U(N)) basis for all half-BPS operators introduced in [15]. The formula given in [17] is:

$$\xi_{p_1\ldots p_n} = \frac{|[\sigma_{p_1\ldots p_n}]|}{p!} \sum_{R\vdash p} \frac{1}{f_R} \chi_R(\sigma_{p_1\ldots p_n}) \chi_R[\phi]\ . \tag{2.41}$$

The relation between the dual basis operators and single particle operators (2.24) together with the observation about S_p characters of cycle permutations (2.28) therefore

[7] More precisely, in all of the many cases we explored, we always find that this formula is valid.

JHEP11(2020)072

gives an explicit formula for SPOs directly in terms of the Schur polynomials of Hook Young diagram of height k, with p boxes in total.

The Young diagrams are R_k^p:

$$R_k^p = [p-k+1, 1^{k-1}] =$$

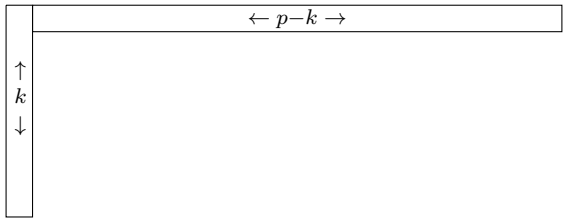

and the operator is

$$\mathcal{O}_p = \sum_{k=1}^{p} \tilde{d}_k(p,N)\chi_{R_k^p}[\phi] \tag{2.42}$$

where

$$\begin{aligned}\tilde{d}_k(p,N) &= p(p-1)(-1)^{k-1}\frac{(N-k+p+1)_{k-1}(N-p+1)_{p-k}}{(N)_p-(N-p+1)_p}\\ &= (-)^k\frac{(p-1)}{p+N}\frac{(N-k+p+1)_k}{(N-k+1)_k}\frac{p}{1-\frac{(N)_p}{(N-p+1)_p}}\end{aligned} \tag{2.43}$$

The last expression is a simple rewriting, to be compared with the one in (2.40).

2.2.4 Examples in the three basis

It is useful at this point to consider some low charges SPOs, and show their representation in the three basis we just constructed.

For $\mathcal{O}_2$,

$$\begin{aligned}\mathcal{O}_2 &= T_2 - \frac{1}{N}T_{11}\\ \mathcal{O}_2 &= \frac{(N-1)}{N}E_{2,1} - \frac{2}{N}E_{2,2}\\ \mathcal{O}_2 &= \frac{(N-1)}{N}\chi_{R_1^2} - \frac{(N+1)}{N}\chi_{R_2^2}\end{aligned} \tag{2.44}$$

For $\mathcal{O}_3$,

$$\begin{aligned}\mathcal{O}_3 &= \frac{2}{N^2}T_{111} - \frac{3}{N}T_{21} + T_3\\ \mathcal{O}_3 &= \frac{(N-2)(N-1)}{N^2}E_{3,1} - \frac{3(N-2)}{N^2}E_{3,2} + \frac{12}{N^2}E_{3,3}\\ \mathcal{O}_3 &= \frac{(N-2)(N-1)}{N^2}\chi_{R_1^3} - \frac{(N-2)(N+2)}{N^2}\chi_{R_2^3} + \frac{(N+1)(N+2)}{N^2}\chi_{R_3^3}\end{aligned} \tag{2.45}$$

For $\mathcal{O}_4$

$$\begin{aligned}\mathcal{O}_4 &= -\frac{(2N^2-3)}{N(N^2+1)}T_{22} + \frac{10}{N^2+1}T_{211} - \frac{5}{N(N^2+1)}T_{1111} - \frac{4}{N}T_{31} + T_4\\ \mathcal{O}_4 &= \frac{(N-3)(N-2)(N-1)}{N(N^2+1)}E_{4,1} - \frac{4(N-3)(N-2)}{N(N^2+1)}E_{4,2}\\ &\quad + \frac{20(N-3)}{N(N^2+1)}E_{4,3} - \frac{120}{N(N^2+1)}E_{4,4}\end{aligned}$$

JHEP11(2020)072

$$\mathcal{O}_4 = \frac{(N-3)(N-2)(N-1)}{N\,(N^2+1)}\chi_{R_1^4} - \frac{(N-3)(N-2)(N+3)}{N\,(N^2+1)}\chi_{R_2^4} + \frac{(N-3)(N+2)(N+3)}{N\,(N^2+1)}\chi_{R_3^4} - \frac{(N+1)(N+2)(N+3)}{N\,(N^2+1)}\chi_{R_4^4} \tag{2.46}$$

A feature of the expansion of the single-particle operator $\mathcal{O}_p$ in the Schur basis is the homogeneous degree in N of its coefficients w.r.t. the partitions of p, i.e. the different basis elements.

2.3 SPOs interpolate between single-trace and giant gravitons

Our definition of single-particle operators can be given directly in $\mathcal{N}=4$ SYM, it involves protected operators and thus is non perturbative. As we anticipated in the introduction, it was strongly motivated by certain properties of the spectrum of KK modes on $AdS_5 \times S^5$, known in supergravity [6–8]. (The ones regarding special features of correlation functions will be further discussed in section 3.2). In this section, we provide additional evidence about the identification of our operators with single-particle half-BPS excitations of $AdS_5 \times S^5$, by studying how the single-particle operator behaves at large N as we vary p, since the latter is well understood in the gravity dual [13, 14].

Recall that the regime of validity of the gravitational description of $\mathcal{N}=4$ SYM is the regime in which N is the largest parameter. For $p \ll N$ the single-particle operators describe AdS_5 KK modes of the type-IIB graviton on the five-sphere, of charge p, and in fact the single-particle operator in the large N limit becomes the single-trace operator

$$\mathcal{O}_p \to T_p + O(1/N)\ . \tag{2.47}$$

The correspondence of the single-trace operators with the KK spectrum in the *strict* large N limit is a very well known fact. Notice that from our formula (2.32), in terms of traces, the limit (2.47) is not immediate, but upon inspection, one can see that the coefficients of multi-trace corrections with m traces, $C_{q_1\dots q_m}$, are indeed $O(1/N^{m-1})$. What happens is that each term of the sum in $C_{q_1\dots q_m}$ is actually $O(N)$, but the alternating sum provides m cancellations, one at each order in N, and this brings it down to $O(1/N^{m-1})$. It is much more direct to see the limit (2.47) from the formula in terms of eigenvalues (2.39)–(2.40), because p is explicit and it is fixed in the limit. By using the Stirling approximation, we find

$$\frac{d_k(p,N)}{d_1(p,N)} \to \frac{(-)^{k-1}}{N^{k-1}}\frac{\Gamma[p+k-1]}{\Gamma[p]} \qquad \text{as} \qquad N\to\infty \tag{2.48}$$

Therefore, unless $k=1$, the contribution is suppressed. But $k=1$ is precisely the contribution $z_1^p + \dots z_N^p$, i.e. the single trace term.

The agreement of the multi-trace admixture in the $1/N$ expansion can be tested from supergravity computations in [6–8], and more generally is consistent with the OPE [4].

Increasing the charge p on the gravity side the authors of [13] predicted an invasion of giant gravitons. The observation is that as the angular momentum (which is equal to the charge p) of the type-IIB graviton increases it becomes less and less pointlike on the

JHEP11(2020)072

sphere, and eventually grows into a D3 brane wrapping an S^3 embedded in the S^5. But the radius of this spherical D3 brane cannot be greater than that of the S^5, the constraint $p/N \leq 1$ follows. We will now show that our single-particle operator perfectly matches the above picture. It cuts off if $p > N$ with both p and N finite, and becomes a giant sphere graviton in the large N limit, with $p \sim N$. In particular, it becomes the operator proposed in [14] as the dual of the spherical D3 brane.

First, let us motivate further the differences between single-particle and single-trace operators. In particular, it is quite evident from our construction that when the charge p of the single-particle operator increases, approaching the number of colours N, it will behave very differently compared to the single trace operator T_p. In fact, if $p > N$, the operator vanishes

$$\mathcal{O}_p = 0 \qquad ; \qquad p > N. \tag{2.49}$$

For example, it is quite immediate to see that this is the case in (2.44), (2.45) and (2.46). In contrast, when $p > N$, the single-trace operators do not vanish, but rather become linear combinations of multi-trace operators. This explains why the single-particle operators vanish: for $p > N$ *all* operators are multi-trace, therefore by definition the single-particle operators are orthogonal to all operators and hence must vanish.

Coming back to the large N limit and the giant graviton picture, where p approaches N from the left, we should consider our single-particle operators in the regime in which

$$p = N - p' \qquad \text{with } p, N \gg 1 \text{ and } p' \geq 0 \text{ fixed}\,. \tag{2.50}$$

In this limit the single-particle operator becomes proportional to the sub-determinant operator $E_{p,p} = z_1 \dots z_p + \dots$ introduced in (2.37). To see this consider the behaviour of a generic coefficients $d_k(p, N)$, normalised w.r.t. $d_p(p, N)$,

$$\mathcal{D}(k') \equiv \frac{d_k(p,N)}{d_p(p,N)} = (-)^{-k'} \frac{\Gamma[2p-1-k']\Gamma[1+p'+k']}{\Gamma[2p-1]\Gamma[1+p']} \qquad ; \qquad k' \equiv p-k \geq 0\,. \tag{2.51}$$

Notice that because p' is fixed, $\mathcal{D}(k')$ is a just function of p and k, or better k'. The giant graviton regime is found for small k' where $\mathcal{D}(k') \sim O(1/(2p)^{k'})$, and since $p \sim N$ at leading order, contributions $E_{p,k}$ are power-law suppressed in the large N limit, apart for the one labelled by $k = p$, which is dominant. Therefore we obtain[8]

$$\mathcal{O}_p \;\to\; (-)^{p+1} p \left(\frac{1}{1+\frac{p}{N}}\right)^{N-p+1} E_{p,p} + O(1/N) \qquad ; \qquad p, N \gg 1 \text{ and } p - N \text{ fixed} \tag{2.52}$$

where the prefactor comes from the limit of $d_p(p, N)$.

The (sub)-determinant operators were proposed in [14] as duals to the D3 branes studied in [13]. We have found that our single-particle operator becomes precisely the sub-determinant operator in the limit (2.50). Recall that the sub-determinant operator

[8] For values of $k' \to N$ we probe the contribution of other $E_{p,k}$ in the sum (2.39), since $k \to 1$. In this limit $\mathcal{D}(k') \sim \sqrt{\pi} N^{1/2+p'} e^{-2N \log 2}$, therefore their contribution is exponentially suppressed, and we can localise the sum on $E_{p,p}$.

JHEP11(2020)072

is also the totally antisymmetric Schur polynomial, labelled by the Young tableau R^p_p, in the sum (2.42). In this notation then, the giant graviton limit localises the single particle operator onto the single column Schur polynomial, as expected [15].

2.4 SPOs in U(N) are SPOs in SU(N)

Single-particle operators can be defined for both SU(N) and U(N) gauge group. As we observed in the low charge examples (2.12), (2.14) and (2.15), the two are closely related. The SU(N) elementary fields are of course different from the U(N) elementary field, and the two theories in general are different. However, the fact that U(N) SPOs represented in the trace basis were shown to give the SU(N) SPOs upon setting Tr(ϕ) to zero, suggests that SPOs in U(N) are SPOs in SU(N). In this section we make this statement rigorous.

The elementary field $\hat{\phi}_r{}^s$ in SU(N) is the traceless part of the elementary field $\phi_r{}^s$ in U(N), namely

$$\hat{\phi}_r{}^s = \phi_r{}^s - \tfrac{1}{N}\delta^s_r\phi_t{}^t \,. \tag{2.53}$$

For any operator $O[\phi]$ in U(N) we define the SU(N) projection as the map,

$$\Pi: \; O[\phi] \;\to\; \hat{O}[\phi] \equiv O[\hat{\phi}(\phi)] \,. \tag{2.54}$$

The operator $\hat{O}[\phi]$ is then a new operator in U(N). For example, the SU(N) projection of $O[\phi] = \mathrm{Tr}(\phi^2)$ is

$$\hat{O}[\phi] = \mathrm{Tr}(\,\hat{\phi}(\phi).\hat{\phi}(\phi)\,) = \underbrace{\mathrm{Tr}(\phi^2)}_{O[\phi]} - \tfrac{1}{N}\,\mathrm{Tr}(\phi)\,\mathrm{Tr}(\phi) \;. \tag{2.55}$$

More generally, we find that an operator $\hat{O}[\phi]$ has the form

$$\hat{O}[\phi] = O[\phi] - [T_1\tilde{O}[\phi]] \qquad ; \qquad T_1 = \mathrm{Tr}[\phi] \tag{2.56}$$

for some operator $\tilde{O}[\phi]$. Notice that $O[\phi]$ is also the leading term in the $1/N$ expansion of $\hat{O}[\phi]$, with the fields ϕ and $\hat{\phi}$ treated as formal variables.

The $\hat{O}[\phi]$ operators in U(N) span a subspace, since they are independent of the trace. The map $\Pi : O \to \hat{O}$ decomposes the space of U(N) operators as $Im(\Pi)\oplus Ker(\Pi)$, with the kernel everything of the form $[T_1\tilde{O}[\phi]]$. To show that the SU(N) projection is orthogonal we have to show that

$$\langle \hat{O}(x_1)\,[T_1\tilde{O}](x_2)\rangle_{\mathrm{U}(N)} = 0 \;. \tag{2.57}$$

The claim follows from the fact that the operator $\hat{O}[\phi]$ is constructed only from the traceless part $\hat{\phi}^r_s$, then by applying Wick's theorem to compute this two-point function we always find a contraction between $\hat{\phi}^r_s(x_1)$ within $\hat{O}(x_1)$ and $T_1(x_2)$. In the U(N) theory with propagator (2.3) we have

$$\langle \hat{\phi}^s_r(x_1) T_1(x_2)\rangle = \langle \phi^s_r(x_1)\phi^t_t(x_2)\rangle - \frac{1}{N}\delta^s_r\langle \phi^u_u(x_1)\phi^t_t(x_2)\rangle = 0 \,. \tag{2.58}$$

JHEP11(2020)072

Thus *any* operator $\hat{O}[\phi]$ constructed only from the traceless part $\hat{\phi}^r_s$ is orthogonal to *any* operator involving the trace as a factor $[T_1\tilde{O}]$.

Single-particle operators $\mathcal{O}$ in U(N) are precisely defined to be orthogonal to all multi-traces, in particular to the operators of the form $[T_1\tilde{O}]$ that we discussed above.[9] Thus single particle operators in U(N) automatically live in the SU(N) subspace. The SU(N) single-particle operator is now candidate to give the U(N) single-particle operator.

Since the two-point orthogonality in U(N) and SU(N) is obtained via Wick's theorem with two different propagators, the only thing remaining to check is that the U(N) inner product restricted on the SU(N) subspace is the same as the inner product of the SU(N) theory. A short computation shows that,

$$\langle\hat{\phi}^s_r(\phi)\hat{\phi}^u_t(\phi)\rangle_{\mathrm{U}(N)} = \left\langle\left(\phi^s_r - \frac{1}{N}\delta^s_r\phi^v_v\right)\left(\phi^u_t - \frac{1}{N}\delta^u_t\phi^v_v\right)\right\rangle_{\mathrm{U}(N)} = \delta^u_r\delta^s_t - \tfrac{1}{N}\delta^s_r\delta^u_t \tag{2.59}$$

which is precisely the SU(N) propagator (2.4).

We conclude that U(N) single-particle operators are SPOs in SU(N) ,

$$\mathcal{O}^{\mathrm{U}(N)}_p[\phi] = \hat{\mathcal{O}}^{\mathrm{SU}(N)}_p[\hat{\phi}] \qquad p \geq 2 \tag{2.60}$$

and any correlators of SPOs of charge 2 or higher computed in either U(N) or SU(N) will be identical.

Our result here manifests, purely in the free theory, the well known feature of $\mathcal{N}$=4 SYM in the context of AdS/CFT that the U(1) part of the gauge group U(N) decouples and only SU(N) remains in the interacting theory. Here we find that the sector of single-particle operators with length greater than one in the U(N) theory is that of the SU(N) theory, and furthermore it is orthogonal to anything we could construct with a T_1.

2.5 Two-point function normalisation

From our study of the SPOs in the trace basis, we can obtain readily their two-point function normalisation. Indeed, it follows from the relation (2.24) that such a normalisation is just the inverse of the ξ_p normalisation from the dual basis, namely

$$\langle\mathcal{O}_p(x_1)\mathcal{O}_p(x_2)\rangle = R_p\, g^p_{12} \qquad ; \qquad \langle\xi_p(x_1)\xi_p(x_2)\rangle = \frac{1}{R_p}g^p_{12} \tag{2.61}$$

where we use the notation R_p to denote the N-dependent color factor. From (2.31) it takes the form

$$R_p = p^2(p-1)\left[\frac{1}{(N-p+1)_{p-1}} - \frac{1}{(N+1)_{p-1}}\right]^{-1}. \tag{2.62}$$

Note that R_p has zeros at $N = 1, \ldots p-1$, reflecting the fact that the operator vanishes when $N < p$, and since it is also symmetric in $N \to -N$ it must contain explicit factors of the form $(N^2 - r^2)$, for $r = 1, \ldots p-1$.

[9] Notice that in the examples (2.12), (2.14) and (2.15), we did not use the basis $Im(\Pi) \oplus Ker(\Pi)$ that instead we are constructing here.

JHEP11(2020)072

It is useful to make these facts manifest by rewriting

$$R_p = \frac{p}{N^{p-2}} \times \prod_{r=1}^{p-1} (N^2 - r^2) \times \frac{1}{Q_p(1/N^2)}\,, \tag{2.63}$$

where $Q_p(1/N^2)$ is a polynomial of degree $\lfloor \frac{p-2}{2} \rfloor$ in $1/N^2$. The first few cases are given by

$$Q_2(1/N^2) = 1\,, \qquad Q_3(1/N^2) = 1\,, \qquad Q_4(1/N^2) = 1 + \frac{1}{N^2}\,. \tag{2.64}$$

whereas the general form of $Q_p(1/N^2)$ is given by

$$Q_{p-2}(N) = \frac{(N+1)_{p-1} - (N-p+1)_{p-1}}{p(p-1)}\,. \tag{2.65}$$

One can manifest the $N \to -N$ symmetry by using rising and lowering factorials instead of always the rising factorial (Pochhammer). With the notation $x^{\overline{p}}$ for the Pochhammer (rising factorial) and $x^{\underline{p}}$ for the falling factorial, we find

$$R_p = p^2(p-1)\frac{(N-1)^{\underline{p-1}}(N+1)^{\overline{p-1}}}{(N+1)^{\overline{p-1}} - (N-1)^{\underline{p-1}}}\,. \tag{2.66}$$

In the form (2.66) it is clear that R_p is the simplest possible rational function of N^2 with the above zeros and of order $O(N^p)$ at large N.

2.6 On multi-particle operators

A complete basis of half-BPS operators in the theory is obtained by taking arbitrary products of the single-particle operators. We call this basis the multi-particle basis.

The statement above can be true also for single-trace operators, modulo the fact that single-traces overcount. Any T_p with $p > N$ is not an independent operator both in SU(N) and U(N), and yet it has non trivial two point functions with other operators. On the other hand, the multi-particle basis does not have this issue. Indeed, if $p > N$ there are only multi-trace operators, and the single-trace operator is not independent. Then, by definition, the single-particle operators are orthogonal to all operators and hence must vanish. Very remarkably, this feature is automatically implemented in the two-point function normalisation (2.66).

The multi-particle basis will not be orthogonal, although of course the single-particle sector will be orthogonal to the multi-particle sector. This is to be contrasted with the Schur polynomial basis of [15] which is both complete and orthogonal, for all half-BPS operators. In particular, operators are in 1-1 correspondence with Young tableau of height no more than N.

Unlike the Schur polynomial basis, the multi-particle basis has the advantage of being a basis both for SU(N) and U(N), depending simply on whether $\mathcal{O}_1$ is included or not.

Requiring orthogonality of multiparticle states is however subtle. To obtain an orthogonal basis one can of course simply implement the Gram Schmidt procedure on a given basis: start with an ordered list of basis elements, then leave the first element unchanged,

JHEP11(2020)072

then run over $n > 1$ by considering the n-th element and add linear combinations of previous elements such that the new element is orthogonal to all previous ones. For example, for the charge six operators we could start with the ordering

$$\begin{aligned} &(T_{111111}, T_{21111}, T_{2211}, T_{3111}, T_{222}, T_{321}, T_{411}, T_{33}, T_{42}, T_{51}, T_6) && \mathrm{U}(N) \\ &(T_{222}, T_{33}, T_{42}, T_6) && \mathrm{SU}(N)\,. \end{aligned} \tag{2.67}$$

Performing Gram-Schmidt orthogonalisation would provide an orthogonal set of operators. (In practise this can be done by cutting appropriately the matrix in (2.9).) However at this point, the single-particle operator is singled out as the last one. In the example above $\mathcal{O}_6$, is the one with greater admixture, in contrast to T_{111111} or T_{222}, but then it is not clear if there is a canonical choice for the ordering of the other operators.

As long as the single-particles are fixed, a completely equivalent way of obtaining the same orthogonal basis is to start with the dual basis, list the operators in reverse order, and perform Gram-Schmidt orthogonalisation. This process yields exactly the same orthogonal basis (up to normalisation). Referring to the same example as above,

$$\begin{aligned} &(\xi_6, \xi_{51}, \xi_{42}, \xi_{33}, \xi_{411}, \xi_{321}, \xi_{222}, \xi_{3111}, \xi_{2211}, \xi_{21111}, \xi_{111111}) && \mathrm{U}(N) \\ &(\xi_6, \xi_{42}, \xi_{33}, \xi_{222}) && \mathrm{SU}(N)\,. \end{aligned} \tag{2.68}$$

In the first approach the operator with the most traces T_{111111} (or T_{222}) remains unchanged whereas the single-particle operator is the most complicated from the point of view of the trace-basis. In the second approach, this is turned on its head. In terms of the dual basis, the single particle operator is – just ξ_p – whereas an operator labelled by a partition with increasing length becomes more intricate from the point of view of the ξ basis. In the end, the most intricate of such operators - a linear combination of all dual operators - must equal T_{11111} (or T_{222}).

We leave the task of extending the single-particle operators to a full orthogonal basis to a future work. Perhaps an AdS/CFT understanding of multi-particle KK modes will help us figuring out a canonical way to fix the multi-particle states in $\mathcal{N} = 4$ SYM.

3 Multipoint orthogonality

In the previous section we obtained explicit expressions for SPOs. From the two-point orthogonality it followed that SPOs are given by a specific admixture of single- and multi-trace operators. In a sense, the SPOs are composites of traces and the richness of this structure would suggest that multipoint correlation functions are rather more complicated than multipoint single-trace correlation functions. However this expectation is too naive and as a first counter-example we show in this section that the defining two-point function orthogonality uplifts to a multipoint orthogonality theorem, which in turn implies vanishing of a large class of diagrams. Let us state our main result.

> *Multipoint orthogonality theorem.* Any propagator structure, which can contribute to any half-BPS correlator, with a single-particle operator $\mathcal{O}_p$ connected to two sub-diagrams, themselves disconnected from each other, has a vanishing color factor. The statement holds for both SU(N) and U(N) free theories.

JHEP11(2020)072

We are considering any propagator structure $\mathcal{F}_{p|\underline{q_1}\dots\underline{q_{n-1}}}$ which becomes disconnected upon removing $\mathcal{O}_p$, and thus has the shape of a dumbbell:

$\mathcal{F}_{p|\underline{q_1}\dots\underline{q_{n-1}}} =$ 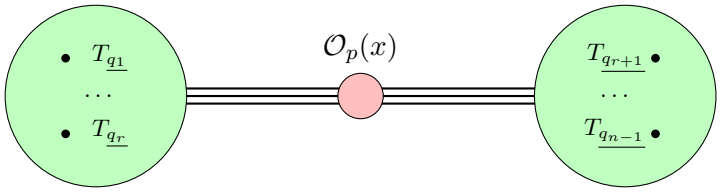

(3.1)

A propagator structure of this sort will have a number of bridges going between points in the two (green) blobs, left and right, and a number of bridges connecting $\mathcal{O}_p(x)$ with points belonging to the left and right blobs. No bridges between left and right blobs.

Our theorem states that

$$\mathcal{F}_{p|\underline{q_1}\dots\underline{q_{n-1}}} = 0. \tag{3.2}$$

We can gain some intuition about the multipoint orthogonality by considering the fact that $\mathcal{F}_{p|\underline{q_1}\dots\underline{q_{n-1}}}$ can be rearranged as a determinant. This follows directly from the representation of $\mathcal{O}_p(x)$ as a determinant, that we mentioned in (2.9). All rows of this determinant, but the last one, are given by the (color factor of the) two points functions $\langle T_{\lambda_i} T_{\lambda_j}\rangle$, where λ_i and λ_j denote partitions of p. The last row is given by (the color factors of) $\langle T_{\lambda_i}(x) T_{\underline{q_1}}(x_1)\dots T_{\underline{q_{n-1}}}(x_{n-1})\rangle$ in the given propagator structure. The determinant will vanish as long as this last row reduces to a linear combination of the others. But this linear combination might be N-dependent and thus hard to chase. We give some examples in appendix C. However, a crucial point is that for *any* two point functions $\langle T_{\lambda_i} T_{\lambda_j}\rangle$ at least one partition has length greater than two. Therefore we might displace a part of it on a fictitious point, and since there cannot be propagators inside a T_λ, this configuration is actually a dumbbell. We learn in this way that, for the determinant to have a chance to vanish, the topology of the $\langle T_{\lambda_i}(x) T_{\underline{q_1}}(x_1)\dots T_{\underline{q_{n-1}}}(x_{n-1})\rangle$ has to have the same feature of the two point functions $\langle T_{\lambda_i} T_{\lambda_j}\rangle$. We can then argue that $\mathcal{F}_{p|\underline{q_1}\dots\underline{q_{n-1}}}$ is a dumbbell, as we draw in (3.1).

The reasoning above leaves a free parameter. In fact, the assignment $\underline{q_1},\dots,\underline{q_{n-1}}$ can be such that

$$\frac{1}{2}\left(-p+\sum_{i=1}^{n-1} q_i\right) = k \geq 0 \tag{3.3}$$

and yet the diagram disconnects as soon as we remove $\mathcal{O}_p$. The value of k measures the excess of $\sum q_i$ to be a partition of p. This is possible precisely because differently from a two-point function, in a multipoint function there can be $k \geq 0$ Wick contractions distributed among the $T_{\underline{q_1}}(x_1)\dots T_{\underline{q_{n-1}}}(x_{n-1})$, such that when $\mathcal{O}_p$ is removed, the diagram still disconnects.

In general, the combinatorics which leads to $\mathcal{F}_{p|\underline{q_1}\dots\underline{q_{n-1}}} = 0$ is hard. It would be very interesting to have a combinatorial proof of our theorem, by using Wick contractions and double line notation, but our proof in the next section will go through a nice alternative route.

JHEP11(2020)072

Some readers might wish to jump directly to section 3.2 at this point. There we use multipoint orthogonality to show that near-extremal n-point functions, defined by the constraint $k \leq n-3$, vanish.

3.1 Proof of the theorem

As long as the topology of $\mathcal{F}_{p|\underline{q_1}\cdots\underline{q_{n-1}}}$ is fixed as in (3.1), we can work with a fixed propagator structure.

To show that $\mathcal{F}_{p|\underline{q_1}\cdots\underline{q_{n-1}}} = 0$, we will first make an argument for the part of the diagram, consisting of $\mathcal{O}_p$ and everything to the right. Take $\mathcal{O}_p(x)T_{\underline{q_{r+1}}}(x_{r+1}), \ldots, T_{\underline{q_{n-1}}}(x_{n-1})$ and consider Wick contracting the fundamental fields in all possible ways consistent with the propagator structure $\mathcal{F}_{p|\underline{q_1}\cdots\underline{q_{n-1}}}$. Since the number of bridges going from $\mathcal{O}_p(x)$ to the right is fixed and less than p, some of the fundamental fields inside $\mathcal{O}_p(x)$ will remain unlinked, thus resulting in a new half-BPS operator of lower charge, say R, inserted at x. For each arrangement of Wick contractions, we can write this new half-BPS operator of charge R in the trace basis, as illustrated below,

$$\prod g_{ij}^{d_{ij}} \sum_{\underline{R}\vdash R} C_{\underline{R}}\, T_{\underline{R}}(x) \;=$$

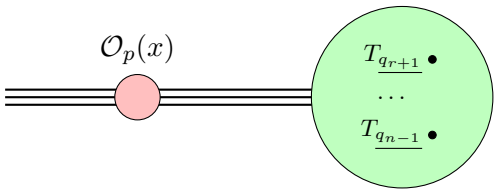

(3.4)

The sum is over operators $T_{\underline{R}}(x)$, indexed by partitions of R, and multiplied by a coefficient $C_{\underline{R}}$. The (partial) propagator structure $\prod g_{ij}^{d_{ij}}$ is the one we assigned and it is factored out.

The initial propagator structure is now computed as

$$\mathcal{F}_{p|\underline{q_1}\cdots\underline{q_{n-1}}} = \prod g_{ij}^{d_{ij}} \sum_{\underline{R}\vdash R} C_{\underline{R}}$$

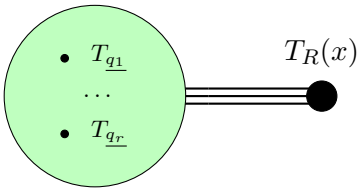

(3.5)

The next step is to find the coefficients C_R, and we do so by sandwiching the equation (3.4) with operators $T_{R'}(x')$ at some auxiliary location x'. Graphically we obtain

$$\prod g_{ij}^{d_{ij}} \sum_{\underline{R'},\underline{R}\vdash R} C_{\underline{R}}\, \langle T_{\underline{R'}}(x') T_{\underline{R}}(x)\rangle =$$

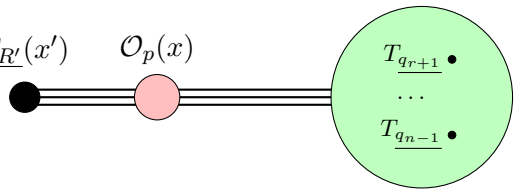

(3.6)

This is a vector equation for $C_{\underline{R}}$, which we can solve by inverting the matrix of two point functions. It follows that the coefficients $C_{\underline{R}}$ are given by computing another dumbbell diagram. The two-point functions $\langle T_{\underline{R'}}(x')T_{\underline{R}}(x)\rangle$ are given by $g^R_{x'x}$, which we can factor out, times the color factor, $\mathcal{C}_{\underline{R},\underline{R'}}$. For clarity we will keep using the notation $\langle T_{\underline{R'}}(x')T_{\underline{R}}(x)\rangle$.

JHEP11(2020)072

We can now replace the $C_{\underline{R}}$ and rewrite the original $\mathcal{F}_{p|\underline{q_1}\cdots\underline{q_{n-1}}}$ as follows,

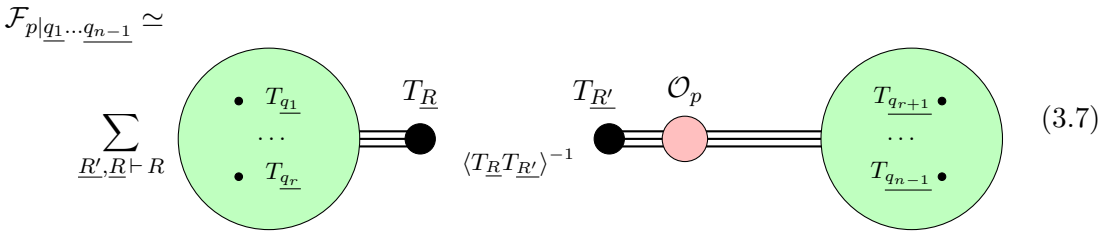

(3.7)

Repeating a similar discussion for the left hand side of $\mathcal{F}_{p|\underline{q_1}\cdots\underline{q_{n-1}}}$ we conclude then that the original propagator structure can be rewritten as

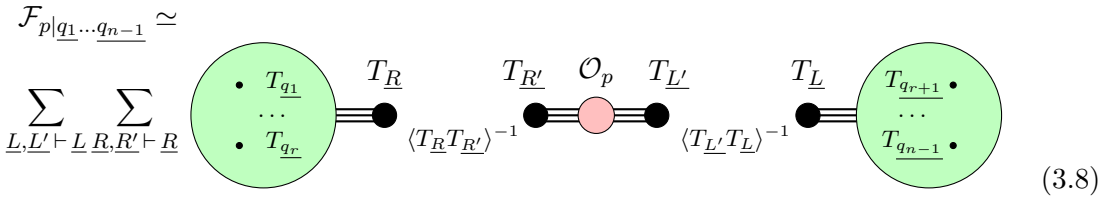

(3.8)

Crucially, the central connected diagram in (3.8) is a three-point function $\langle \mathcal{O}_p T_{\underline{Q}} T_{\underline{R}}\rangle$ with $p = Q + R$, thus extremal. To conclude we then have to show that any extremal three-point function vanishes, i.e.

$$\langle \mathcal{O}_p T_{\underline{Q}} T_{\underline{R}}\rangle = 0 \qquad ; \qquad p = Q + R\,. \tag{3.9}$$

This is a direct consequence of the two-point function orthogonality, which we used in (2.8) to define the SPOs, together with the fact that extremal 3-point functions are directly related to the corresponding two-point function obtained by bringing points 2 and 3 together (since there are no propagators between $T_{\underline{Q}}$ and $T_{\underline{R}}$)

$$\langle \mathcal{O}_p T_{\underline{Q}} T_{\underline{R}}\rangle = \left(\frac{g_{13}}{g_{12}}\right)^R \langle \mathcal{O}_p [T_{\underline{Q}} T_{\underline{R}}]\rangle = 0\,. \tag{3.10}$$

This concludes our proof. We thus have shown that any propagator structure involving a single $\mathcal{O}_p$, which becomes disconnected on removing $\mathcal{O}_p$ vanishes.

3.2 Near-extremal correlators vanish

When discussing n-point functions of half-BPS operators it is useful to introduce the degree of extremality k defined as follows. Let p be the largest charge, and $q_{i=1,\ldots n-1}$ the others, then

$$k = \tfrac{1}{2}\left(-p + \sum_{i=1}^{n-1} q_i\right)\,. \tag{3.11}$$

This definition of k should be now familiar from (3.3).

JHEP11(2020)072

For $k < 0$ correlators vanish purely by SU(4) symmetry. Extremal ($k = 0$) and next-to-extremal ($k = 1$) correlators, they all were shown to be non-renormalised in [19–23].[10]

In [18] the concept of "near-extremal" correlators was introduced. These are correlators in which the degree of extremality k is not too close to the number of points. Specifically

$$\text{near extremal correlator:} \qquad k \leq n-3 \ . \tag{3.12}$$

Notice that for $n \geq 5$, the near-extremal correlators go beyond the extremal- and next-to-extremal cases mentioned above.

We claim that any near-extremal SU(N) correlator *in free theory*, where the largest charge operator is a single-particle operator, vanishes:[11]

$$\langle \mathcal{O}_p(x) T_{\underline{q_1}}(x_1) \dots T_{\underline{q_{n-1}}}(x_{n-1}) \rangle = 0 \qquad k \leq n-3 \ . \tag{3.13}$$

As usual, $T_{\underline{q_i}}$ stands for any half-BPS operator with total charge q_i. We remark that *any* refers to any single- or multi-trace operator or any combination of these. A corollary of this is that any near-extremal correlator involving only SPOs vanishes.

$$\langle \mathcal{O}_p(x) \mathcal{O}_{q_1}(x_1) \dots \mathcal{O}_{q_{n-1}}(x_{n-1}) \rangle = 0 \qquad k \leq n-3 \ . \tag{3.14}$$

A similar statement can also be made in the U(N) theory, with the caveat that then it is only true for connected correlators: any *connected* near-extremal U(N) correlator where the largest charge operator is a single-particle operator vanishes.

In order to prove (3.13) we will now show that every propagator structure contributing to this correlator has the dumbbell shape, as in (3.1), namely it becomes disconnected on removing $\mathcal{O}_p$.

Let us first show that there are too few propagators between the operators $T_{\underline{q_i}}$ to connect them all together, and therefore there will be two green blobs as in (3.1). Indeed, since there are p legs coming out of $\mathcal{O}_p$, and k is the excess of $\sum q_i$ to be a partition of p, there are k propagators among the $T_{\underline{q_i}}$s. But $k \leq n-3$ and there are $n-1$ operators $T_{\underline{q_i}}$. The minimal scenario to link all the $T_{\underline{q_i}}$ would be to have a necklace with $k = n-1$ bridges, which is not possible, both for SU(N) and U(N). We would need at least two more points.

We understood that the topology of $\mathcal{O}_p(x) T_{\underline{q_1}}(x_1) \dots T_{\underline{q_{n-1}}}(x_{n-1})$ is such that it is not possible to connect all $T_{\underline{q_i}}$. This would imply the diagram is dumbbell, but for the case in which the diagram is actually made of two disconnected parts, i.e. one green blob is actually on its own. For concreteness let's say $T_{\underline{q_1}}(x_1) \dots T_{\underline{q_r}}(x_r)$ is disconnected from $\mathcal{O}_p(x) T_{\underline{q_{r+1}}}(x_1) \dots T_{\underline{q_n}-1}(x_{n-1})$, for some value of r. Let us see when this can happen: the number of bridges among the $T_{\underline{q_{r+1}}}, \dots, T_{\underline{q_{n-1}}}$ which are not connecting with $\mathcal{O}_p$ is

$$k_R = \frac{1}{2}\left(-p + \sum_{i=r+1}^{n-1} q_i \right) . \tag{3.15}$$

[10] It is quite nice to see how the non-renormalisation works diagrammatically, in specific cases. For the simplest case of two-point functions see for example [24, 25].

[11] The results of [18] could be used to argue that the near-extremal connected correlators vanish in the supegravity limit, to all order in $1/N$, and to leading order in g_{YM}. Notice that $\mathcal{O}_{p,there} = T_{p,here}$.

JHEP11(2020)072

We can assume $\mathcal{O}_p(x)T_{\underline{q_{r+1}}}(x_{r+1}),\ldots,T_{\underline{q_{n-1}}}(x_{n-1})$ to remain connected on removing $\mathcal{O}_p$, and since there are $n-r-2$ operators $T_{\underline{q_{r+1}}}(x_{r+1}),\ldots,T_{\underline{q_{n-1}}}(x_{n-1})$, the minimum scenario would be to have them forming a tree, thus $k_R \geq n-r-2$. If we now recall the inequality on k we find

$$k=\frac{1}{2}\Big(-p+\sum_{i=r+1}^{n-1}q_i+\sum_{i=1}^{r}q_i\Big)\leq n-3 \quad \Rightarrow \quad \frac{1}{2}\sum_{i=1}^{r}q_i\leq n-3-k_R\leq r-1\,. \tag{3.16}$$

But $\frac{1}{2}\sum_{i=1}^{r}q_i$ is the total number of bridges among the fields $T_{\underline{q_1}}(x_1)\ldots T_{\underline{q_r}}(x_r)$, which recall are disconnected from the rest of the diagram. Therefore, we learn that at most they form a tree. In a tree, some operators will necessarily be connected to others just with a single bridge. For the U(N) theory this is possible if a number of $\mathcal{O}_1$ fields are inserted in the original correlator. For SU(N) theory there is not such a possibility.

We conclude that all SU(N) diagrams contributing to near extremal correlators have a dumbbell shape (3.1) and hence vanish. Similarly for all connected U(N) diagrams.

3.2.1 More cases: coincident points and multi-trace splitting

A useful corollary of the vanishing of near-extremal correlators occurs for lower point correlators, say m-points, which are not near-extremal but have a number of multi-trace operators,

$$\langle\mathcal{O}_p(x)T_{\underline{q_1}}(x_1)\ldots T_{\underline{q_{m-1}}}(x_{m-1})\rangle \qquad ; \qquad k=\frac{1}{2}\Big(-p+\sum q_i\Big)\geq m-3\,. \tag{3.17}$$

The idea is that when a number r of operators are genuinely multi-trace, we can think of (3.17) as a correlator $\mathcal{F}$ with $n\geq m$ points (with specific propagator structure since there cannot be propagators inside a multi-trace). Namely

$$\langle\mathcal{O}_p(x)T_{\underline{q_1}}(x_1)\ldots T_{\underline{q_{m-1}}}(x_{m-1})\rangle \quad \rightarrow \quad \mathcal{F}(p|\underline{q_1'}\ldots\underline{q_n'})\,. \tag{3.18}$$

The number of new points n depends on the way we want to think of the multi-trace operators. The max we can do is to put all its parts on fictitious points. So if $l(\underline{q_i})$ measures the number of parts of $\underline{q_i}$, then

$$m\leq n\leq (m-r)+\sum_{i=1}^{r}l(\underline{q_i})\,. \tag{3.19}$$

If there is a value of n such that $k\leq n-3$, the original correlator vanishes, since it can be though of as an n-point near-extremal correlator.

A simple example. For three-point functions we find

$$\text{if } \exists\ i \text{ such that } l(\underline{q_i})\geq 2 \text{ and } k\leq 1 \quad \Rightarrow \quad \langle\mathcal{O}_p(x)T_{\underline{q_1}}(x_1)T_{\underline{q_2}}(x_2)\rangle=0\,. \tag{3.20}$$

The claim follows because in this case we can always think of the three-point function as a near-extremal four-point function, which vanishes.

Another example is

$$\text{if } \exists\ i \text{ such that } l(\underline{q_i})\geq 2 \text{ and } k\leq m-2 \quad \Rightarrow \quad \langle\mathcal{O}_p(x)T_{\underline{q_1}}(x_1)\ldots T_{\underline{q_{m-1}}}(x_{m-1})\rangle=0\,. \tag{3.21}$$

There are many possibilities involving splitting of more than one operator, but we do not list them all, since it should be clear how to generalise the examples above.

JHEP11(2020)072

4 Exact results for correlators of SPOs

4.1 Maximally-extremal correlators

Given the vanishing of all near-extremal correlators of SPOs in (3.12), the next cases to consider are

$$\langle \mathcal{O}_p(x)\mathcal{O}_{q_1}(x_1)\dots\mathcal{O}_{q_{n-1}}(x_{n-1})\rangle \quad ; \quad k=n-2 \quad ; \quad k=\frac{1}{2}\Big(-p+\sum q_i\Big) \tag{4.1}$$

which we call Maximally-Extremal (ME).

We will compute all ME correlators *in free theory*, beginning with three-points and generalising the argument to n-points. From now on we focus on the SU(N) theory. The final result will have the following flavor,

$$\langle \mathcal{O}_p(x)\mathcal{O}_{q_1}(x_1)\cdots\mathcal{O}_{q_{n-1}}(x_{n-1})\rangle_{\text{connected}} = \langle \mathcal{O}_p\mathcal{O}_p\rangle \left(\sum_{\text{trees}\,\mathcal{T}} |\mathcal{W}[\mathcal{T}]|\; \mathcal{T}\begin{bmatrix} d_1 & & b_{ij} \\ & \ddots & \\ & & d_{n-1}\end{bmatrix}\right) \tag{4.2}$$

where the sum is over all trees $\mathcal{T}$ on $n-1$ points, each point with associated degree $d_i \geq 1$ (number of legs per point) such that $\sum_{i=1}^{n-1} d_i = 2(n-2)$. The tree is specified by a sub-propagator structure b_{ij} which we arrange into a matrix, and finally,

$$|\mathcal{W}[\mathcal{T}]| = \prod_{i=1}^{n-1} q_i(q_i-1)\dots(q_i-d_i+1)\,. \tag{4.3}$$

We will progressively get to this result.

4.1.1 3-point functions

ME three-points functions are also next-to-extremal three-point functions since $k=1$. In order to compute them, notice first that

$$\langle \mathcal{O}_p(x)\mathcal{O}_{q_1}(x_1)\mathcal{O}_{q_2}(x_2)\rangle = \langle \mathcal{O}_p(x)T_{q_1}(x_1)T_{q_2}(x_2)\rangle\,, \qquad p=q_1+q_2-2\,, \tag{4.4}$$

In fact, the difference between the two is a sum of three-point functions with at least a multi-trace. By the results in section 3.2.1, they all vanish.

In the three-point function $\langle \mathcal{O}_p T_{q_1} T_{q_2}\rangle$ there is a single propagator between T_{q_1} and T_{q_2}, and therefore a single Wick contraction to do in between x_1 and x_2. If at the same time we bring together these two insertion points, we obtain the following result,

$$\lim_{x_1\to x_2} \mathrm{Tr}(\underbrace{\phi(x_1).\dots.\phi(x_1)}_{q_1})\,\mathrm{Tr}(\underbrace{\phi(x_2).\dots.\phi(x_2)}_{q_2}) \simeq \mathrm{Tr}(\underbrace{\phi(x_2).\dots.\phi(x_2)}_{p}) + \dots \tag{4.5}$$

Intuitively, since each trace is cyclic invariant we are always considering a configuration which in double line notation looks like the following drawing (with many more free legs),

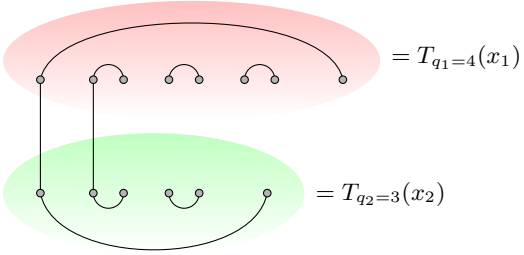

(4.6)

JHEP11(2020)072

But in general we find all the contributions of an OPE of scalars on the r.h.s. of (4.5), however since we will contract that with the half-BPS operator $\mathcal{O}_p$, any other term does not survive. Clearly there are $q_1 q_2$ ways to perform this Wick contraction and we arrive at

$$\langle \mathcal{O}_p T_{q_1} T_{q_2} \rangle = q_1 q_2 \langle \mathcal{O}_p T_p \rangle \,. \tag{4.7}$$

Finally we have that $\langle \mathcal{O}_p T_p \rangle = \langle \mathcal{O}_p \mathcal{O}_p \rangle$ from the defining orthogonality of $\mathcal{O}_p$.

Putting all this together we arrive at the result that next-to-extremal three-point functions are simply expressed in terms of two-point functions,

$$\langle \mathcal{O}_p \mathcal{O}_{q_1} \mathcal{O}_{q_2} \rangle = q_1 q_2 \langle \mathcal{O}_p \mathcal{O}_p \rangle \qquad ; \qquad p = q_1 + q_2 - 2 \,. \tag{4.8}$$

4.1.2 n-point functions

Now consider maximally extremal n-point functions.

As in the case of three-points in (4.4), note that we can replace all operators, apart from the one with the largest charge, by single trace operators,

$$\langle \mathcal{O}_p(x) \mathcal{O}_{q_1}(x_1) \cdots \mathcal{O}_{q_n}(x_{n-1}) \rangle = \langle \mathcal{O}_p(x) T_{q_1}(x_1) \cdots T_{q_{n-1}}(x_{n-1}) \rangle \quad ; \quad k = n - 2 \,. \tag{4.9}$$

The difference between the two is a sum of n-point functions involving at least one multi-trace operator. By the results in section 3.2.1, they all vanish.

A non-vanishing connected diagram contributing to the correlator (4.9) is such that, upon deleting $\mathcal{O}_p$ and all the bridges attached to it, there will be $n-2$ propagators amongst the $n-1$ operators T_{q_i}, just enough to connect the T_{q_i}s all together in a tree. We draw a five-point example here below for clarity,

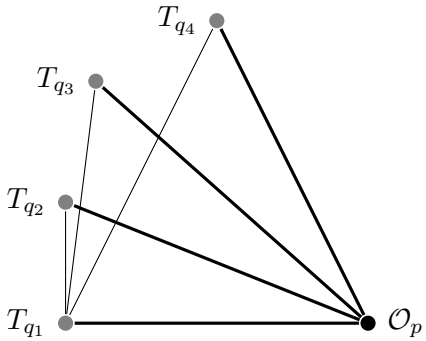

(4.10)

In this case the tree consists of T_{q_1} connected to T_{q_2}, T_{q_3} and T_{q_4}. Notice that in a tree there is one and only one bridge which connects pairs of operators. On each point we can have at most an n-pointed star with some $n \geq 1$.

We have understood that a propagator structure contributing to a ME n-point correlator (4.9) contains a sub-propagator structure which is a tree $\mathcal{T}$. We can represent it by using our same notation for propagator structures in appendix B, namely

$$\mathcal{T} \simeq \begin{bmatrix} d_1 & b_{12} & b_{13} & \dots & b_{1n-1} \\ & d_2 & b_{23} & \dots & \vdots \\ & & \ddots & & \\ & & & & \\ & & & & d_{n-1} \end{bmatrix} \quad ; \quad \begin{matrix} d_i \geq 1 \\ \\ b_{(ij)} \in \{0, 1\} \end{matrix} \tag{4.11}$$

JHEP11(2020)072

where now $d_i \leq p_i$ is the number of legs of T_{q_i} entering the tree, and the number of bridges b_{ij} from point i to point j can only take two possible values, $b_{(ij)} \in \{0, 1\}$. The latter does not yet guarantees that (4.11) is a tree (for example necklace configurations can be arranged with $b_{ij} = 1$). A unique way to label a tree is to use a Prüfer sequence $s = (s_1 \ldots)$. We explain how the Prüfer algorithm works in appendix B.2. This point of view allows to reduce the pairwise computation of Wick contractions to a sequence, and in particular, gives us the result

$$|\mathcal{W}[\mathcal{T}]| = \prod_{i=1}^{n-1} q_i(q_i - 1)\ldots(q_i - d_i + 1)\,. \tag{4.12}$$

More details can be found in appendix B.2.

At this point, recall that the legs of the T_{q_i}s which do not enter the tree, form a bridge with the single-particle operator $\mathcal{O}_p$. By performing the Wick contraction on the tree, leaf by leaf as in the Prüfer algorithm, each time bringing together the points, we can use the same argument of section 4.1.1 to infer that the net result of the tree is to glue together the T_{q_i}s to form a new single trace operator of charge T_p, together with higher trace terms. These higher-trace terms will not contribute in the full ME correlator according to the discussion in section 3.2.1.

The entire connected part of the ME correlator can thus be written as a sum over trees, multiplying the two point function $\langle \mathcal{O}_p \mathcal{O}_p \rangle$ overall:

$$\langle \mathcal{O}_p(x)\mathcal{O}_{q_1}(x_1)\cdots\mathcal{O}_{q_{n-1}}(x_{n-1})\rangle_{\text{connected}} = \langle \mathcal{O}_p\mathcal{O}_p\rangle \left(\sum_{trees\,\mathcal{T}} |\mathcal{W}[\mathcal{T}]|\; \mathcal{T}\begin{bmatrix} d_1 & & b_{ij} \\ & \ddots & \\ & & d_{n-1} \end{bmatrix} \right) \tag{4.13}$$

where the sum is restricted to $d_i \geq 1$ such that $\sum_{i=1}^{n-1} d_i = 2(n-2)$.

Note that the total number of trees contributing to this correlator is well known and given by Cayley's formula:

$$(n-1)^{n-3}\,. \tag{4.14}$$

Note also that many trees correspond to the same arrangement of degrees, $d_{i=1,\ldots n-1}$. Therefore many trees have the same value of $|\mathcal{W}[\mathcal{T}]|$. (In fact the tree is uniquely specified only once the configuration of bridges is also specified.) This degeneracy is counted by the multinomial coefficient

$$\frac{(n-3)!}{\prod_{i=1}^{n-1}(d_i - 1)!}\,. \tag{4.15}$$

Disconnected contributions. The ME correlator can have disconnected contributions even in the SU(N) theory. Indeed there can be a disconnected component if and only if at least two of the T_{q_i} operators are $\mathcal{O}_2$. These are precisely necklace configurations of SU(N), and products thereof.[12] For example, we might have

$$\langle \prod_{i=1}^{K} \mathcal{O}_2(x_i)\mathcal{O}_{q_{k+1}}\ldots\mathcal{O}_{q_{n-1}}\mathcal{O}_p\rangle_{\text{discon.}} = \langle \prod_{i=1}^{K} \mathcal{O}_2(x_i)\rangle_{\text{necklace}} \langle \mathcal{O}_{q_{k+1}}\ldots\mathcal{O}_{q_{n-1}}\mathcal{O}_p\rangle_{\text{conn.}}\,. \tag{4.16}$$

[12] Following a discussion similar to the one around (3.16), we conclude that at least one of the connected components has to be made up entirely of $\mathcal{O}_2$s.

JHEP11(2020)072

Note that the factored expressions on the r.h.s are themselves maximally extremal. In fact if there are K $\mathcal{O}_2$, then $n \to n' \equiv n - K$, and we find

$$n-2 = \frac{1}{2}\Big(-p + 2K + \sum_{i=\ell+1}^{n-1} q_i \Big) \qquad \to \qquad (n'-2) = \frac{1}{2}\Big(-p + \sum_{i=\ell+1}^{n-1} q_i \Big) . \tag{4.17}$$

Any other type of disconnected component will vanish as at least one of the connected pieces will be near extremal.

Let us conclude this section with some examples.

4-pt function. Here there are three possible trees, or equivalently arrangements for the possible values of the number of legs at positions $i = 1, 2, 3$ in the tree, $d_{i=1,2,3}$, where $\mathcal{O}_p$ is located at position 4. We can have $d_1 = 2, d_2 = d_3 = 1$, which gives the tree $g_{12}g_{13}$, and two other permutations of this. There is no degeneracy (4.15), thus the full result is

$$\begin{aligned} \langle \mathcal{O}_p \mathcal{O}_{q_1} \mathcal{O}_{q_2} \mathcal{O}_{q_3} \rangle_{\text{connected}} = q_1 q_2 q_3 \, \langle \mathcal{O}_p \mathcal{O}_p \rangle \Big[& (q_1 - 1) g_{41}^{q_1-2} g_{42}^{q_2-1} g_{43}^{q_3-1} \overbrace{g_{12} g_{13}}^{\text{tree } \mathcal{T}} \\ & + (q_2 - 1) g_{41}^{q_1-1} g_{42}^{q_2-2} g_{43}^{q_3-1} \, g_{12} g_{23} \\ & + (q_3 - 1) g_{41}^{q_1-1} g_{42}^{q_2-1} g_{43}^{q_3-2} g_{13} g_{23} \Big] . \end{aligned} \tag{4.18}$$

5-pt function. The number of trees in this case is $4^2 = 16$ and furthermore this is a case with degeneracy. If the tree goes in between points $i = 1, 2, 3, 4$, the four non-degenerate configurations are

$$\begin{aligned} & d_1 = 3 \, , \, d_{j=2,3,4} = 1 \quad ; && d_2 = 3 \, , \, d_{j=1,3,4} = 1 \quad ; \\ & d_3 = 3 \, , \, d_{j=1,2,4} = 1 \quad ; && d_4 = 3 \, , \, d_{j=1,2,3} = 1 \, . \end{aligned} \tag{4.19}$$

Then, there are twice the configurations

$$\begin{aligned} & d_{i=1,2} = 2 \, , \, d_{i=3,4} = 1 \quad ; && d_{i=1,3} = 2 \, , \, d_{i=2,4} = 1 \\ & d_{i=1,4} = 2 \, , \, d_{i=2,3} = 1 \quad ; && d_{i=2,3} = 2 \, , \, d_{i=1,4} = 1 \\ & d_{i=2,4} = 2 \, , \, d_{i=1,3} = 1 \quad ; && d_{i=3,4} = 2 \, , \, d_{i=1,2} = 1 \, . \end{aligned} \tag{4.20}$$

In fact, the degeneracy is two, as counted by (4.15). The total number of trees count twelve (above) plus the four non-degenerate, equals sixteen.

Finally, let us also notice that the contribution of some tree might vanish for low charges. For example, associated to $d_1 = 3, d_{j=2,3,4} = 1$ is $q_1 q_2 q_3 q_4 (q_1 - 1)(q_1 - 2)$, which vanishes in the case $q_1 = 2$. Therefore, in the case of $\langle \mathcal{O}_2(x_5) \mathcal{O}_2 \mathcal{O}_2 \mathcal{O}_2 \mathcal{O}_2 \rangle$ we are left with the twelve degenerate trees, all contributing with coefficient $q_1 q_2 q_3 q_4 = 16$.

4.2 Next-to-maximally-extremal correlators

Going down in extremality, we consider Next-to-Maximally-Extremal (NME). These are n-point correlators with $k = n - 1$, i.e.

$$\langle \mathcal{O}_p(x) \mathcal{O}_{q_1}(x_1) \dots \mathcal{O}_{q_{n-1}}(x_{n-1}) \rangle \quad ; \quad k = n-1 \quad ; \quad k = \frac{1}{2}\Big(-p + \sum q_i \Big) . \tag{4.21}$$

We will first study three-point functions and them move to n-point functions *in free theory*.

4.2.1 3-point functions

Starting with $n = 3$ we are studying next-next-to-extremal three-point functions

$$\langle \mathcal{O}_p(x)\mathcal{O}_{q_1}(x_1)\mathcal{O}_{q_2}(x_2)\rangle \qquad ; \qquad p = q_1 + q_2 - 4. \tag{4.22}$$

As for the NE case, these can be related to the corresponding two point function $\langle \mathcal{O}_p\mathcal{O}_p\rangle$, but with a more complicated coefficient containing non-factorisable polynomials.

To evaluate the three-point function, we replace $\mathcal{O}_{q_1}$ and $\mathcal{O}_{q_2}$ by their respective expansions in the trace basis (2.32). Differently from what happens in the ME case, see section 4.1.1, this time the expansion truncates for any term involving higher than double-trace operators at a single point. These higher-traces will result in vanishing diagrams with $n \geq 5$ points, according to our general results in section 3.2.1. For the same reason we can replace the double trace terms with products of single particle operators. Therefore we conclude that:

$$\langle \mathcal{O}_p(x)\mathcal{O}_{q_1}(x_1)\mathcal{O}_{q_2}(x_2)\rangle = \langle \mathcal{O}_p(x)T_{q_1}(x_1)T_{q_2}(x_2)\rangle \tag{4.23}$$

$$+ \sum_{p_1=2}^{\frac{q_1}{2}} C_{p_1(q_1-p_1)} \langle \mathcal{O}_p(x) \left[\mathcal{O}_{p_1}\mathcal{O}_{q_1-p_1}\right](x_1)\mathcal{O}_{q_2}(x_2)\rangle \tag{4.24}$$

$$+ \sum_{p_2=2}^{\frac{q_2}{2}} C_{p_2(q_2-p_2)} \langle \mathcal{O}_p(x)\mathcal{O}_{q_1}(x_1) \left[\mathcal{O}_{p_2}\mathcal{O}_{q_2-p_2}\right](x_2)\rangle \tag{4.25}$$

where $C_{(p_1p_2)}$ is the mixing coefficient between single-particle states and double-trace operators $T_{p_1}T_{p_2}$. (We have written its explicit form in appendix, see (A.5)).

The terms involving double-traces are equivalent to the four-point ME diagrams given in the previous section. Precisely in (4.18). We find,

$$\langle \mathcal{O}_p(x) \left[\mathcal{O}_{p_1}\mathcal{O}_{q_1-p_1}\right](x_1)\mathcal{O}_{q_2}(x_2)\rangle = q_2(q_2-1)p_1(q_1-p_1)\, g_{xx_1}^{q_1-2} g_{xx_2}^{q_2-2} g_{x_1x_2}^2 \langle \mathcal{O}_p\mathcal{O}_p\rangle \tag{4.26}$$

$$\langle \mathcal{O}_p(x)\mathcal{O}_{q_1}(x_1) \left[\mathcal{O}_{p_2}\mathcal{O}_{q_2-p_2}\right](x_2)\rangle = q_1(q_1-1)p_2(q_2-p_2)\, g_{xx_1}^{q_1-2} g_{xx_2}^{q_2-2} g_{x_1x_2}^2 \langle \mathcal{O}_p\mathcal{O}_p\rangle\,. \tag{4.27}$$

In each case there is only one term compared to (4.18) because there cannot be a bridge within $\left[\mathcal{O}_{p_1}\mathcal{O}_{q_1-p_1}\right](x_1)$ or $\left[\mathcal{O}_{p_2}\mathcal{O}_{q_2-p_2}\right](x_2)$.

The only unknown is therefore $\langle \mathcal{O}_p(x)T_{q_1}(x_1)T_{q_2}(x_2)\rangle$. This consists of diagrams with two propagators between T_{q_1} and T_{q_2} which always count $q_1(q_1-1)q_2(q_2-1)/2$ Wick contractions, according to the general results in appendix B (see (B.17)). However the net color factor has $2^2 = 1+1+2$ contributions for each arrangement of Wick contraction, depending on which part of the SU(N) propagator in (2.4) we consider, i.e. whether we use the U(N) part or the other one, $-\frac{1}{N}\delta_r^s\delta_t^u$, which we call the capping part.

If we consider the two Wick contraction between $T_{q_1}(x_1)T_{q_2}(x_2)$ but we use just the capping part since that caps on the matrix indexes on each end of the propagator, we find effectively a dumbbell diagram, which vanishes.

If we consider the two Wick contraction between $T_{q_1}(x_1)T_{q_2}(x_2)$ but we use just the U(N) propagator, we expect to produce effective operators of charge $q_1 + q_2 - 4$ labelled

JHEP11(2020)072

by partitions of 4. In SU(N), we find two, the single trace and a double trace. Consider now that *generically* we produce an effective double trace operator $[T_{q_1-2}T_{q_2-2}]$ and thus another dumbell diagram, which will vanish. We illustrate this mechanism with an example in double line notation,

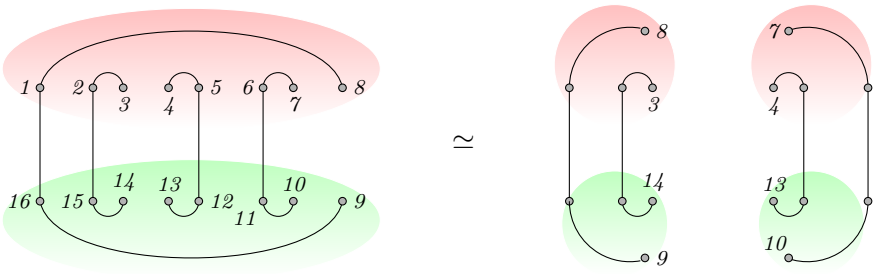

(4.28)

Instead, there are two ways of achieving a non vanishing result, in which the glued operator looks like the single-trace operator T_p. We can have U(N) propagators one adjacent to the other, then

$$\mathrm{Tr}(\underbrace{\ldots\phi_{ab}\phi_{bc}\ldots}_{q_1})\,\mathrm{Tr}(\underbrace{\ldots\phi_{de}\phi_{ef}\ldots}_{q_2})\delta^a_f\delta^e_b\delta^b_e\delta^d_c = N\,\mathrm{Tr}(\underbrace{\phi\ldots\phi}_{p})\,. \tag{4.29}$$

In this case only pq Wick contractions are non zero. Finally, we can take a connected and a disconnected part, resulting in

$$\mathrm{Tr}(\underbrace{\ldots\phi^a_b\ldots\phi^c_d\ldots}_{q_1})\,\mathrm{Tr}(\underbrace{\ldots\phi^e_f\ldots\phi^g_h\ldots}_{q_2})\Big(-\delta^a_h\delta^g_b\;\frac{1}{N}\delta^c_d\delta^e_f-\frac{1}{N}\delta^a_b\delta^g_h\;\delta^c_f\delta^e_d\Big) = -\frac{2}{N}\,\mathrm{Tr}(\underbrace{\phi\ldots\phi}_{p})\,. \tag{4.30}$$

Now, upon inputting (4.29) and (4.30) into a vev with $\mathcal{O}_p$ and using that $\langle T_p\mathcal{O}_p\rangle = \langle\mathcal{O}_p\mathcal{O}_p\rangle$ gives the final result,

$$\langle T_{q_1}T_{q_2}\mathcal{O}_p\rangle = q_1q_2\left[N-\frac{(q_1-1)(q_2-1)}{N}\right]\langle\mathcal{O}_p\mathcal{O}_p\rangle\;. \tag{4.31}$$

The computation above yields an explicit formula for the next-next-to-extremal three-point functions of single-particle operators

$$\begin{aligned}\langle\mathcal{O}_p(x)\mathcal{O}_{q_1}(x_1)\mathcal{O}_{q_2}(x_2)\rangle = \langle\mathcal{O}_p\mathcal{O}_p\rangle\Bigg[&q_1q_2\left[N-\frac{(q_1-1)(q_2-1)}{N}\right]\\ &+\sum_{p_1=2}^{\lfloor\frac{q_1}{2}\rfloor}C_{p_1(q_1-p_1)}q_2(q_2-1)p_1(q_1-p_1)\\ &+\sum_{p_2=2}^{\lfloor\frac{q_2}{2}\rfloor}C_{p_2(q_2-p_2)}q_1(q_1-1)p_2(q_2-p_2)\Bigg]\,.\end{aligned} \tag{4.32}$$

JHEP11(2020)072

The two sums are symmetric and can be performed with the explicit knowledge of $C_{p_1(q_1-p_1)}$ given in appendix (see (A.5)). We find

$$\sum_{p_1=2}^{\lfloor \frac{q_1}{2} \rfloor} C_{p_1(q_1-p_1)} p_1(q_1-p_1)$$
$$= \frac{q_1}{2N(q_1-2)} \left[2N^2 + (q_1-1)_2 N + 2(q_1-2)_2 + \frac{2(q_1-1)_2 N(N)_{q_1}}{(N-q_1+1)_{q_1} - (N)_{q_1}} \right] . \quad (4.33)$$

4.2.2 *n*-point functions

NME n-point functions can be obtained in a way similar to the three-point functions and in this section we sketch how the computation goes.

The definition of $k = \frac{1}{2}(-p + \sum q_i) = 2$ selects an operator $\mathcal{O}_p$, and we call the others "light". Start by expanding all these "light" operators in terms of the trace basis, and note that almost all terms in the expansion vanish since they produce correlators equivalent to near-extremal higher point diagrams. The result is the following generalisation of the three-point expansion in (4.23), namely

$$\langle \mathcal{O}_{q_1} \dots \mathcal{O}_{q_{n-1}} \mathcal{O}_p \rangle = \langle T_{q_1} \dots T_{q_{n-1}} \mathcal{O}_p(x_n) \rangle + \sum_{i=1}^{n-1} \sum_{p_i=2}^{\lfloor \frac{q_i}{2} \rfloor} C_{p_i(q_i-p_i)} \langle \mathcal{O}_{q_1} \dots \mathcal{O}_{q_{i-1}} [O_{p_i} \mathcal{O}_{q_i-p_i}] \mathcal{O}_{q_{i+1}} \dots \mathcal{O}_p(x_n) \rangle \ . \quad (4.34)$$

This equation can be thought of as a separate equation for each contributing Feynman diagram independently. Note that the correlators in the sum are all contributions to $n+1$-point N^{n-1}-extremal correlators which are maximally extremal and given in the previous section. The first term can then be computed by doing the partial Wick contractions $n-1$ in total on the singe trace operators $T_{p_1} \dots T_{p_{n-1}}$, only keeping the relevant terms just as in (4.29).

4.3 3-point functions as multi-particle 2-point functions

The work done in the previous sections has been to start from ME and NME three-point functions, compute them, and understand how to generalise the technique to n-points. In order to deal with the three-point functions we substituted two out of three SPOs with their corresponding expansion in the trace basis, and we reduced part of the job to compute a three point function with one single-particle and two traces. In this section instead we note an interesting feature of three-point function of SPO which does not require passing to the trace basis, and it is valid for any extremality. The relation works as follows,

$$\langle \mathcal{O}_p \mathcal{O}_q \mathcal{O}_r \rangle = \frac{1}{2^k k!} \langle [\mathcal{O}_p \mathcal{O}_q] \, [\mathcal{O}_r \overbrace{\mathcal{O}_2 \cdots \mathcal{O}_2}^{k}] \rangle_{\text{connected}}, \qquad p+q-r = 2k \ . \quad (4.35)$$

where the equality is for the color factor of the l.h.s. being the same as that of a two-point functions of multi-particle operators of SPOs on the r.h.s.

JHEP11(2020)072

Let us first illustrate the case $k = 3$ with the following picture,

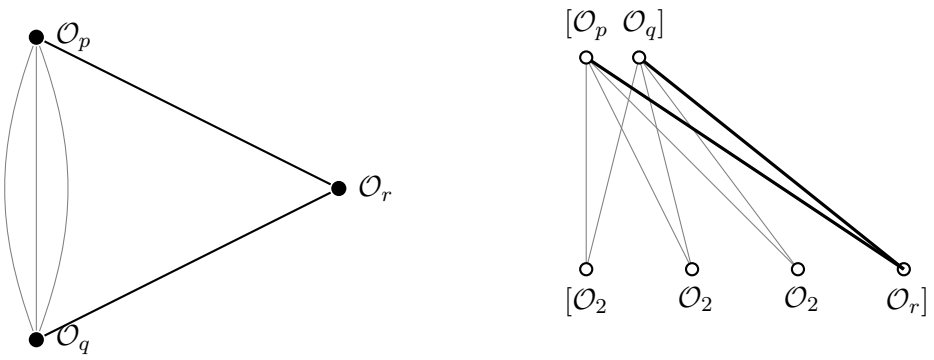

(4.36)

The diagram on the left is the single diagram contributing to $\langle \mathcal{O}_p \mathcal{O}_q \mathcal{O}_r \rangle$, whereas the one on the right is the only type of diagram contributing to $\langle [\mathcal{O}_p \mathcal{O}_q]\, [\mathcal{O}_r \mathcal{O}_2 \mathcal{O}_2 \mathcal{O}_2\,] \rangle$.

To show (4.35), consider where the two legs out of an $\mathcal{O}_2$ can end. They can not go to $\mathcal{O}_r$ as they are at the same point. If they both went to $\mathcal{O}_p$, this would result in a diagram of the form of a dumbbell in (3.1) (centered around $\mathcal{O}_p$) which thus vanishes. Similarly if both legs go to $\mathcal{O}_q$. The only exception to this is if p or q equals two in which case you can have a completely disconnected contribution - which also is absent since we specify the connected component. The only remaining possibility is then that one leg goes to $\mathcal{O}_p$ and one to $\mathcal{O}_q$ resulting in the diagram shown on the right. There are clearly $2^k k!$ different but equivalent diagrams of this sort, arising from the $k!$ possibilities of swapping the propagators from $\mathcal{O}_p$ to the $\mathcal{O}_2$s and from the cyclic symmetry around each $\mathcal{O}_2$.

The color factor of $\langle \mathcal{O}_p \mathcal{O}_q \mathcal{O}_r \rangle$ is the same of one of the equivalent configuration of $\langle [\mathcal{O}_p \mathcal{O}_q]\, [\mathcal{O}_r \mathcal{O}_2 \ldots \mathcal{O}_2\,] \rangle$ described above. This follows from the fact that

$$\phi_b^a \bullet\!\!-\!\!-\!\!\bullet\ \phi_d^c \ = \overbracket{\phi_b^a \phi_d^c} = \delta_d^a \delta_b^c - \frac{1}{N} \delta_b^a \delta_d^c,$$

$$\phi_b^a \overset{\mathcal{O}_2}{\bullet\!\!-\!\!\bullet\!\!-\!\!\bullet}\ \phi_d^c \ = \overbracket{\phi_b^a \phi_f^e} \overbracket{\phi_e^f \phi_d^c} = \delta_d^a \delta_b^c - \frac{1}{N} \delta_b^a \delta_d^c\,. \tag{4.37}$$

which conclude our proof of (4.35).[13]

While the right hand side of (4.35) is restricted to the connected part of the two point function (thinking of it as a limit of a higher point function), rather than the full two-point function, we need this distinction only when p or q equals 2 and $k = 1$, where instead we have

$$\langle \mathcal{O}_q \mathcal{O}_2 \mathcal{O}_q \rangle = \frac{1}{2} \left(\langle [\mathcal{O}_q \mathcal{O}_2]\, [\mathcal{O}_q \mathcal{O}_2] \rangle - \langle \mathcal{O}_q \mathcal{O}_q \rangle \langle \mathcal{O}_2 \mathcal{O}_2 \rangle \right). \tag{4.38}$$

Note that the condition giving the value of k in (4.35) is dependent on the order of $\mathcal{O}_p$, $\mathcal{O}_q$ and $\mathcal{O}_r$; in particular it distinguishes $\mathcal{O}_r$ from the other two operators. However the color factor of the three-point function *does not depend on this ordering.* For example,

[13] The ideas of our proof here can be generalised to multipoint correlators as well. For example those which are equivalent to the l.h.s. of (4.40).

JHEP11(2020)072

consider the three point function of $\mathcal{O}_3$, $\mathcal{O}_4$ and $\mathcal{O}_5$, we can have three multi-particle two-point functions with $k = 1, 2, 3$ respectively,

$$\begin{array}{ccccccc} \langle \mathcal{O}_3\mathcal{O}_4\mathcal{O}_5\rangle & = & \langle \mathcal{O}_3\mathcal{O}_5\mathcal{O}_4\rangle & = & \langle \mathcal{O}_4\mathcal{O}_5\mathcal{O}_3\rangle & = & \dfrac{60\prod_{i=1}^{4}(N^2-i^2)}{N(5+N^2)}\,. \\ \| & & \| & & \| & & \\ \dfrac{1}{2}\langle[\mathcal{O}_3\mathcal{O}_4]\,[\mathcal{O}_5\mathcal{O}_2]\rangle & & \dfrac{1}{8}\langle[\mathcal{O}_3\mathcal{O}_5]\,[\mathcal{O}_4\mathcal{O}_2\mathcal{O}_2]\rangle & & \dfrac{1}{48}\langle[\mathcal{O}_4\mathcal{O}_5]\,[\mathcal{O}_3\mathcal{O}_2\mathcal{O}_2\mathcal{O}_2]\rangle & & \end{array} \tag{4.39}$$

All three multi-particle two-point functions are then equal!.

We conclude that for a triplet of single-particle operators all multi-particle two-point functions which correspond to different dispositions of the three SPOs give the same color factor up to a multiplicity counted by $2^k k!$.

Also note that while the discussion above required $\mathcal{O}_p$ and $\mathcal{O}_q$ to be SPOs, it nowhere relied on $\mathcal{O}_r$ to be an SPO. Thus the following more general relation holds for any half-BPS operator $T_{r_1,\ldots,r_l}$:

$$\langle \mathcal{O}_p\mathcal{O}_q T_{r_1,\ldots,r_l}\rangle = \frac{1}{2^k k!}\langle[\mathcal{O}_p\mathcal{O}_q]\,[T_{r_1,\ldots,r_l}\overbrace{\mathcal{O}_2\cdots\mathcal{O}_2}^{k}]\rangle|_{\text{connected}}, \tag{4.40}$$

with $r_1 + \ldots + r_l = r$ and $p + q - r = 2k$.

4.4 On correlators with lower extremality

We understood how to classify free theory correlators according to their degree of extremality w.r.t. ME correlator. Lowering this degree increases the complexity of the computation. ME are the simplest non vanishing correlators and are computed in terms of tree graph. As function of the charges $p, q_{i=1,\ldots,n-1}$, the charge dependence is fully factorised for each tree graph, with the factor having a clean interpretation. NME showed more structure. We expect that NNME will have more, and so on so forth.

The complexity of NNME is already evident in the three-point functions. For example $\langle \mathcal{O}_p\mathcal{O}_{q_1}\mathcal{O}_{q_2}\rangle$ with $r = p + q - 6$ will have a contribution of the form $\langle \mathcal{O}_p T_{q_1} T_{q_2}\rangle$, with three bridges between T_{q_1} and T_{q_2}. We show few cases are

$$\langle \mathcal{O}_6 T_6 T_6\rangle = \left(300 + \frac{7200}{N^2} + 36N^2\right)\langle \mathcal{O}_6\mathcal{O}_6\rangle \tag{4.41}$$

$$\langle \mathcal{O}_7 T_7 T_6\rangle = \left(840 + \frac{12600}{N^2} + 42N^2\right)\langle \mathcal{O}_7\mathcal{O}_7\rangle \tag{4.42}$$

$$\langle \mathcal{O}_8 T_8 T_6\rangle = \left(1680 + \frac{20160}{N^2} + 48N^2\right)\langle \mathcal{O}_8\mathcal{O}_8\rangle \tag{4.43}$$

$$\langle \mathcal{O}_8 T_7 T_7\rangle = \left(1911 + \frac{22050}{N^2} + 49N^2\right)\langle \mathcal{O}_8\mathcal{O}_8\rangle \tag{4.44}$$

$$\langle \mathcal{O}_9 T_8 T_7\rangle = \left(3528 + \frac{35280}{N^2} + 56N^2\right)\langle \mathcal{O}_9\mathcal{O}_9\rangle \tag{4.45}$$

and we attach an ancillary file to show the reader how complicated are the correlators $\langle T_{\underline{p}} T_{q_1} T_{q_2}\rangle$ before we convert those to the single-particle operator $\mathcal{O}_p$. About (4.41)–(4.45), we can say a number of things based on the possible scenarios in double-line notation:

JHEP11(2020)072

(1) $O(1/N^2)$ contributions can only arise from picking the three SU(N) propagators in the configuration: two capping parts ($-\frac{1}{N}\delta^s_r\delta^u_t$) and a U($N$) part in (2.4). When the two capping parts are used we are left with $T_{q_1-2}(x_1)T_{q_2-2}(x_2)$ with no link in between. The U(N) propagator has the effect of producing an effective T_p operator.

(2) $O(1/N)$ contributions can only arise from picking the propagators in the configuration: one capping part and two U(N) parts, and these two U(N) propagators have to be generic, i.e. not consecutive. When the capping part is used, we reduce the number of legs to $T_{q_1-1}(x_1)T_{q_2-1}(x_2)$ with no link in between. When we attach the two U(N) propagators we are in a situation like NME (see (4.28)) and the result will vanish.

(3) $O(N)$ contributions can only arise from picking the propagators in the configuration: three U(N) parts, but two U(N) propagators have to be consecutive and one generic. The consecutive propagators produce a factor of N, reduce the number of legs to $T_{q_1-2}(x_1)T_{q_2-2}(x_2)$ and link the operators. Considering the other generic U(N) propagators we are again in a situation like NME (see (4.28)) and the result will vanish.

(4) $O(N^2)$ contributions can only arise from picking the propagators in the configuration: three U(N) parts, but all consecutive.

(5) $O(1)$ contributions can arise from two configurations: a) one capping part and two U(N) parts, but these two have to be consecutive. b) three U(N) parts, generic. Notice that a) is necessarily negative, whereas b) is positive.

The number of Wick contractions is $(q_1-2)_3(q_1-2)_3/3!$, and for each arrangement we have a multiplicity $2^3 = 1+1+3+3$, depending on the way we pick the propagators, i.e. whether we consider the U(N) or the capping part. It is clear that item (1) contributes fully, and item (4) contributes only with q_1q_2. Thus we have found

$$\langle \mathcal{O}_p T_{q_1} T_{q_2}\rangle = \left[q_1q_2N^2 + 3\times\frac{(q_1-2)_3(q_2-2)_3}{3!N^2} + \left(-\frac{1}{N}(Nc_a)+c_b\right)\right]\langle \mathcal{O}_p\mathcal{O}_p\rangle$$

where $c_a, c_b > 0$ and depend on the charges q_1 and q_2.[14]

It is not straightforward at this point to extract further information from the combinatorics, and in practise the dependence on the charges becomes hidden in the combinatorics. Nevertheless, the lesson we learn from our considerations about NNME three point function above is the surprising simplicity of the final result, that once more points to the possibility of understanding single-particle multipoint correlators in a way that eschews from a brute force computation. We hope to make this observation more concrete in the future.

5 The half-BPS OPE

In this section we illustrate an alternative approach to obtaining multi-point correlation functions, the half-BPS OPE, which among many interesting features offers a different

[14] A simple guess is $c_b - c_a = (q_1-1)_2(q_2-1)_2(\frac{1}{3}(q_1-5)(q_2-5) - \frac{1}{4}(q_1-6)(q_2-6))$.

JHEP11(2020)072

understanding of the colour dependence of the correlators. The idea of the half-BPS OPE is simply to bootstrap the free theory correlators by projecting it onto the half-BPS states.[15]

The half-BPS OPE follows directly from the full super OPE in $\mathcal{N}$=4 analytic superspace [28], and can be defined as the limit,

$$\lim_{x_1\to x_2} g_{12}^P\Big[\mathcal{O}_{p_1}(x_1)\mathcal{O}_{p_2}(x_2)\Big] = \sum_{\underline{t}\vdash t} C^{\underline{t}}_{p_1p_2}\ \mathcal{O}_{\underline{t}}(x_2), \qquad t = p_1+p_2-2P. \tag{5.1}$$

The symbol $g_{12}^P[\mathcal{O}_{p_1}(x_1)\mathcal{O}_{p_2}(x_2)]$ specifies that out of the full super OPE on the l.h.s. we are picking the term with Y dependence of the form Y_{12}^{2P}.[16] The result on the r.h.s. is intuitive, what happens is that by fusing the P bridges between $\mathcal{O}_{p_1}$ and $\mathcal{O}_{p_2}$, we find an expansion over the half-BPS operators with $t = p_1+p_2-2P$ legs, i.e. t is the twist of the operator. We refer to this projection as the 'half-BPS OPE at twist t'.

One can pick any basis of half-BPS operators to express the r.h.s. of (5.1). For definiteness we have written it in terms of the basis generated by products of SPOs, $\mathcal{O}_{\underline{t}} = [\mathcal{O}_{t_1}\dots\mathcal{O}_{t_m}]$ where $\underline{t} = (t_1,\dots,t_m)$ is a partition of t.

The coefficients $C^{\underline{t}}_{p_1p_2}$ can be related more precisely to three-point functions, by taking the vev with other half BPS operators. We first find

$$\langle \mathcal{O}_{p_1}\mathcal{O}_{p_2}\mathcal{O}_{\underline{t}'}\rangle = \sum_{\underline{t}\vdash t} C^{\underline{t}}_{p_1p_2} g_{\underline{t}\underline{t}'}\,, \tag{5.2}$$

where g is the matrix of two-point functions of half-BPS operators of twist t,

$$g_{\underline{t}\underline{t}'} = \langle \mathcal{O}_{\underline{t}}\mathcal{O}_{\underline{t}'}\rangle\,. \tag{5.3}$$

Inverting (5.2) as a vector equation we obtain

$$C^{\underline{t}}_{p_1p_2} = \sum_{\underline{t}'\vdash t}\langle \mathcal{O}_{p_1}\mathcal{O}_{p_2}\mathcal{O}_{\underline{t}'}\rangle (g^{-1})_{\underline{t}'\underline{t}}\,. \tag{5.4}$$

Free theory correlators decompose into propagator structures: if we arrange the operators at the corners of a square and as usual we draw a line between point i and point j to represent a propagator g_{ij}, we can in fact represent the correlator as a sum over all possible propagator structures,

$$\langle \mathcal{O}_{p_1}\dots\mathcal{O}_{p_n}\rangle = \sum_{\{b_{ij}\}} \alpha_{\{b_{ij}\}} \prod_{i<j} g_{ij}^{b_{ij}}\,, \qquad \sum_{i\neq j} b_{ij} = p_i\,, \quad b_{ji} = b_{ij}\,, \quad b_{ii} = 0\,. \tag{5.5}$$

The color factors $\alpha_{\{b_{ij}\}}$ can in principle be computed by Wick contractions. However, a brute force computation is quite expensive, since the single particle operators are admixture of single and multi-trace operators. Therefore intermediate steps are cumbersome. Nevertheless, we already saw for the NNME three-point functions in section 4.4 that the final result is much simpler than the intermediate steps. Thus, the idea of the half-BPS OPE is to constrain the $\alpha_{\{b_{ij}\}}$ and compute them by using the consistency of the general

[15] This approach has been pursued also in [27] at order $1/N^2$.

[16] Multiplying by X_{12}^{2P} we can take $X_1 \to X_2$, and this limit will now project on $\mathcal{O}_{\underline{t}}$

JHEP11(2020)072

OPE, projected onto the simpler sector of half-BPS operators. To illustrate the power and simplicity of this procedure we will now consider four-point functions $\langle \mathcal{O}_{p_1}\mathcal{O}_{p_2}\mathcal{O}_{p_3}\mathcal{O}_{p_4}\rangle$.

In the following analysis we will always take p_4 to be the largest charge. We have three 'channels' to perform the OPE, depending on which operator $\mathcal{O}_{p_{i=1,2,3}}$ we bring close to $\mathcal{O}_{p_4}$. Schematically, (12) $\leftrightarrow$ (34), (23) $\leftrightarrow$ (14) and (13) $\leftrightarrow$ (24). Let us consider the first channel, for illustration. The reasoning will be similar for the others.

If we perform the half-BPS OPE $(\mathcal{O}_{p_1} \times \mathcal{O}_{p_2})$ we find the twist t to lie in the range $max(|p_{12}|, |p_{43}|) \leq t \leq min(p_1 + p_2, p_3 + p_4)$, where $p_{ij} \equiv p_i - p_j$ throughout this section. The extrema are special, and will be discussed separately. For any other value of t in $max(|p_{12}|, |p_{43}|) < t < min(p_1 + p_2, p_3 + p_4)$, we obtain a relation for a linear combination of the coefficients α, of the form

$$\sum_{b_{12}+b_{13}+b_{23}+b_{24}=t} \alpha_{\{b_{ij}\}} = \sum_{\underline{t},\underline{t}' \vdash t} \langle \mathcal{O}_{p_1}\mathcal{O}_{p_2}\mathcal{O}_{\underline{t}}\rangle (g^{-1})_{\underline{t}\underline{t}'} \langle \mathcal{O}_{\underline{t}'}\mathcal{O}_{p_3}\mathcal{O}_{p_4}\rangle \,. \tag{5.6}$$

The sum on the l.h.s. above is specified by the condition $b_{12} + b_{13} + b_{23} + b_{24} = t$ so that it involves only diagrams with t propagators between the pair $(\mathcal{O}_{p_1}, \mathcal{O}_{p_2})$ and the pair $(\mathcal{O}_{p_3}, \mathcal{O}_{p_4})$.

A feature of using the basis generated by products of SPOs is that the single-particle space is orthogonal to the multiparticle sector (by the definition of SPOs). Therefore the r.h.s of (5.6) can be split into a single particle contribution and a multiparticle contribution,

$$\sum_{b_{12}+b_{13}+b_{23}+b_{24}=t} \alpha_{\{b_{ij}\}} = \langle \mathcal{O}_{p_1}\mathcal{O}_{p_2}\mathcal{O}_{t}\rangle \langle \mathcal{O}_{t}\mathcal{O}_{t}\rangle^{-1} \langle \mathcal{O}_{t}\mathcal{O}_{p_3}\mathcal{O}_{p_4}\rangle \tag{5.7}$$

$$+ \sum_{\underline{t},\underline{t}' \vdash t} \langle \mathcal{O}_{p_1}\mathcal{O}_{p_2}\mathcal{K}_{\underline{t}}\rangle (\tilde{g}^{-1})_{\underline{t}\underline{t}'} \langle \mathcal{K}_{\underline{t}'}\mathcal{O}_{p_3}\mathcal{O}_{p_4}\rangle \,. \tag{5.8}$$

Here the sum in the second term is over only partitions $\underline{t}, \underline{t}'$ of length at least two. We use the notation $\mathcal{K}$ to emphasise that there is always more than one factor in the operator $\mathcal{K}_{\underline{t}} = [\mathcal{O}_{t_1} \dots \mathcal{O}_{t_m}]$, i.e. $(m \geq 2)$ and we write $\tilde{g}_{\underline{t}\underline{t}'} = \langle \mathcal{K}_{\underline{t}}\mathcal{K}_{\underline{t}'}\rangle$ for the metric projected on the multi-particle sector.

Referring to (5.7) and (5.8), we can appreciate that considering the lowest possible twist, i.e. $t = max(|p_{12}|, |p_{43}|) > 0$, we find in any case extremal three point functions, which vanish according to our general discussion in section 3.2. For the highest value instead, $t = min(p_1 + p_2, p_3 + p_4)$, we find that (5.7) is again extremal, thus vanishing, but (5.8) instead gives a sum over three point functions with multi-particle states. However, these three-point functions are of the same kind of the original four-point function we want to bootstrap, therefore do not lead to useful constraints. Rather, we will show that can be used to obtain multi-particle two-point functions.

5.1 N^{2}E correlators

Let us fix ideas by re-considering the simplest ME four-point functions first addressed in section 4.1. These are the next-to-next-to-extremal (N^{2}E) correlators, and obey,

$$s = p + q + r - 4 \,, \tag{5.9}$$

JHEP11(2020)072

where we always take s to be the largest charge. The condition (5.9) implies that all but two propagators are connected to $\mathcal{O}_s$, leaving six possible topologies which can contribute to the correlator, depicted below

$$\langle \mathcal{O}_p \mathcal{O}_q \mathcal{O}_r \mathcal{O}_s \rangle = \alpha_1 + \alpha_2 + \alpha_3 + \tilde{\alpha}_1 + \tilde{\alpha}_2 + \tilde{\alpha}_3 \,. \tag{5.10}$$

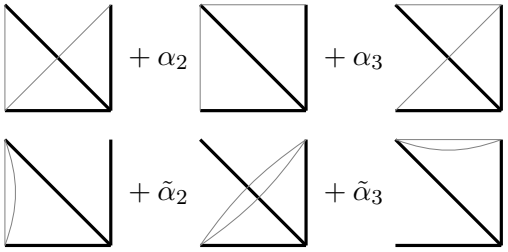

The operator $\mathcal{O}_s$ sits at right corner on the bottom of each square. Here the thin lines correspond to single propagators not connected to $\mathcal{O}_s$ whereas the thick lines represent multiple propagators (as many as needed to match the charges p, q, r, s).

Let us consider the half-BPS OPE $(\mathcal{O}_p \times \mathcal{O}_q)$ at twist $t = (p+q-4)$. This means we project onto the Y dependence Y_{12}^P with $P = 2$. The only surviving diagram is the first one on the second line of (5.10) and we obtain the following equation,

$$\tilde{\alpha}_1 = \sum_{\underline{t},\underline{t}' \vdash t} \langle \mathcal{O}_p \mathcal{O}_q \mathcal{O}_{\underline{t}} \rangle (g^{-1})_{\underline{t}\underline{t}'} \langle \mathcal{O}_{\underline{t}'} \mathcal{O}_r \mathcal{O}_s \rangle \,. \tag{5.11}$$

If $t > 0$, the three-point functions $\langle \mathcal{O}_{\underline{t}'} \mathcal{O}_r \mathcal{O}_s \rangle$ all vanish. This is because $\mathcal{O}_s$ is a SPO of charge $s = p+q+r-4 = t+r$ and the three-point function is therefore extremal. We conclude $\tilde{\alpha_1} = 0$ and a similar analysis of the $(\mathcal{O}_p \times \mathcal{O}_r)$ and $(\mathcal{O}_q \times \mathcal{O}_r)$ OPEs reveals that also $\tilde{\alpha}_2 = \tilde{\alpha}_3 = 0$. This same conclusion was already reached in [11] where we argued that free theory propagator topologies in all SPO four-point functions are absent when one of the operators is only connected to one other. The assumption $t > 0$ excludes the identity operator, and implies that the diagrams we considered are connected.

Now let us perform the half-BPS OPE $(\mathcal{O}_p \times \mathcal{O}_q)$ at twist $t = (p+q-2)$. We have to project the Y dependence onto Y_{12}^P with $P = 1$, giving us

$$\alpha_1 + \alpha_2 = \langle \mathcal{O}_p \mathcal{O}_q \mathcal{O}_t \rangle \langle \mathcal{O}_t \mathcal{O}_t \rangle^{-1} \langle \mathcal{O}_t \mathcal{O}_r \mathcal{O}_s \rangle \,. \tag{5.12}$$

In the second equality we have used the fact that the three-point functions $\langle \mathcal{K}_{\underline{t}} \mathcal{O}_r \mathcal{O}_s \rangle$ can be splitted at least on four-point auxiliary points with $k = s-r-(p+q+2) = 1$. It follows that such three-point functions are near-extremal and vanish according to the discussion in section 3.2.1. Using our previous computation for $\langle \mathcal{O}_t \mathcal{O}_r \mathcal{O}_s \rangle$ (see (4.8)) we arrive at

$$\alpha_1 + \alpha_2 = pqr(p+q-2) \langle \mathcal{O}_s \mathcal{O}_s \rangle \,. \tag{5.13}$$

Repeating the analysis above in the other two OPE channels we obtain two more similar equations with the unique solution

$$\alpha_1 = pqr(p-1)\langle \mathcal{O}_s \mathcal{O}_s \rangle, \quad \alpha_2 = pqr(q-1)\langle \mathcal{O}_s \mathcal{O}_s \rangle, \quad \alpha_3 = pqr(r-1)\langle \mathcal{O}_s \mathcal{O}_s \rangle \,. \tag{5.14}$$

This is exactly the same solution we derived in equation (4.18) with different means.

JHEP11(2020)072

As we anticipated, performing the half-BPS OPE at twist $t = p + q$ does not yield further constraints on the coefficients α_i. Instead we obtain the relation

$$\alpha_3 + \langle \mathcal{O}_p \mathcal{O}_r \rangle \langle \mathcal{O}_q \mathcal{O}_s \rangle + \langle \mathcal{O}_p \mathcal{O}_s \rangle \langle \mathcal{O}_q \mathcal{O}_r \rangle = \sum_{\underline{t},\underline{t}' \vdash t} \langle \mathcal{O}_p \mathcal{O}_q \mathcal{K}_{\underline{t}} \rangle (\tilde{g}^{-1})_{\underline{t}\underline{t}'} \langle \mathcal{K}_{\underline{t}'} \mathcal{O}_r \mathcal{O}_s \rangle \,. \tag{5.15}$$

On the l.h.s. we have been careful to include the disconnected contributions that can be present. The contribution $\langle \mathcal{O}_p \mathcal{O}_q \mathcal{O}_t \rangle$ is extremal and vanishing, thus only multi-particles exchanged appear in the second equality above. Moreover, from the fact that there are no bridges between $\mathcal{O}_p$ and $\mathcal{O}_q$ due to extremality, we find that the three point function $\langle \mathcal{O}_p \mathcal{O}_q \mathcal{K}_{\underline{t}} \rangle$ is equal to the two-point function $\langle [\mathcal{O}_p \mathcal{O}_q] \mathcal{K}_{\underline{t}} \rangle = \tilde{g}_{(p,q),\underline{t}}$. The r.h.s. above thus simplifies and we obtain

$$\alpha_3 + \langle \mathcal{O}_p \mathcal{O}_r \rangle \langle \mathcal{O}_q \mathcal{O}_s \rangle + \langle \mathcal{O}_p \mathcal{O}_s \rangle \langle \mathcal{O}_q \mathcal{O}_r \rangle = \langle [\mathcal{O}_p \mathcal{O}_q] \mathcal{O}_r \mathcal{O}_s \rangle . \tag{5.16}$$

This is equivalent to taking the coincidence limit $x_1 \to x_2$ on the original four-point function $\langle \mathcal{O}_p \mathcal{O}_q \mathcal{O}_r \mathcal{O}_s \rangle$ which yields immediately

$$\langle [\mathcal{O}_p \mathcal{O}_q] \mathcal{O}_r \mathcal{O}_s \rangle = pqr(r-1) \langle \mathcal{O}_s \mathcal{O}_s \rangle + \langle \mathcal{O}_p \mathcal{O}_r \rangle \langle \mathcal{O}_q \mathcal{O}_s \rangle + \langle \mathcal{O}_p \mathcal{O}_s \rangle \langle \mathcal{O}_q \mathcal{O}_r \rangle \,. \tag{5.17}$$

where $s = p + q + r - 4$ as before and we have used the derived result (5.14) for α_3. The other coincidence limit $x_3 \to x_4$ gives us

$$\langle \mathcal{O}_p \mathcal{O}_q [\mathcal{O}_r \mathcal{O}_s] \rangle = \delta_{2r} 2pq \langle \mathcal{O}_s \mathcal{O}_s \rangle + \langle \mathcal{O}_p \mathcal{O}_r \rangle \langle \mathcal{O}_q \mathcal{O}_s \rangle + \langle \mathcal{O}_p \mathcal{O}_s \rangle \langle \mathcal{O}_q \mathcal{O}_r \rangle \,. \tag{5.18}$$

The connected part only contributes for $r = 2$. The double coincidence limit ($x_1 \to x_2, x_3 \to x_4$) then gives two-point functions of product operators.

$$\langle [\mathcal{O}_p \mathcal{O}_q] [\mathcal{O}_r \mathcal{O}_s] \rangle = \delta_{2r} 2pq \langle \mathcal{O}_s \mathcal{O}_s \rangle + \langle \mathcal{O}_p \mathcal{O}_r \rangle \langle \mathcal{O}_q \mathcal{O}_s \rangle + \langle \mathcal{O}_p \mathcal{O}_s \rangle \langle \mathcal{O}_q \mathcal{O}_r \rangle \,. \tag{5.19}$$

The case of $\langle \mathcal{O}_2 \mathcal{O}_q \mathcal{O}_r \mathcal{O}_s \rangle$. At four points, whenever one of the charges takes (the smallest possible) value $p = 2$, the correlator contributes to a single $su(4)$ representation in each OPE channel. Such four-point functions are also called next-to-next-to extremal, and in principle have six propagator structures. Here we focus on the three topologies shown below,

$$\langle \mathcal{O}_2 \mathcal{O}_q \mathcal{O}_r \mathcal{O}_s \rangle_c = \alpha_1$$  $$+ \alpha_2$$ 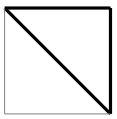 $$+ \alpha_3$$  . (5.20)

Diagrams where one of the operators is connected to only one are omitted, since the color factor vanish by exactly the same arguments as above. We also omit cases in which diagrams are disconnected.

Performing the half BPS OPE ($\mathcal{O}_2 \times \mathcal{O}_q$) at twist q gives

$$\alpha_1 + \alpha_2 = \frac{\langle \mathcal{O}_2 \mathcal{O}_q \mathcal{O}_q \rangle \langle \mathcal{O}_q \mathcal{O}_r \mathcal{O}_s \rangle}{\langle \mathcal{O}_q \mathcal{O}_q \rangle} = 2q \langle \mathcal{O}_q \mathcal{O}_r \mathcal{O}_s \rangle \,, \tag{5.21}$$

JHEP11(2020)072

where we simplified the result using our previous results for maximally extremal three-point functions. Again we obtain two similar equations from the other crossing channels and finally we arrive at

$$\begin{aligned}\alpha_1 &= (q+r-s)\langle \mathcal{O}_q \mathcal{O}_r \mathcal{O}_s\rangle\,,\\ \alpha_2 &= (q+s-r)\langle \mathcal{O}_q \mathcal{O}_r \mathcal{O}_s\rangle\,,\\ \alpha_3 &= (r+s-q)\langle \mathcal{O}_q \mathcal{O}_r \mathcal{O}_s\rangle\,.\end{aligned} \tag{5.22}$$

Note that setting $s = q+r-2$ above we find agreement with (5.14) in the case $p = 2$. The coincidence limit $x_1 \to x_2$ then gives three-point functions involving products of single-particle operators,

$$\langle [\mathcal{O}_2\mathcal{O}_q]\mathcal{O}_r\mathcal{O}_s\rangle = (r+s-q)\langle \mathcal{O}_q\mathcal{O}_r\mathcal{O}_s\rangle + \langle \mathcal{O}_2\mathcal{O}_r\rangle\langle \mathcal{O}_q\mathcal{O}_s\rangle + \langle \mathcal{O}_2\mathcal{O}_s\rangle\langle \mathcal{O}_q\mathcal{O}_r\rangle\,. \tag{5.23}$$

5.2 N^{3}E correlators

Let us now consider N^3-extremal 4-point functions where $s = p+q+r-6$. We focus on the seven connected diagrams (out of ten) depicted below,

$\langle \mathcal{O}_p\mathcal{O}_q\mathcal{O}_r\mathcal{O}_s\rangle_c =$ α_1 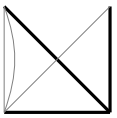 $+\alpha_2$ 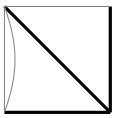 $+\alpha_3$ 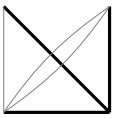 $+\alpha_4$ 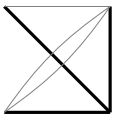

$+\alpha_5$ 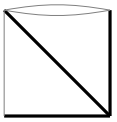 $+\alpha_6$ 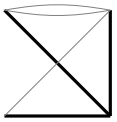 $+\alpha_7$ 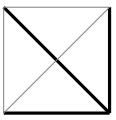 . (5.24)

Again, we are omitting three diagrams where one operator is connected to only one other, which would vanish. Recall that the operator $\mathcal{O}_s$ sits at the right corner on the bottom of each square.

Performing the half-BPS OPE $(\mathcal{O}_p \times \mathcal{O}_q)$ at twist $t = p+q-4$, i.e. by projection onto Y_{12}^P with $P = 2$, yields

$$\alpha_1+\alpha_2 = \frac{\langle \mathcal{O}_p\mathcal{O}_q\mathcal{O}_{p+q-4}\rangle\,\langle \mathcal{O}_{p+q-4}\mathcal{O}_r\mathcal{O}_s\rangle}{\langle \mathcal{O}_{p+q-4}\mathcal{O}_{p+q-4}\rangle} = (p+q-4)r\frac{\langle \mathcal{O}_p\mathcal{O}_q\mathcal{O}_{p+q-4}\rangle}{\langle \mathcal{O}_{p+q-4}\mathcal{O}_{p+q-4}\rangle}\,\langle \mathcal{O}_s\mathcal{O}_s\rangle\,. \tag{5.25}$$

The multi-particle term vanishes by extremality and the contribution $\langle \mathcal{O}_{p+q-4}\mathcal{O}_r\mathcal{O}_s\rangle$ is ME, thus it simplifies to give the second equality above. We obtain two similar equations from the other OPEs $(\mathcal{O}_p \times \mathcal{O}_r)$ and $(\mathcal{O}_q \times \mathcal{O}_r)$. These only involve the pairs $\alpha_3+\alpha_4$ and $\alpha_5+\alpha_6$. The color factor α_7 does not enter any of these constraints.

From the OPE $(\mathcal{O}_p \times \mathcal{O}_q)$ at twist $t = p+q-2$ we obtain

$$\alpha_3+\alpha_5+\alpha_7 = pq\,\langle \mathcal{O}_{p+q-2}\mathcal{O}_r\mathcal{O}_s\rangle + \sum_{\underline{t},\underline{t}'\vdash t}\langle \mathcal{O}_p\mathcal{O}_q\mathcal{K}_{\underline{t}}\rangle\,(\tilde{g}^{-1})_{\underline{t}\underline{t}'}\,\langle \mathcal{K}_{\underline{t}'}\mathcal{O}_r\mathcal{O}_s\rangle\,. \tag{5.26}$$

In general both single-particle and multi-particle terms contribute. The multi-particle contribution have more structure than previous cases, but let us note that the three-point

JHEP11(2020)072

function $\langle \mathcal{K}_{\underline{t}'} \mathcal{O}_r \mathcal{O}_s \rangle$ is only non-zero if $\mathcal{K}_{\underline{t}'} = [\mathcal{O}_{t'_1} \mathcal{O}_{t-t'_1}]$, namely a product of two single-particle operators. A contribution with more than two single-particle operators can be understood as a near-extremal five-point function and vanishes according to the discussion in section 3.2.1. Then, we are in a favourable position since the three point function $\langle [\mathcal{O}_{t'_1} \mathcal{O}_{t-t'_1}] \mathcal{O}_r \mathcal{O}_s \rangle$ can be computed as the coincidence limit of the N^{2}E four-point functions described in (5.17). In particular,

$$\langle \mathcal{K}_{\underline{t}'} \mathcal{O}_r \mathcal{O}_s \rangle = \langle [\mathcal{O}_{t'_1} \mathcal{O}_{t-t'_1}] \mathcal{O}_r \mathcal{O}_s \rangle = t'_1 (t - t'_1) r (r-1) \langle \mathcal{O}_s \mathcal{O}_s \rangle \,. \tag{5.27}$$

We obtain two similar equations from the other OPEs $(\mathcal{O}_p \times \mathcal{O}_r)$ and $(\mathcal{O}_q \times \mathcal{O}_r)$. These involve $\alpha_2 + \alpha_4$ with α_7, and, $\alpha_1 + \alpha_6$ with α_7.

In total we have six equations with particular structure. If we consider the last three equations that we derived, and we subtract the first three equation, we obtain a single equation for $3\alpha_7$. Thus we determine α_7 completely,

$$\begin{aligned} \alpha_7 = \frac{1}{3} \Bigg(& pq \, \langle \mathcal{O}_{p+q-2} \mathcal{O}_r \mathcal{O}_s \rangle + \sum_{\underline{t}, \underline{t}' \vdash t} \langle \mathcal{O}_p \mathcal{O}_q \mathcal{K}_{\underline{t}} \rangle \, (\tilde{g}^{-1})_{\underline{t}\underline{t}'} \, \langle \mathcal{K}_{\underline{t}'} \mathcal{O}_r \mathcal{O}_s \rangle \\ & - (p+q-4) r \frac{\langle \mathcal{O}_p \mathcal{O}_q \mathcal{O}_{p+q-4} \rangle}{\langle \mathcal{O}_{p+q-4} \mathcal{O}_{p+q-4} \rangle} \langle \mathcal{O}_s \mathcal{O}_s \rangle \Bigg) + \text{ cyc}(p,q,r) \,. \end{aligned} \tag{5.28}$$

The remaining equations determine five of the remaining coefficients in terms of one remaining, α_1 say. In specific cases additional conditions can come from crossing symmetry constraints. In appendix D we discuss various examples with different degree of crossing symmetry.

In all examples discussed in appendix D, the coefficients $\alpha_1, \ldots, \alpha_6$ are consistent with the following solution

$$\begin{aligned} &\alpha_1 = F(p,q,r) \, \langle \mathcal{O}_s \mathcal{O}_s \rangle \,, \quad \alpha_2 = F(q,p,r) \, \langle \mathcal{O}_s \mathcal{O}_s \rangle \,, \quad \alpha_3 = F(p,r,q) \, \langle \mathcal{O}_s \mathcal{O}_s \rangle \,, \\ &\alpha_4 = F(r,p,q) \, \langle \mathcal{O}_s \mathcal{O}_s \rangle \,, \quad \alpha_5 = F(q,r,p) \, \langle \mathcal{O}_s \mathcal{O}_s \rangle \,, \quad \alpha_6 = F(r,q,p) \, \langle \mathcal{O}_s \mathcal{O}_s \rangle \,, \end{aligned} \tag{5.29}$$

where

$$F(p,q,r) = (p-2) r \frac{\langle \mathcal{O}_p \mathcal{O}_q \mathcal{O}_{p+q-4} \rangle}{\langle \mathcal{O}_{p+q-4} \mathcal{O}_{p+q-4} \rangle} \,. \tag{5.30}$$

The bootstrap problem allows the deformation $F(p,q,r) \to F(p,q,r) + \tilde{F}(p,q,r)$, where $\tilde{F}(p,q,r)$ is totally antisymmetric and unconstrained. In all cases we studied we have found that the deformation $\tilde{F} = 0$.[17]

6 Conclusions

We have considered a new basis of half-BPS operators in $\mathcal{N}$=4 SYM, namely the single particle operators (and products of these). These are the natural duals to single-particle supergravity states on $AdS_5 \times S^5$. In particular we have seen that they naturally interpolate

[17] If we consider the correlators $\langle T_p T_q T_r \mathcal{O}_s \rangle$ instead of $\langle \mathcal{O}_p \mathcal{O}_q \mathcal{O}_r \mathcal{O}_s \rangle$ we find that all coefficients are a simple Laurent polynomial in N multiplied by $\langle \mathcal{O}_s \mathcal{O}_s \rangle$. For example, from the results presented in appendix D with $p = 3 \leq q \leq r$ we can see that $\alpha_7 = 6qr(N - 3(q-1)(r-1)/N)$.

JHEP11(2020)072

between point-like gravitons and giant gravitons, as they should. We have also considered the free theory, all N, correlators of these operators. Interestingly, all near extremal correlators of SPOs, namely n-point correlators with extremality degree strictly less than $n-2$, vanish, and this is presumably tied to the conjecture in [18] that the corresponding supergravity couplings vanish. Going away from this case, we studied maximally extrema correlators, which have a very simple form, then we considered next-to-maximally extremal correlators. The complexity increases by lowering the extremality, but even in such a case we have found additional simplicity, compared to the single-trace correlators.

It is interesting to revisit past discussions involving half-BPS operators, especially concerning large N limits and the relation to string theory computations via AdS/CFT, in the light of our new basis of SPOs. As we have seen in section 2.3 the SPOs correctly interpolate between single trace operators and the operators conjectured to be dual to S^5 giant graviton operators. In [29] the half-BPS three-point functions of two giant graviton operators and one point-like graviton was performed and compared with the analogous computation in gauge theory. The gauge theory was computed using two large Schur polynomial operators and one single trace operator. The results were found to not quite agree and it was conjectured this was to do with the inability of the Schur polynomials to correctly interpolate between giant and point-like gravitons. The SPOs on the other hand do precisely interpolate between the two as show in section 2.3. On the other hand,the extremal correlators of SPOs simply vanish! In [30] this issue was revisited and it was argued that indeed there were subtleties in the extremal case which are not present in the N-extremal case. The NE with two giant gravitons and one point-like graviton were computed in gauge theory (using Schur polynomials for the giant gravitons and single trace operators for the pointlike operator) as well as in string theory and this time found agreement. Since we have explicit formulae for the NE 3-point functions we can check this agrees here also.

We start with the next-to-extremal three-point function of unit normalised single particle operators. From (4.8) we have

$$\frac{\langle \mathcal{O}_p \mathcal{O}_q \mathcal{O}_r \rangle}{\sqrt{\langle \mathcal{O}_p \mathcal{O}_p \rangle \langle \mathcal{O}_q \mathcal{O}_q \rangle \langle \mathcal{O}_r \mathcal{O}_r \rangle}} = pq \sqrt{\frac{\langle \mathcal{O}_r \mathcal{O}_r \rangle}{\langle \mathcal{O}_p \mathcal{O}_p \rangle \langle \mathcal{O}_q \mathcal{O}_q \rangle}}, \quad p+q=r+2. \tag{6.1}$$

Now consider the limit $N \to \infty$ with p staying finite, but $q, r \to \infty$ such that $q' = q/N, r' = r/N$ are fixed. Taking the appropriate limits of the two point functions (2.62) we find

$$\frac{\langle \mathcal{O}_p \mathcal{O}_q \mathcal{O}_r \rangle}{\sqrt{\langle \mathcal{O}_p \mathcal{O}_p \rangle \langle \mathcal{O}_q \mathcal{O}_q \rangle \langle \mathcal{O}_r \mathcal{O}_r \rangle}} \to \sqrt{p} \frac{r}{N} \left(1 - \frac{r}{N}\right)^{\frac{p-2}{2}}, \quad p+q=r+2 \tag{6.2}$$

which is in precise agreement with [30].

We can also compute the normalised next-to-next-to-extremal three-point function given by (4.32)–(4.33) in the same limit, $N \to \infty$ with $p, q' = q/N, r' = r/N$ fixed

$$\frac{\langle \mathcal{O}_p \mathcal{O}_q \mathcal{O}_r \rangle}{\sqrt{\langle \mathcal{O}_p \mathcal{O}_p \rangle \langle \mathcal{O}_q \mathcal{O}_q \rangle \langle \mathcal{O}_r \mathcal{O}_r \rangle}} \to \sqrt{p} \frac{r}{N} \left(1 - \frac{r}{N}\right)^{\frac{p-4}{2}} \left(1 - \frac{(p-1)r}{2N}\right), \quad p+q=r+4. \tag{6.3}$$

It would be interesting to compare with the corresponding string theory computation.

JHEP11(2020)072

There are a number of further avenues one could go down from here. Firstly one could try to generalise our story beyond the half-BPS sector. Bases for more general operators in $\mathcal{N} = 4$ SYM have been given, for example [32–38] and it would be interesting to look again at these from the perspective of single-particle operators.

The same definition of SPOs presumably holds also for orthogonal and symplectic gauge groups in $\mathcal{N} = 4$ SYM which can be obtained via a $\mathbb{Z}_2$ orientifold projection of the standard $AdS_5 \times S^5$ setup [39]. Half-BPS operators in these theories have been studied in [40–43] and it would be interesting to consider single-particle operators in that context. It would also be interesting to study-single particle states for other AdS$\times S$ backgrounds, for example in AdS_3, as it was pointed out in [44], ABJM, and for the mysterious six-dimensional (2,0) theory on $AdS_7 \times S^4$.

Finally, it would be very interesting to consider aspects of the dynamics of the single-particle operators that have not been explored yet, and go beyond the computation of the one-loop amplitudes in [4], along the lines suggested in [53]. For instance, the trace basis is widely used in the context of integrability and in turn integrability based techniques allow the computation of exact correlators. The simplest four-point correlator one could study, i.e. the octagon configuration of [45],[18] was firstly obtained by using hexagonalization from weak coupling, and later re-derived in other beautiful ways [46–49]. From the OPE point of view at weak coupling, many properties of the correlators are due to single-trace stringy states acquiring an anomalous dimension with universal features. This mechanism is quite democratic and perhaps the distinction between single-traces and single-particle external states does not matter at weak coupling. On the other hand, the situation in the supergravity regime is quite different, and the half-BPS single-particle operators are properly the dual of the KK modes, beyond the planar limit. It would be very interesting to understand how integrability based techniques [50, 51] modify or adapt when correlators of single-particle operators are considered.

Acknowledgments

FA would like to thank Pedro Vieira, Frank Coronado, and Till Bargheer for stimulating discussions. We also thank an anonymous referee for providing valuable insights. FA is partially supported by the ERC-STG grant 637844- HBQFTNCER. FS is supported by the Italian Ministry of Research under grant PRIN 20172LNEEZ and by the INFN under GRANT73/CALAT. JD, HP were supported in part by the ERC Consolidator grant 648630 IQFT. MS is supported by a Mayflower studentship from the University of Southampton. AS is supported by an STFC studentship and PH acknowledges support from STFC grant ST/P000371/1 and the European Union's Horizon 2020 research and innovation programme under the Marie Skłodowska-Curie grant agreement No. 764850 "SAGEX".

[18] See [52] for a five-point analog, called the decagon.

JHEP11(2020)072

A Trace sector formulae

In section 2.2 and 2.2.1 we obtained the result

$$\mathcal{O}_p = \sum_{\{q_1 \dots q_m\} \vdash p} C_{q_1,\dots,q_m} T_{q_1,\dots q_m} \tag{A.1}$$

$$C_{q_1,\dots q_m} = \frac{|[\sigma_{q_1\dots q_m}]|}{(p-1)!} \sum_{s \in \mathcal{P}(\{q_1,\dots,q_m\})} \frac{(-1)^{|s|+1}(N+1-p)_{p-\Sigma(s)}(N+p-\Sigma(s))_{\Sigma(s)}}{(N)_p - (N+1-p)_p} \tag{A.2}$$

which is explicit in p and $q_1 \dots q_m$, and depends on group theory data which we explained in section 2.2.1.

The value of m distinguishes the splitting of $\mathcal{O}_p$ in number of traces and below we give explicit examples for the double trace sector $m = 2$, and the triple trace sector $m = 3$.

A.1 Double trace sector

Consider the partition $q_1 + q_2 = p$. The powerset in the sum is

$$\mathcal{P}\left(\{q_1 q_2\}\right) = \{\{\}, \{q_1\}, \{q_2\}, \{q_1, q_2\}\} \tag{A.3}$$

and the corresponding values of Σ are

$$\Sigma(\{\}) = 0\ ,\ \Sigma(\{q_1\}) = q_1\ ,\ \Sigma(\{q_2\}) = q_2\ ,\ \Sigma(\{q_1, q_2\}) = q_1 + q_2 = p. \tag{A.4}$$

Furthermore the size of the conjugacy class is $|[q_1 q_2]| = p!/(q_1 q_2)$ as long as $q_1 \neq q_2$. Otherwise $q_1 = q_2 = p/2$ and $|[q_1 q_2]| = p!/(2q_1 q_2) = (p-1)!/(2p)$. With these informations, the coefficient of $T_{q_1} T_{q_2}$ in $\mathcal{O}_p$, from (A.2), is

$$C_{q_1 q_2} = \begin{cases} \dfrac{p}{q_1 q_2} \times \dfrac{-(N-p+1)_p - (N)_p + (N-p+1)_{q_2}(N+q_2)_{p-q_2} + (N-p+1)_{q_1}(N+q_1)_{p-q_1}}{(N)_p - (N-p+1)_p} \\ \dfrac{2}{p} \times \dfrac{-(N-p+1)_p - (N)_p + 2(N-p+1)_{p/2}(N+p/2)_{p/2}}{(N)_p - (N-p+1)_p} \end{cases} . \tag{A.5}$$

As we pointed out, the above formula holds for the coefficients of the double trace contributions to the single particle operator of any weight.

A.2 Triple trace sector

Consider the partition $q_1 + q_2 + q_3 = p$. By making explicit (A.2) we find,

$$\begin{aligned} C_{q_1 q_2 q_3} =& \frac{p}{q_1 q_2 q_3} \frac{-(N-p+1)_p + (N)_p}{(N)_p - (N-p+1)_p} \\ &+ \frac{p}{q_1 q_2 q_3} \frac{-\sum_{i=1}^3 (N-p+1)_{q_i}(N+q_i)_{p-q_i} + \sum_{i=1}^3 (N-p+1)_{p-q_i}(N+p-q_i)_{q_i}}{(N)_p - (N-p+1)_p} . \end{aligned} \tag{A.6}$$

The other two possible cases, in which $q_i = q_j$ and $q_1 = q_2 = q_3 = p/3$, only differ compared to the result above by the size of the conjugacy class. In the first case we have to further divide by 2, and in the second case by 6. This formula thus cover all possible triple trace contributions to single particle operators of any weight.

For any value of m, i.e. trace sector, our function $C_{\underline{q}}$ can be made very explicit, as in the examples discussed above.

JHEP11(2020)072

B Wick contractions

Given the set of all admissible propagator structures for a correlator, say

$$\texttt{PropStruct} = \Big\{\mathcal{P}_1, \dots \Big\} \tag{B.1}$$

we will now determine the associated Wick contractions.

Recall that an elementary fields of $\mathcal{N} = 4$ transforms under SO(6) of R-symmetry, i.e. ϕ^I, but itself is an $N \times N$ matrix in the adjoint of the gauge group. For the rest of this section we will then assume the replacement

$$\left(\phi^I(X)\right)_{\alpha\beta} \qquad \to \qquad \sum_i \phi^I_i(X)\, \mathcal{T}^i_{\alpha\beta} \tag{B.2}$$

where $\mathcal{T}^i_{\alpha\beta}$ are a basis of generators for the representation under the gauge group. This replacement on the trace basis becomes,

$$\begin{aligned}
T_p(X) \quad &\to \quad Y_{I_1} \dots Y_{I_p} \sum_{i_1,\dots i_p} \phi^I_{i_1} \dots \phi^{I_p}_{i_p}(X) \times \mathcal{T}^{i_1}_{\alpha_1\alpha_2} \dots \mathcal{T}^{i_p}_{\alpha_{2p-1}\alpha_1} \qquad \text{(B.3)}\\
T_{\{p_1,p_2\}}(X) \quad &\to \quad Y_{I_1} \dots Y_{I_p} \sum_{i_1,\dots i_p} \phi^I_{i_1} \dots \phi^{I_p}_{i_p}(X) \times \mathcal{T}^{i_1}_{\alpha_1\alpha_2} \dots \mathcal{T}^{i_{p_1}}_{\alpha_{2p_1-1}\alpha_1} \\
&\qquad\qquad\qquad\qquad\qquad\qquad\qquad\qquad \times \mathcal{T}^{i_{p_1+1}}_{\beta_1\beta_2} \dots \mathcal{T}^{i_p}_{\beta_{2p_2-1}\beta_1} \\
&\quad \vdots
\end{aligned}$$

and so on so forth, i.e. if the operator is multi-trace, the trace is splitted accordingly.

For what concerns finding the Wick contractions of an assigned propagator structure, the trace structure of the operators can be ignored. (Even though sometimes we can use the cyclic symmetry of the traces.) If we draw a blob to represent the operator, the only relevant information at this stage will be the number of SO(6) indexes, i.e. legs attached to the blob. Single- or multi-trace, we will draw the same blob. For each Wick contraction, or bridge between legs (belonging to different blobs), say α_1 and β_2, we insert a $\delta_{\alpha_1\beta_2}$ which links the generators. For SU(N) the sum over generators is then replaced by

$$\sum_{i=1}^{N-1} \mathcal{T}^i_{\alpha_1\alpha_2} \mathcal{T}^i_{\alpha_3\alpha_4} = \delta_{\alpha_1\alpha_4}\delta_{\alpha_2\alpha_3} - \frac{1}{N}\delta_{\alpha_1\alpha_2}\delta_{\alpha_3\alpha_4}\,. \tag{B.4}$$

The color factor depends crucially on the trace structure of the operators and the type of propagator, whether SU(N) or U(N).

To enumerate the Wick contractions we need two standard combinatorial objects:

1. Define $\mathscr{C}(k \subseteq n)$ as the *combinations* of k integers in the set $\{1, \dots, n\}$. These are ordered sets. For example, if $n = 3$ and $k = 2$ the combinations are $12, 13, 23$. The number of the combinations is the binomial coefficient

$$|\mathscr{C}(k \subseteq n)| = \binom{n}{k} = \frac{n!}{(n-k)!k!}\,. \tag{B.5}$$

JHEP11(2020)072

2. Define $\mathscr{D}(k \subseteq n)$ as the *dispositions* of k integers in the set $\{1, \ldots, n\}$. These are not ordered sets. For example, if $n = 3$ and $k = 2$, the dispositions are $12, 13, 23, 21, 31, 32$. The number of dispositions is indeed the number of k-combinations acted with k-permutations,

$$|\mathscr{D}(k \subseteq n)| = \binom{n}{k} k! = \frac{n!}{(n-k)!} \,. \tag{B.6}$$

To begin with, consider a simple example, the two-point function $\langle T_3, T_3 \rangle$. There is obviously a single propagator structure, with three brigdes, $b_{(12)} = 3$, Starting with $\phi^{I_1}\phi^{I_2}\phi^{I_3}(X_1)\phi^{I_4}\phi^{I_5}\phi^{I_6}(X_2)$, there are six Wick contractions, and we can rearrange them as follows,

$$\underbrace{\phi^{I_1}(X_1)\phi^{I_4}(X_2)} \quad \underbrace{\phi^{I_2}(X_1)\phi^{I_5}(X_2)} \quad \underbrace{\phi^{I_3}(X_1)\phi^{I_6}(X_2)} \quad \vdots \tag{B.7}$$

These six Wick contractions are indexed by $\mathscr{C}(3 \subseteq 3)$ (legs-out), which has dimension 1, paired with $\mathscr{D}(3 \subseteq 3)$ (legs-in), which has dimension 6. In other words,

$$\begin{array}{cccccc} 1\,2\,3 & 1\,2\,3 & 1\,2\,3 & 1\,2\,3 & 1\,2\,3 & 1\,2\,3 \\ 1'2'3' & 1'3'2' & 2'1'3' & 2'3'1' & 3'1'2' & 3'2'1' \end{array} \tag{B.8}$$

where the $'$ alphabet is $\{1' \to 4,\ 2' \to 5,\ 3' \to 6\}$.

Generating Wick contractions for a propagator structure $\mathcal{P} = \{b_{(12)}, \ldots b_{(ij)}, \ldots\}$ is slightly more involved but the logic is similar to the example above. First organise $\mathcal{P} = \{b_{(12)}, \ldots b_{(ij)}, \ldots\}$ as a matrix of the following form

$$\begin{bmatrix} p_1 & b_{(12)} & \cdots & b_{(1i)} & \cdots & \cdots & \cdots & b_{(1j)} & \cdots & \cdots \\ & \ddots & & & & & & & & \\ & & & p_i & \cdots & \cdots & \cdots & b_{(ij)} & \cdots & \vdots \\ & & & & p_{i+1} & b_{(i+1,i+2)} & & \vdots & & \vdots \\ & & & & & \ddots & & & & \vdots \\ & & & & & & p_{j-1} & b_{(j-1,j)} & & \vdots \\ & & & & & & & p_j & b_{(jj+1)} & \vdots \\ & & & & & & & & p_{j+1} & \vdots \\ & & & & & & & & & \ddots \ \vdots \\ & & & & & & & & & p_n \end{bmatrix} . \tag{B.9}$$

Conservation of charge at the blob p_i means

$$p_i = \sum_{k=1}^{i-1} b_{(ki)} + \sum_{k=i+1}^{n} b_{(ik)} \tag{B.10}$$

pictorially the r.h.s. is the sum over all the numbers on the hook having p_i at the corner.

JHEP11(2020)072

We will start enumerating the Wick contractions by going along the rows of the matrix, starting from the $b_{(12)}$. Upon visiting a $b_{(ij)}$, we define the *updated* values of p_i and p_j given by

$$p_{[ij]} \equiv - \underbrace{\sum_{k=1}^{i-1} b_{(ki)}}_{\#\text{ on the rows above } (i,i)} + p_i \; - \underbrace{\sum_{k=i+1}^{j-1} b_{(ik)}}_{\#\text{ on the cln before } (i,j)} \tag{B.11}$$

$$p_{[ji]} \equiv - \underbrace{\sum_{k=1}^{i-1} b_{(kj)}}_{\#\text{ on the rows above } (i,i)} + p_j \, . \tag{B.12}$$

The idea is that when we visit an entry (ij) we assign b_{ij} of the free legs of $p_{[ij]}$. These are legs out, and we link them with free legs of $p_{[ji]}$. The latter are legs in. Thus changing row index we consider legs in, and changing column index we consider legs out.

Define now the Wick contractions $\mathcal{W}[b_{(ij)}]$ for the bridges going from blob i with $p_{[ij]}$ legs-out, reaching blob j with $p_{[ji]}$ legs-in. These are enumerated by

$$\mathcal{W}[b_{(ij)}] = \mathscr{C}(b_{(ij)} \subseteq p_{[ij]}) \otimes \mathscr{D}(b_{(ij)} \subseteq p_{[ji]}) \, . \tag{B.13}$$

The dimension of $\mathcal{W}[b_{(ij)}]$ is simply

$$|\mathcal{W}[b_{(ij)}]| = |\mathscr{C}(b_{(ij)} \subseteq p_{[ij]})| \times |\mathscr{D}(b_{(ij)} \subseteq p_{[ji]})| \, . \tag{B.14}$$

The set of all possible Wick contractions for $\mathcal{P} = \{b_{(12)}, b_{(13)}, \ldots\}$ is given by

$$\mathcal{W}[\mathcal{P}] = \otimes_{1 \le i < j \le n} \mathcal{W}[b_{(ij)}] \tag{B.15}$$

with dimension $|\mathcal{W}[\mathcal{P}]| = \prod_{i<j} |\mathcal{W}[b_{(ij)}]|$. By using the explicit formulae,

$$|\mathscr{C}(k \subseteq n)| = \frac{n!}{(n-k)!k!} \qquad ; \qquad |\mathscr{D}(k \subseteq n)| = \frac{n!}{(n-k)!} \tag{B.16}$$

we find

$$|\mathcal{W}[\mathcal{P}]| = \prod_{1 \le i < j \le n} \frac{1}{b_{ij}!} \left(- \sum_{k=1}^{i-1} b_{ki} + p_i - \sum_{k=i+1}^{j} b_{ik} + 1 \right)_{b_{ij}} \times \left(p_j - \sum_{k=1}^{i} b_{kj} + 1 \right)_{b_{ij}} \tag{B.17}$$

where $(a)_b$ is the Pochhammer symbol.

Consider some explicit examples to fix ideas.

At three points we find that

$$|\mathcal{W}[\langle \mathcal{O}_p \mathcal{O}_q \mathcal{O}_r \rangle]| = \frac{p!q!r!}{(\frac{q+r-p}{2})!(\frac{p+r-q}{2})!(\frac{p+q-r}{2})!} \tag{B.18}$$

which is indeed fully symmetric.

At four points we find

$$\texttt{Legs\_out} = \overbrace{c_1 \ldots c_{d_{(12)}}}^{\mathscr{C}(b_{(12)} \subseteq p_{[12]})} \overbrace{c_1 \ldots c_{d_{(13)}}}^{\mathscr{C}(b_{(13)} \subseteq p_{[13]})} \overbrace{c_1 \ldots c_{d_{(14)}}}^{\mathscr{C}(b_{(14)} \subseteq p_{[14]})} \overbrace{c_1 \ldots c_{d_{(23)}}}^{\mathscr{C}(b_{(23)} \subseteq p_{[23]})} \overbrace{c_1 \ldots c_{d_{(24)}}}^{\mathscr{C}(b_{(24)} \subseteq p_{[24]})} \overbrace{c_1 \ldots c_{d_{(34)}}}^{\mathscr{C}(b_{(34)} \subseteq p_{[34]})}$$

$$\texttt{Legs\_in} = \underbrace{d_1 \ldots d_{d_{(12)}}}_{\mathscr{D}(b_{(12)} \subseteq p_{[21]})} \underbrace{d_1 \ldots d_{d_{(13)}}}_{\mathscr{D}(b_{(13)} \subseteq p_{[31]})} \underbrace{d_1 \ldots d_{d_{(14)}}}_{\mathscr{D}(b_{(14)} \subseteq p_{[41]})} \underbrace{d_1 \ldots d_{d_{(23)}}}_{\mathscr{D}(b_{(23)} \subseteq p_{[32]})} \underbrace{d_1 \ldots d_{d_{(24)}}}_{\mathscr{D}(b_{(24)} \subseteq p_{[42]})} \underbrace{d_1 \ldots d_{d_{(34)}}}_{\mathscr{D}(b_{(34)} \subseteq p_{[43]})} \, .$$

JHEP11(2020)072

Combinations c_i and dispositions d_i generated so far, do not refer to the specific numbering of the legs of the correlator. What we have done so far has been to enumerate Wick contractions. The final task is to assign them to the indexes from 1 to $\sum_{i=1}^{n} p_i$. In the example above the color-code denotes which subset of numbers belong to the same blob.

B.1 Digits

Let us introduce the characteristic vector of a combination in $\mathscr{C}(k \subseteq n)$. This is a digit of n bits, i.e. 0 or 1, with k values of 1 distributed in the digit. The positions of the 1 give the combination, for example

$$\{1,3,5\} \in \mathscr{C}(3 \subseteq 5) \qquad \longleftrightarrow \qquad [10101]\,. \tag{B.19}$$

It is simple to think of the combinations in this way, since the only operation one has to do is to sequenciate the 1s to the right or the 0s to the left, starting from the configuration $[111100\ldots]$ with k values of 1s at the beginning. The integer corresponding to a given combination is computed by the Gosper's hack in `C++`.[19] This is the fastest way to do it, and it works well for low charges (since there is an obvious bound provided by the number of bits of the machine.)

The idea of sequenciating is useful to generate dispositions as well. Recall that $\mathscr{D}(k \subseteq n)$ is obtained by acting with the symmetry group S_k on each combination in $\mathscr{C}(k \subseteq n)$. So we pick a $k-$combination $C = \{c_1, \ldots c_k\}$. (It is ordered, but otherwise it is not necessary). Starting form the subset of length one $C_1 = \{c_1\}$ we generate the set

$$C_2 = \{\{c_1, 0\}, \{0, c_1\}\}/.\{0 \to c_2\}\,. \tag{B.20}$$

Then for each element in C_2 we generate all sets obtained by sequenciating an extra 0. For example,

$$C_{3,1} = \{\{c_1, c_2, 0\}, \{c_1, 0, c_2\}, \{0, c_1, c_2\}\}/.\{0 \to c_3\} \tag{B.21}$$

$$C_{3,2} = \{\{c_2, c_1, 0\}, \{c_2, 0, c_1\}, \{0, c_2, c_1\}\}/.\{0 \to c_3\} \tag{B.22}$$

and so on. This recursive procedure on the length of the subsets in C gives all the dispositions of C.

For the Wick contractions, there are no repetitions in the $\{c_i\}$, since they come from the combinations.

Instead, in the context of the trees we encountered in section 4.1.2, more precisely in order to generate all possible values of d_i, i.e. number of legs per point, it is useful to consider cases with repetitions. These values, $d_1, \ldots d_{n-1}$ can be obtained by taking all partitions of $2(n-2) = \sum_{i=1}^{n-1} d_i$ (this is the constraint on the tree) and considering all dispositions of these partitions. Recall that the parts can have repetitions, i.e. some $d_i = d_j$ and so on.

The minor modification of the algorithm above is the following. The idea is to collect the repetitions in the original sequence as vectors $\vec{c}_i$ with $\vec{c}_i \neq \vec{c}_j$ if $i \neq j$. The recursive

[19] See for example https://en.wikipedia.org/wiki/Combinatorial_number_system.

JHEP11(2020)072

procedure will now work upon replacing the 0 with these vectors at each step. For example, start from $C = \{c_1 c_1, c_2 c_2, c_3 \ldots\}$. Then we generate

$$C_2 = \{\{c_1, c_1, 0\}, \{c_1, 0, c_1\}, \{0, c_1, c_1\}\}/.\{0 \to \vec{c}_2\}\,. \tag{B.23}$$

We go on with

$$\begin{aligned} C_{3,1} = \{&\{c_1, c_1, c_2, c_2, 0\}, \{c_1, c_1, c_2, 0, c_2\}, \\ &\{c_1, c_1, 0, c_2, c_2\}, \{c_1, 0, c_1, c_2, c_2\}, \{0, c_1, c_1, c_2, c_2\}\}/.\{0 \to c_3\} \\ &\vdots \end{aligned} \tag{B.24}$$

B.2 Prüfer sequences and trees

A unique way to label a tree is to use a Prüfer sequence $s = (s_1 \ldots)$, constructed as follows [54]. Consider the tree made of points at positions $1, \ldots n-1$, each point with d_i legs attached, as described above. For the example in (4.10), this is

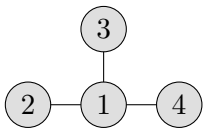

(B.25)

We define a *leaf* in the tree as a pair of positions $\ell_1 - \ell_2$ in which ℓ_1 is connected to ℓ_2 with one and only one bridge. At step k of the Prüfer algorithm, remove the leaf $\ell_1 - \ell_2$ with the *smallest* labelled position ℓ_1 and assign $s_k = \ell_2$ to the sequence. Then, write

$$|\mathcal{W}[\ell_1 - \ell_2]| = (q_{\ell_1} - d_{\ell_1} + 1) \times (q_{\ell_2} - \#(\ell_2)) \tag{B.26}$$

to count the Wick contractions corresponding to that leaf, where $\#(\ell_2)$ is the number of times ℓ_2 appeared in the sequence previously (step $< k$). We stop when there is only one leaf left. Here below we give another example, (rich enough to illustrate the various steps)

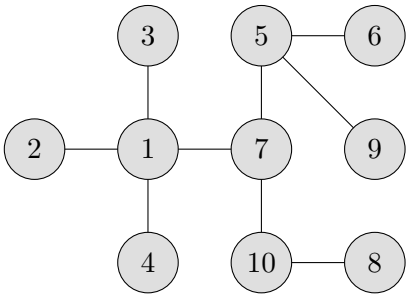

$$\begin{aligned} s_1 &= 1 \quad (q_1)(q_2) \\ s_2 &= 1 \quad (q_3)(q_1 - 1) \\ s_3 &= 1 \quad (q_4)(q_1 - 2) \\ s_4 &= 7 \quad (q_1 - 3)(q_7) \\ s_5 &= 5 \quad (q_6)(q_5) \\ s_5 &= 10 \quad (q_8)(q_{10}) \\ s_6 &= 5 \quad (q_9)(q_5 - 1) \\ s_6 &= 7 \quad (q_5 - 2)(q_7 - 1) \\ s_7 &= 10 \quad (q_7 - 2)(q_{10} - 1) \end{aligned} \tag{B.27}$$

The nice feature of the Prüfer algorithm is that it reduces the pairwise computation of Wick contractions, which follows from our results in (B.17),

$$|\mathcal{W}[\mathcal{T}]| = \prod_{\substack{i<j \\ b_{ij}=1}} \left(q_i - d_i + \sum_{k=j}^{n-1} b_{ik}\right) \times \left(q_j - \sum_{k=1}^{i-1} b_{kj}\right) \tag{B.28}$$

JHEP11(2020)072

(where we used conservation of charge on the tree) to a sequence. In particular, it gives a more efficient ordering of the b_{ij} to count $|\mathcal{W}[\mathcal{T}]|$. For instance, the pairs $(ij) = \{(56), (57), (59)\}$ in the example above would count differently, even though the total result does not change. Thus we can use the Prüfer algorithm to rearrange the counting.

In the Prüfer algorithm it is clear that the first time two operators i and j appear in the sequence, they count with $q_i q_j$, because necessarily $d_i = 1$ or $d_j = 1$. The second time one of this operators appears again, it counts with $q_i - 1$ or $q_j - 1$, and so on. The total number of Wick contractions is then,

$$|\mathcal{W}[\mathcal{T}]| = \prod_{i=1}^{n-1} q_i(q_i - 1)\dots(q_i - d_i + 1) \tag{B.29}$$

which is the result we quoted in (4.12).

C Low charge examples for multipoint orthogonality

In this section we reconsider the idea of phrasing the multi-point orthogonality theorem as an identity of the form $det = 0$, and we discuss some examples to have an idea about how the combinatorics works. Let us recall our setup of section 3. We want to study,

$$\mathcal{F}_{p|\underline{q_1}\dots\underline{q_{n-1}}}(x, x_1 \dots x_{n-1}) = \langle \mathcal{O}_p(x) T_{\underline{q_1}}(x_1) \dots T_{\underline{q_{n-1}}}(x_{n-1}) \rangle \tag{C.1}$$

where $\underline{q_i}$ can be a partition of q_i and $n \geq 3$. We can use the arrangement of $\mathcal{O}_p(x)$ in (2.9) as a determinant, to rewrite our correlator as another determinant

$$\mathcal{F}_{p|\underline{q_1},\dots,\underline{q_{n-1}}} = \frac{1}{\mathcal{N}_p} \det \begin{pmatrix} \mathcal{C}_{\lambda_1|\lambda_1} & \mathcal{C}_{\lambda_2|\lambda_1} & \dots & \mathcal{C}_{p|\lambda_1} \\ \vdots & \vdots & \dots & \vdots \\ \mathcal{C}_{\lambda_1|\lambda_{P-1}} & \mathcal{C}_{\lambda_2|\lambda_{P-1}} & \dots & \mathcal{C}_{p|\lambda_{P-1}} \\ \hline \mathcal{C}_{\lambda_1|\underline{q_1}\dots\underline{q_{n-1}}} & \mathcal{C}_{\lambda_2|\underline{q_1}\dots\underline{q_{n-1}}} & \dots & \mathcal{C}_{p|\underline{q_1}\dots\underline{q_{n-1}}} \end{pmatrix} . \tag{C.2}$$

Notice that differently from $\mathcal{F}_{p|\underline{q_1}\dots\underline{q_{n-1}}}$, the (color factor of the) correlator $\mathcal{C}_{\lambda_i|\underline{q_1}\dots\underline{q_{n-1}}}$ now involves only traces,

$$\mathcal{C}_{\lambda_i|\underline{q_1},\dots,\underline{q_{n-1}}} = \langle T_{\lambda_i}(x) T_{\underline{q_1}}(x_1) \dots T_{\underline{q_{n-1}}}(x_{n-1}) \rangle . \tag{C.3}$$

As we noticed in the main text of section 3, a feature of writing the correlator as a determinant is that if a propagator structure is such that the rows of the matrix are not independent, the determinant will vanish. The two-point functions from which we started our story are an obvious example, but also a trivial multipoint generalisation of that. Take the list of $\underline{q_1}, \dots, \underline{q_{n-1}}$ to coincide with a partition of p, say λ_I. Then, passing to the double line notation, it is clear that $\mathcal{C}_{\lambda_j|\underline{q_1},\dots,\underline{q_{n-1}}}$ has the same color factor of the corresponding two-point function regardless of the number of points.

More generally, the property we want to assign to the propagator structure in such a way that the determinant vanishes is that

$$\mathcal{C}_{\lambda_j|\underline{q_1},\dots,\underline{q_{n-1}}} = \sum_{I=1,\dots P-1} K_I \, \mathcal{C}_{\lambda_j|\lambda_I} \qquad j = 1, 2 \dots P \tag{C.4}$$

JHEP11(2020)072

for some K_I. Namely, the vector made by $\mathcal{C}_{\lambda_j|\underline{q_1},\ldots,\underline{q_{n-1}}}$, is a linear combination of the rows in (C.2). This translates into a requirement about the topology of the diagram, since *all partitions* $\lambda_{I=1,\ldots P-1}$ involved in (C.4) have at least length two, i.e. $\lambda_P = \{p\}$ is excluded, and there cannot be self-contractions within T_{λ_I} in the two point functions $\mathcal{C}_{\lambda_j|\lambda_I}$. We conclude that a necessary condition for $\mathcal{F}_{p|\underline{q_1},\ldots,\underline{q_{n-1}}}$ to vanish is that the diagram disconnects as soon as we remove $\mathcal{O}_p$.

The reasoning above leaves a free parameter. In fact, the assignment $\underline{q_1},\ldots,\underline{q_{n-1}}$ can be such that

$$\frac{1}{2}\left(-p+\sum_{i=1}^{n-1} q_i\right) = k \geq 0 \tag{C.5}$$

and yet the diagram disconnects as soon as we remove $\mathcal{O}_p$. The value of k measures the excess of $\sum q_i$ to be a partition of p. This is possible precisely because differently from a two-point function, in a multipoint function there can be $k \geq 0$ Wick contractions distributed among the $T_{\underline{q_1}}(x_1)\ldots T_{\underline{q_{n-1}}}(x_{n-1})$, such that when $\mathcal{O}_p$ is removed, the diagram still disconnects.

Example (I). Consider the SU(N) single-particle operator $\mathcal{O}_4$, which is the SPO with the simplest admixture, $T_{\{22\}}$ and T_4, and take the four-point function $\langle \mathcal{O}_4(x) T_2(x_1) T_2(x_2) T_2(x_3)\rangle$. This is an example with $k = 1$, and there is only one possible propagator structure,

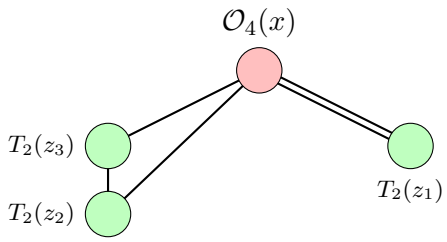

(C.6)

namely, $\mathcal{F}_{4|2,2,2} \simeq g_{x1}^2 g_{x2} g_{x3} g_{23}$. In formulae we will now find that $\mathcal{F}_{4|2,2,2}$ vanishes,

$$\mathcal{F}_{4|222} \simeq \frac{1}{\mathcal{N}_4} \det \begin{pmatrix} \mathcal{C}_{\{22\}|\{22\}} & \mathcal{C}_{4|\{22\}} \\ \mathcal{C}_{\{22\}|2,2,2} & \mathcal{C}_{4|2,2,2} \end{pmatrix} = 0 \tag{C.7}$$

where

$$\begin{matrix} \mathcal{C}_{\{22\}|\{22\}} = 8(N^4-1) \\ \mathcal{C}_{\{22\}|2,2,2} = 32(N^4-1) \end{matrix} \quad ; \quad \begin{matrix} \mathcal{C}_{4|\{22\}} = 8(N^2-1)(2N^2-3)/N \\ \mathcal{C}_{4|2,2,2} = 32(N^2-1)(2N^2-3)/N \end{matrix} . \tag{C.8}$$

We see here that $\mathcal{F}_{4|2,2,2} = 0$ is a consequence of the four-point functions in the second line of (C.8) being proportional by a factor of four to the two-point functions in the first line. The figure below provides some more intuition. We draw $\mathcal{F}_{4|2,2,2}$, and by looking at a single contribution to the color factor of $\mathcal{C}_{4|2,2,2}$, we illustrate that its double line

JHEP11(2020)072

notation is the same as that of the two-point function $\mathcal{C}_{4|\{22\}}$, i.e. in double line notation $T_2(x_1)T_2(x_2)T_2(x_3)$ "behaves" like the operator T_{22},

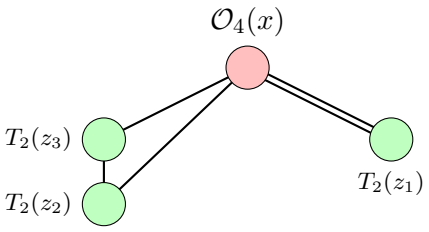

$\mathcal{F}_{4|222} \simeq g_{x1}^2 g_{x2} g_{x3} g_{23}$

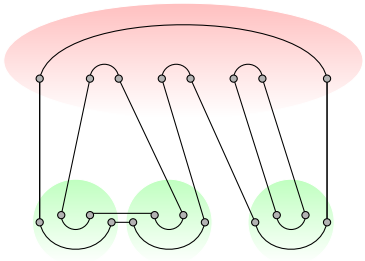

A contribution to the color factor

(C.9)

Notice also that the factor of four in (C.8) is the number of ways we can contract $T_2(x_2)T_2(x_3)$ with $k = 1$ Wick contractions. Precisely because of this Wick contraction, we can see in (C.9) that the loop counting is the same for both the four- and the two- point functions.

Example (II). In the next example we consider the four-point function $\langle \mathcal{O}_4(x)T_2(z_1)T_2(z_2)T_4(z_3)\rangle$, which corresponds to a case with $k = 2$. There are six propagator structures, but we are interested in the one drawn below, since it will have a vanishing color factor,

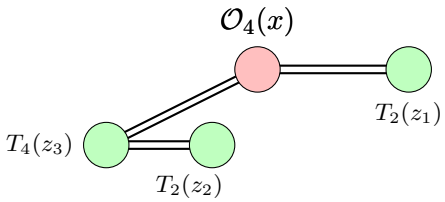

$\mathcal{F}_{4|422} \simeq g_{x1}^2 g_{x3}^2 g_{23}^2$

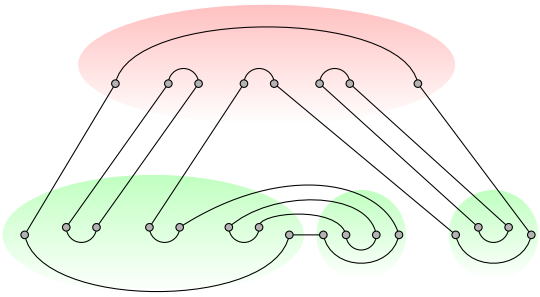

A contribution to the color factor

(C.10)

By a mechanism similar to the previous example, we will now see that $\mathcal{F}_{4|4,2,2} = 0$. However, this new example shows that the combinatorics in general is subtle/complicated.

In formulae we find that $\mathcal{F}_{4|4,2,2}$ gives

$$\mathcal{F}_{4|4,2,2} \simeq \frac{1}{\mathcal{N}_4} \det \begin{pmatrix} \mathcal{C}_{\{22\}|\{22\}} & \mathcal{C}_{4|\{22\}} \\ \mathcal{C}_{\{22\}|4,2,2} & \mathcal{C}_{4|4,2,2} \end{pmatrix} = 0 \tag{C.11}$$

where

$$\begin{aligned} \mathcal{C}_{\{22\}|\{22\}} &= 8(N^4-1) \\ \mathcal{C}_{\{22\}|4,2,2} &= 32(N^4-1)(2N^2-3)/N \end{aligned} \quad ; \quad \begin{aligned} \mathcal{C}_{4|\{22\}} &= 8(N^2-1)(2N^2-3)/N \\ \mathcal{C}_{4|4,2,2} &= 32(N^2-1)(2N^2-3)^2/N^2 \end{aligned} \quad . \tag{C.12}$$

JHEP11(2020)072

This time the four-point functions in the second line of (C.12) are proportional to the two-point functions on the first line by an N-dependent factor. This feature can be seen in the double line diagram (C.10), in which we can count four loops instead of three, and three was the counting of the previous example (C.9). From the combinatorial point of view is then non trivial that $\mathcal{F}_{4|4,2,2}$ vanishes.

In general, the determinant argument we started with, only leads to a relation between rows which eventually can get complicated. It would be very interesting to have a more direct combinatorial argument, alternative to the proof we gave in section 3.1.

D More N^{3}E correlators at 4-pt

Here we give a few more details on the N^{3}E four-point functions analysed with the half-BPS OPE as in section 5.2. Thus focussing on the following diagrams,

$$\langle \mathcal{O}_p \mathcal{O}_q \mathcal{O}_r \mathcal{O}_s \rangle_c = \alpha_1 + \alpha_2 + \alpha_3 + \alpha_4 + \alpha_5 + \alpha_6 + \alpha_7 \,. \tag{D.1}$$

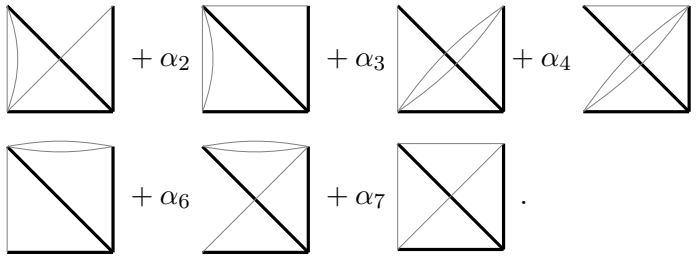

Recall that the operator $\mathcal{O}_s$ sits at the right corner on the bottom of each square.

Example: $\langle \mathcal{O}_3 \mathcal{O}_3 \mathcal{O}_3 \mathcal{O}_3 \rangle$. In this case crossing symmetry implies

$$\alpha_1 = \alpha_2 = \alpha_3 = \alpha_4 = \alpha_5 = \alpha_6 \tag{D.2}$$

The relevant equations, (5.25) and (5.26), respectively, simplify to become

$$\alpha_1 = 18 \frac{\langle \mathcal{O}_3 \mathcal{O}_3 \rangle^2}{\langle \mathcal{O}_2 \mathcal{O}_2 \rangle} = 81 \frac{(N^2-1)(N^2-4)^2}{N^2} . \tag{D.3}$$

$$2\alpha_1 + \alpha_7 = 9 \langle \mathcal{O}_3 \mathcal{O}_3 \mathcal{O}_4 \rangle + \frac{\langle \mathcal{O}_3 \mathcal{O}_3 [\mathcal{O}_2 \mathcal{O}_2] \rangle^2}{\langle [\mathcal{O}_2 \mathcal{O}_2][\mathcal{O}_2 \mathcal{O}_2] \rangle} = 324 \frac{(N^2-1)(N^2-4)(N^2-8)}{N^2} . \tag{D.4}$$

In the latter, which comes from (5.26), we find that only $\mathcal{K} = [\mathcal{O}_2 \mathcal{O}_2]$ is relevant, and also that the corresponding three-point function is simply obtained from the results in (5.23). Combining the above results we find the remaining coefficient,

$$\alpha_7 = 162 \frac{(N^2-1)(N^2-4)(N^2-12)}{N^2} = 54 \frac{N^2-12}{N} \langle \mathcal{O}_3 \mathcal{O}_3 \rangle \,. \tag{D.5}$$

Taking coincidence limits then gives

$$\langle [\mathcal{O}_3 \mathcal{O}_3] \mathcal{O}_3 \mathcal{O}_3 \rangle = \langle [\mathcal{O}_3 \mathcal{O}_3][\mathcal{O}_3 \mathcal{O}_3] \rangle = 2\alpha_1 + 2 \langle \mathcal{O}_3 \mathcal{O}_3 \rangle^2 = 18 \frac{(N^2-1)(N^2-4)^2(N^2+8)}{N^2} , \tag{D.6}$$

where the $\langle \mathcal{O}_3 \mathcal{O}_3 \rangle^2$ term comes from the disconnected contributions to the four-point function.

JHEP11(2020)072

Example: $\langle \mathcal{O}_4\mathcal{O}_4\mathcal{O}_4\mathcal{O}_6\rangle$. This example obeys the maximal crossing symmetry conditions (D.2). We have

$$\alpha_1 = 8\frac{\langle \mathcal{O}_4\mathcal{O}_4\mathcal{O}_4\rangle\langle \mathcal{O}_6\mathcal{O}_6\rangle}{\langle \mathcal{O}_4\mathcal{O}_4\rangle} \tag{D.7}$$

and

$$2\alpha_1 + \alpha_7 = 16\langle \mathcal{O}_4\mathcal{O}_6\mathcal{O}_6\rangle + \sum_{\underline{t},\underline{t}'\vdash 6}\langle \mathcal{O}_4\mathcal{O}_4\mathcal{K}_{\underline{t}}\rangle(\tilde{g}^{-1})_{\underline{t}\underline{t}'}\langle \mathcal{K}_{\underline{t}'}\mathcal{O}_4\mathcal{O}_6\rangle\,. \tag{D.8}$$

The solution for α_7 reads

$$\alpha_7 = 64\frac{(2N^4 - 187N^2 + 81)}{N(N^2+1)}\langle \mathcal{O}_6\mathcal{O}_6\rangle\,. \tag{D.9}$$

For $\langle T_4T_4T_4\mathcal{O}_6\rangle$ we have

$$\alpha_7 \to 64\frac{2N^2 - 81}{N}\langle \mathcal{O}_6\mathcal{O}_6\rangle\,. \tag{D.10}$$

Example: $\langle \mathcal{O}_3\mathcal{O}_3\mathcal{O}_4\mathcal{O}_4\rangle$. In this case crossing symmetry requires

$$\alpha_1 = \alpha_2\,, \quad \alpha_3 = \alpha_5 \quad \alpha_4 = \alpha_6\,, \tag{D.11}$$

So we only have four independent coefficients. From equation (5.25) and its crossing we find

$$\alpha_1 = 24\frac{\langle \mathcal{O}_3\mathcal{O}_3\rangle\langle \mathcal{O}_4\mathcal{O}_4\rangle}{\langle \mathcal{O}_2\mathcal{O}_2\rangle} \tag{D.12}$$

$$\alpha_3 + \alpha_4 = 9\frac{\langle \mathcal{O}_3\mathcal{O}_4\mathcal{O}_3\rangle\langle \mathcal{O}_4\mathcal{O}_4\rangle}{\langle \mathcal{O}_3\mathcal{O}_3\rangle} = 81\frac{\langle \mathcal{O}_4\mathcal{O}_4\rangle^2}{\langle \mathcal{O}_3\mathcal{O}_3\rangle} \tag{D.13}$$

From equation (5.26) and its crossing we obtain

$$2\alpha_3 + \alpha_7 = 9\langle \mathcal{O}_4\mathcal{O}_4\mathcal{O}_4\rangle + \frac{\langle \mathcal{O}_3\mathcal{O}_3[\mathcal{O}_2\mathcal{O}_2]\rangle\langle [\mathcal{O}_2\mathcal{O}_2]\mathcal{O}_4\mathcal{O}_4\rangle}{\langle [\mathcal{O}_2\mathcal{O}_2][\mathcal{O}_2\mathcal{O}_2]\rangle} \tag{D.14}$$

$$\alpha_1 + \alpha_4 + \alpha_7 = 34\langle \mathcal{O}_3\mathcal{O}_4\mathcal{O}_5\rangle + \frac{\langle [\mathcal{O}_2\mathcal{O}_3]\mathcal{O}_3\mathcal{O}_4\rangle^2}{\langle [\mathcal{O}_2\mathcal{O}_3][\mathcal{O}_2\mathcal{O}_3]\rangle}\,. \tag{D.15}$$

The two-particle operators entering the above equations are $\mathcal{K} = [\mathcal{O}_2\mathcal{O}_2]$ and $\mathcal{K} = [\mathcal{O}_2\mathcal{O}_3]$. Notice also the appereance of $\langle \mathcal{O}_4\mathcal{O}_4\mathcal{O}_4\rangle$ which is NME three point function computed in section 4.2.1. In sum we have four equations and thus we can determine the independent coefficients,

$$\begin{aligned}
\alpha_1 &= 36\frac{(N^2-4)}{N}\langle \mathcal{O}_4\mathcal{O}_4\rangle = 24\frac{\langle \mathcal{O}_3\mathcal{O}_3\rangle\langle \mathcal{O}_4\mathcal{O}_4\rangle}{\langle \mathcal{O}_2\mathcal{O}_2\rangle}\,,\\
2\alpha_3 = \alpha_4 &= 72\frac{N(N^2-9)}{N^2+1}\langle \mathcal{O}_4\mathcal{O}_4\rangle = 54\frac{\langle \mathcal{O}_4\mathcal{O}_4\rangle^2}{\langle \mathcal{O}_3\mathcal{O}_3\rangle}\,,\\
\alpha_7 &= 72\frac{N^4 - 25N^2 - 6}{N(N^2+1)}\langle \mathcal{O}_4\mathcal{O}_4\rangle\,.
\end{aligned}$$

JHEP11(2020)072

Having obtained the four-point correlator we then find the coincidence limits,

$$\langle[\mathcal{O}_3\mathcal{O}_3]\mathcal{O}_4\mathcal{O}_4\rangle = 144\frac{N(N^2-9)}{N^2+1}\langle\mathcal{O}_4\mathcal{O}_4\rangle\,.$$
$$\langle[\mathcal{O}_3\mathcal{O}_4]\mathcal{O}_3\mathcal{O}_4\rangle = \langle[\mathcal{O}_3\mathcal{O}_4][\mathcal{O}_3\mathcal{O}_4]\rangle = 72\frac{N^4-6N^2-2}{N(N^2+1)}\langle\mathcal{O}_4\mathcal{O}_4\rangle + \langle\mathcal{O}_3\mathcal{O}_3\rangle\langle\mathcal{O}_4\mathcal{O}_4\rangle\,. \quad \text{(D.16)}$$

If we consider instead $\langle T_3T_3T_4\mathcal{O}_4\rangle$ we find α_1 is unchanged while

$$2\alpha_3 = \alpha_4 \to 72\frac{N^2-6}{N}\langle\mathcal{O}_4\mathcal{O}_4\rangle\,, \quad \alpha_7 \to 72\frac{N^2-18}{N}\langle\mathcal{O}_4\mathcal{O}_4\rangle\,. \quad \text{(D.17)}$$

Example: $\langle\mathcal{O}_3\mathcal{O}_3\mathcal{O}_5\mathcal{O}_5\rangle$. This is the first case where we need to consider more than one possible exchanged multi-particle operator in an OPE channel. The crossing symmetry conditions (D.11) still apply but now from equation (5.25) and crossing we have

$$\alpha_1 = 30\frac{\langle\mathcal{O}_3\mathcal{O}_3\rangle\langle\mathcal{O}_5\mathcal{O}_5\rangle}{\langle\mathcal{O}_2\mathcal{O}_2\rangle}\,,$$
$$\alpha_3+\alpha_4 = \frac{\langle\mathcal{O}_3\mathcal{O}_4\mathcal{O}_5\rangle^2}{\langle\mathcal{O}_4\mathcal{O}_4\rangle} = 144\frac{\langle\mathcal{O}_5\mathcal{O}_5\rangle^2}{\langle\mathcal{O}_4\mathcal{O}_4\rangle}\,. \quad \text{(D.18)}$$

From equation (5.26) we find,

$$2\alpha_3+\alpha_7 = 9\langle\mathcal{O}_4\mathcal{O}_5\mathcal{O}_5\rangle + \frac{\langle\mathcal{O}_3\mathcal{O}_3[\mathcal{O}_2\mathcal{O}_2]\rangle\langle[\mathcal{O}_2\mathcal{O}_2]\mathcal{O}_5\mathcal{O}_5\rangle}{\langle[\mathcal{O}_2\mathcal{O}_2][\mathcal{O}_2\mathcal{O}_2]\rangle}\,, \quad \text{(D.19)}$$

Its crossing transformation has more structure:

$$\alpha_1+\alpha_4+\alpha_7 = 15\langle\mathcal{O}_3\mathcal{O}_5\mathcal{O}_6\rangle + \sum_{\underline{t},\underline{t}'\vdash 6}\langle\mathcal{O}_3\mathcal{O}_5\mathcal{K}_{\underline{t}}\rangle(\tilde{g}^{-1})_{\underline{t}\underline{t}'}\langle\mathcal{K}_{\underline{t}'}\mathcal{O}_3\mathcal{O}_5\rangle\,. \quad \text{(D.20)}$$

Here $\mathcal{K}$ runs over the set of twist six multiparticle operators $\{[\mathcal{O}_2\mathcal{O}_4],[\mathcal{O}_3\mathcal{O}_3],[\mathcal{O}_2\mathcal{O}_2\mathcal{O}_2]\}$. The matrix of their two-point functions and hence its inverse can be determined from results on coincidence limits presented earlier. We find

$$\langle\mathcal{K}_{\underline{t}}\mathcal{K}_{\underline{t}'}\rangle = \begin{pmatrix} 2(N^2+7)\langle\mathcal{O}_4\mathcal{O}_4\rangle & 18\langle\mathcal{O}_4\mathcal{O}_4\rangle & 0 \\ 18\langle\mathcal{O}_4\mathcal{O}_4\rangle & 4(N^2+8)\frac{\langle\mathcal{O}_3\mathcal{O}_3\rangle^2}{\langle\mathcal{O}_2\mathcal{O}_2\rangle} & 48\langle\mathcal{O}_3\mathcal{O}_3\rangle \\ 0 & 48\langle\mathcal{O}_3\mathcal{O}_3\rangle & 24(N^2+1)(N^2+3)\langle\mathcal{O}_2\mathcal{O}_2\rangle \end{pmatrix}. \quad \text{(D.21)}$$

In sum, the above equations determine all the coefficients,

$$\alpha_1 = 30\frac{\langle\mathcal{O}_3\mathcal{O}_3\rangle\langle\mathcal{O}_5\mathcal{O}_5\rangle}{\langle\mathcal{O}_2\mathcal{O}_2\rangle}\,,$$
$$3\alpha_3 = \alpha_4 = 108\frac{\langle\mathcal{O}_5\mathcal{O}_5\rangle^2}{\langle\mathcal{O}_4\mathcal{O}_4\rangle}\,,$$
$$\alpha_7 = 90\frac{(N^4-43N^2-72)}{N(N^2+5)}\langle\mathcal{O}_5\mathcal{O}_5\rangle\,. \quad \text{(D.22)}$$

If we consider instead $\langle T_3T_3T_5\mathcal{O}_5\rangle$ we again find α_1 is unchanged while

$$3\alpha_3 = \alpha_4 \to 135\frac{N^2-8}{N}\langle\mathcal{O}_5\mathcal{O}_5\rangle\,, \quad \alpha_7 \to 90\frac{N^2-24}{N}\langle\mathcal{O}_5\mathcal{O}_5\rangle\,. \quad \text{(D.23)}$$

JHEP11(2020)072

Example: $\langle \mathcal{O}_3\mathcal{O}_3\mathcal{O}_6\mathcal{O}_6\rangle$. This example is very similar to the previous one with the crossing conditions (D.11) still valid and three twist seven multiparticle operators participating in the crossing transformation of equation (5.26). We simply quote the results here,

$$\begin{aligned}
\alpha_1 &= 36\frac{\langle\mathcal{O}_3\mathcal{O}_3\rangle\langle\mathcal{O}_6\mathcal{O}_6\rangle}{\langle\mathcal{O}_2\mathcal{O}_2\rangle}\,,\\
4\alpha_3 = \alpha_4 &= 180\frac{\langle\mathcal{O}_6\mathcal{O}_6\rangle^2}{\langle\mathcal{O}_5\mathcal{O}_5\rangle}\,,\\
\alpha_7 &= 108\frac{(N^6-65N^4-408N^2-80)}{N(N^4+15N^2+8)}\langle\mathcal{O}_6\mathcal{O}_6\rangle\,.
\end{aligned} \tag{D.24}$$

If we consider instead $\langle T_3T_3T_6\mathcal{O}_6\rangle$ we find

$$4\alpha_3 = \alpha_4 \to 216\frac{N^2-10}{N}\langle\mathcal{O}_6\mathcal{O}_6\rangle\,,\quad \alpha_7 \to 108\frac{N^2-30}{N}\langle\mathcal{O}_6\mathcal{O}_6\rangle\,. \tag{D.25}$$

Example: $\langle \mathcal{O}_3\mathcal{O}_4\mathcal{O}_4\mathcal{O}_5\rangle$. In this case crossing symmetry implies a different set of conditions,

$$\alpha_1=\alpha_3\,,\quad \alpha_2=\alpha_4\,,\quad \alpha_5=\alpha_6\,. \tag{D.26}$$

equation (5.25) nd its crossing transformation become

$$\begin{aligned}
\alpha_1+\alpha_2 = 108\frac{\langle\mathcal{O}_4\mathcal{O}_4\rangle\langle\mathcal{O}_5\mathcal{O}_5\rangle}{\langle\mathcal{O}_3\mathcal{O}_3\rangle}\,2\alpha_5 \qquad &= 12\frac{\langle\mathcal{O}_4\mathcal{O}_4\mathcal{O}_4\rangle\langle\mathcal{O}_5\mathcal{O}_5\rangle}{\langle\mathcal{O}_4\mathcal{O}_4\rangle}\,.
\end{aligned} \tag{D.27}$$

Equation (5.26) becomes

$$\alpha_1+\alpha_5+\alpha_7 = 12\langle\mathcal{O}_4\mathcal{O}_5\mathcal{O}_5\rangle + \frac{\langle\mathcal{O}_3\mathcal{O}_4[\mathcal{O}_2\mathcal{O}_3]\rangle\langle[\mathcal{O}_2\mathcal{O}_3]\mathcal{O}_4\mathcal{O}_5\rangle}{\langle[\mathcal{O}_2\mathcal{O}_3][\mathcal{O}_2\mathcal{O}_3]\rangle}\,, \tag{D.28}$$

Its crossing involves the two-particle operators $\{[\mathcal{O}_2\mathcal{O}_4],[\mathcal{O}_3\mathcal{O}_3],[\mathcal{O}_2\mathcal{O}_2\mathcal{O}_2]\}$. These are precisely the same operators of the previous example. Thus

$$2\alpha_2+\alpha_7 = 15\langle\mathcal{O}_4\mathcal{O}_4\mathcal{O}_6\rangle + \sum_{\underline{t},\underline{t}'\vdash 6}\langle\mathcal{O}_4\mathcal{O}_4\mathcal{K}_{\underline{t}}\rangle(\tilde{g}^{-1})_{\underline{t}\underline{t}'}\langle\mathcal{K}_{\underline{t}'}\mathcal{O}_3\mathcal{O}_5\rangle\,. \tag{D.29}$$

The solution obtained is

$$\begin{aligned}
\alpha_1 &= 36\frac{\langle\mathcal{O}_4\mathcal{O}_4\rangle\langle\mathcal{O}_5\mathcal{O}_5\rangle}{\langle\mathcal{O}_3\mathcal{O}_3\rangle}\,, & \alpha_2 &= 72\frac{\langle\mathcal{O}_4\mathcal{O}_4\rangle\langle\mathcal{O}_5\mathcal{O}_5\rangle}{\langle\mathcal{O}_3\mathcal{O}_3\rangle}\,,\\
\alpha_5 &= 6\frac{\langle\mathcal{O}_4\mathcal{O}_4\mathcal{O}_4\rangle\langle\mathcal{O}_5\mathcal{O}_5\rangle}{\langle\mathcal{O}_4\mathcal{O}_4\rangle}\,, & \alpha_7 &= 96\frac{(N^4-50N^2+9)}{N(N^2+1)}\langle\mathcal{O}_5\mathcal{O}_5\rangle\,.
\end{aligned} \tag{D.30}$$

If we consider instead $\langle T_3T_4T_4\mathcal{O}_5\rangle$ we find

$$2\alpha_1=\alpha_2\to 96\frac{N^2-6}{N}\langle\mathcal{O}_5\mathcal{O}_5\rangle\,,\quad \alpha_5\to 96\frac{N^2-9}{N}\langle\mathcal{O}_5\mathcal{O}_5\rangle\,,\quad \alpha_7\to 96\frac{N^2-27}{N}\langle\mathcal{O}_5\mathcal{O}_5\rangle\,. \tag{D.31}$$

JHEP11(2020)072

Example: $\langle \mathcal{O}_3\mathcal{O}_4\mathcal{O}_5\mathcal{O}_6\rangle$. This is the first example with no crossing symmetry conditions. We have confirmed with explicit Wick contraction computation that our solution in (5.29)–(5.30) is reproduced. We quote the coefficient α_7

$$\alpha_7 = 120\frac{(N^6 - 82N^4 - 231N^2 + 12)}{N(N^2+1)(N^2+5)}\langle \mathcal{O}_6\mathcal{O}_6\rangle \tag{D.32}$$

For $\langle T_3T_4T_5\mathcal{O}_6\rangle$ we have

$$\alpha_7 \to 120\frac{N^2 - 36}{N}\langle \mathcal{O}_6\mathcal{O}_6\rangle\,. \tag{D.33}$$

References

[1] F. Aprile, J.M. Drummond, P. Heslop and H. Paul, *Quantum gravity from conformal field theory*, *JHEP* **01** (2018) 035 [arXiv:1706.02822] [INSPIRE].

[2] L.F. Alday and S. Caron-Huot, *Gravitational S-matrix from CFT dispersion relations*, *JHEP* **12** (2018) 017 [arXiv:1711.02031] [INSPIRE].

[3] F. Aprile, J.M. Drummond, P. Heslop and H. Paul, *Loop corrections for Kaluza-Klein AdS amplitudes*, *JHEP* **05** (2018) 056 [arXiv:1711.03903] [INSPIRE].

[4] F. Aprile, J. Drummond, P. Heslop and H. Paul, *One-loop amplitudes in $AdS_5 \times S^5$ supergravity from $\mathcal{N} = 4$ SYM at strong coupling*, *JHEP* **03** (2020) 190 [arXiv:1912.01047] [INSPIRE].

[5] L.F. Alday and X. Zhou, *Simplicity of AdS supergravity at one loop*, *JHEP* **09** (2020) 008 [arXiv:1912.02663] [INSPIRE].

[6] G. Arutyunov and S. Frolov, *Some cubic couplings in type IIB supergravity on $AdS_5 \times S^5$ and three point functions in SYM(4) at large N*, *Phys. Rev. D* **61** (2000) 064009 [hep-th/9907085] [INSPIRE].

[7] G. Arutyunov and S. Frolov, *On the correspondence between gravity fields and CFT operators*, *JHEP* **04** (2000) 017 [hep-th/0003038] [INSPIRE].

[8] L. Rastelli and X. Zhou, *How to succeed at holographic correlators without really trying*, *JHEP* **04** (2018) 014 [arXiv:1710.05923] [INSPIRE].

[9] G. Arutyunov, R. Klabbers and S. Savin, *Four-point functions of all-different-weight chiral primary operators in the supergravity approximation*, *JHEP* **09** (2018) 023 [arXiv:1806.09200] [INSPIRE].

[10] G. Arutyunov, R. Klabbers and S. Savin, *Four-point functions of 1/2-BPS operators of any weights in the supergravity approximation*, *JHEP* **09** (2018) 118 [arXiv:1808.06788] [INSPIRE].

[11] F. Aprile, J. Drummond, P. Heslop and H. Paul, *Double-trace spectrum of $N = 4$ supersymmetric Yang-Mills theory at strong coupling*, *Phys. Rev. D* **98** (2018) 126008 [arXiv:1802.06889] [INSPIRE].

JHEP11(2020)072

[12] J.M. Maldacena and A. Strominger, *AdS_3 black holes and a stringy exclusion principle*, *JHEP* **12** (1998) 005 [hep-th/9804085] [INSPIRE].

[13] J. McGreevy, L. Susskind and N. Toumbas, *Invasion of the giant gravitons from Anti-de Sitter space*, *JHEP* **06** (2000) 008 [hep-th/0003075] [INSPIRE].

[14] V. Balasubramanian, M. Berkooz, A. Naqvi and M.J. Strassler, *Giant gravitons in conformal field theory*, *JHEP* **04** (2002) 034 [hep-th/0107119] [INSPIRE].

[15] S. Corley, A. Jevicki and S. Ramgoolam, *Exact correlators of giant gravitons from dual $N = 4$ SYM theory*, *Adv. Theor. Math. Phys.* **5** (2002) 809 [hep-th/0111222] [INSPIRE].

[16] R. de Mello Koch and R. Gwyn, *Giant graviton correlators from dual $\mathrm{SU}(N)$ super Yang-Mills theory*, *JHEP* **11** (2004) 081 [hep-th/0410236] [INSPIRE].

[17] T.W. Brown, *Half-BPS $\mathrm{SU}(N)$ correlators in $N = 4$ SYM*, *JHEP* **07** (2008) 044 [hep-th/0703202] [INSPIRE].

[18] E. D'Hoker, J. Erdmenger, D.Z. Freedman and M. Pérez-Victoria, *Near extremal correlators and vanishing supergravity couplings in AdS/CFT*, *Nucl. Phys. B* **589** (2000) 3 [hep-th/0003218] [INSPIRE].

[19] E. D'Hoker, D.Z. Freedman, S.D. Mathur, A. Matusis and L. Rastelli, *Extremal correlators in the AdS/CFT correspondence*, hep-th/9908160 [INSPIRE].

[20] M. Bianchi and S. Kovacs, *Nonrenormalization of extremal correlators in $N = 4$ SYM theory*, *Phys. Lett. B* **468** (1999) 102 [hep-th/9910016] [INSPIRE].

[21] B. Eden, P.S. Howe, C. Schubert, E. Sokatchev and P.C. West, *Extremal correlators in four-dimensional SCFT*, *Phys. Lett. B* **472** (2000) 323 [hep-th/9910150] [INSPIRE].

[22] J. Erdmenger and M. Pérez-Victoria, *Nonrenormalization of next-to-extremal correlators in $N = 4$ SYM and the AdS/CFT correspondence*, *Phys. Rev. D* **62** (2000) 045008 [hep-th/9912250] [INSPIRE].

[23] B.U. Eden, P.S. Howe, E. Sokatchev and P.C. West, *Extremal and next-to-extremal n point correlators in four-dimensional SCFT*, *Phys. Lett. B* **494** (2000) 141 [hep-th/0004102] [INSPIRE].

[24] S. Penati, A. Santambrogio and D. Zanon, *Two point functions of chiral operators in $N = 4$ SYM at order g^4*, *JHEP* **12** (1999) 006 [hep-th/9910197] [INSPIRE].

[25] S. Penati, A. Santambrogio and D. Zanon, *More on correlators and contact terms in $N = 4$ SYM at order g^4*, *Nucl. Phys. B* **593** (2001) 651 [hep-th/0005223] [INSPIRE].

[26] G. Arutyunov, S. Penati, A. Santambrogio and E. Sokatchev, *Four point correlators of BPS operators in $N = 4$ SYM at order g^4*, *Nucl. Phys. B* **670** (2003) 103 [hep-th/0305060] [INSPIRE].

[27] S. Caron-Huot and A.-K. Trinh, *All tree-level correlators in $AdS_5 \times S_5$ supergravity: hidden ten-dimensional conformal symmetry*, *JHEP* **01** (2019) 196 [arXiv:1809.09173] [INSPIRE].

[28] P.J. Heslop and P.S. Howe, *OPEs and three-point correlators of protected operators in $N = 4$ SYM*, *Nucl. Phys. B* **626** (2002) 265 [hep-th/0107212] [INSPIRE].

[29] A. Bissi, C. Kristjansen, D. Young and K. Zoubos, *Holographic three-point functions of giant gravitons*, *JHEP* **06** (2011) 085 [arXiv:1103.4079] [INSPIRE].

[30] P. Caputa, R. de Mello Koch and K. Zoubos, *Extremal versus non-extremal correlators with giant gravitons*, *JHEP* **08** (2012) 143 [arXiv:1204.4172] [INSPIRE].

JHEP11(2020)072

[31] A. Hashimoto, S. Hirano and N. Itzhaki, *Large branes in AdS and their field theory dual*, *JHEP* **08** (2000) 051 [hep-th/0008016] [INSPIRE].

[32] T.W. Brown, P.J. Heslop and S. Ramgoolam, *Diagonal multi-matrix correlators and BPS operators in $N = 4$ SYM*, *JHEP* **02** (2008) 030 [arXiv:0711.0176] [INSPIRE].

[33] R. Bhattacharyya, S. Collins and R. de Mello Koch, *Exact multi-matrix correlators*, *JHEP* **03** (2008) 044 [arXiv:0801.2061] [INSPIRE].

[34] T.W. Brown, P.J. Heslop and S. Ramgoolam, *Diagonal free field matrix correlators, global symmetries and giant gravitons*, *JHEP* **04** (2009) 089 [arXiv:0806.1911] [INSPIRE].

[35] R. de Mello Koch, J. Smolic and M. Smolic, *Giant gravitons — With strings attached. Part I*, *JHEP* **06** (2007) 074 [hep-th/0701066] [INSPIRE].

[36] R. de Mello Koch, J. Smolic and M. Smolic, *Giant gravitons — With strings attached. Part II*, *JHEP* **09** (2007) 049 [hep-th/0701067] [INSPIRE].

[37] D. Bekker, R. de Mello Koch and M. Stephanou, *Giant gravitons — With strings attached. Part III*, *JHEP* **02** (2008) 029 [arXiv:0710.5372] [INSPIRE].

[38] C. Lewis-Brown and S. Ramgoolam, *Quarter-BPS states, multi-symmetric functions and set partitions*, arXiv:2007.01734 [INSPIRE].

[39] E. Witten, *Baryons and branes in Anti-de Sitter space*, *JHEP* **07** (1998) 006 [hep-th/9805112] [INSPIRE].

[40] O. Aharony, Y.E. Antebi, M. Berkooz and R. Fishman, *'Holey sheets': Pfaffians and subdeterminants as D-brane operators in large N gauge theories*, *JHEP* **12** (2002) 069 [hep-th/0211152] [INSPIRE].

[41] P. Caputa, R. de Mello Koch and P. Diaz, *A basis for large operators in $N = 4$ SYM with orthogonal gauge group*, *JHEP* **03** (2013) 041 [arXiv:1301.1560] [INSPIRE].

[42] P. Caputa, R. de Mello Koch and P. Diaz, *Operators, correlators and free fermions for* SO(N) *and* Sp(N), *JHEP* **06** (2013) 018 [arXiv:1303.7252] [INSPIRE].

[43] C. Lewis-Brown and S. Ramgoolam, *BPS operators in $\mathcal{N} = 4$* SO(N) *super Yang-Mills theory: plethysms, dominoes and words*, *JHEP* **11** (2018) 035 [arXiv:1804.11090] [INSPIRE].

[44] M. Taylor, *Matching of correlators in AdS_3/CFT_2*, *JHEP* **06** (2008) 010 [arXiv:0709.1838] [INSPIRE].

[45] F. Coronado, *Perturbative four-point functions in planar $\mathcal{N} = 4$ SYM from hexagonalization*, *JHEP* **01** (2019) 056 [arXiv:1811.00467] [INSPIRE].

[46] F. Coronado, *Bootstrapping the simplest correlator in planar $\mathcal{N} = 4$ supersymmetric Yang-Mills theory to all loops*, *Phys. Rev. Lett.* **124** (2020) 171601 [arXiv:1811.03282] [INSPIRE].

[47] A.V. Belitsky and G.P. Korchemsky, *Exact null octagon*, *JHEP* **05** (2020) 070 [arXiv:1907.13131] [INSPIRE].

[48] A.V. Belitsky and G.P. Korchemsky, *Octagon at finite coupling*, *JHEP* **07** (2020) 219 [arXiv:2003.01121] [INSPIRE].

[49] A.V. Belitsky and G.P. Korchemsky, *Crossing bridges with strong Szego limit theorem*, arXiv:2006.01831 [INSPIRE].

JHEP11(2020)072

[50] T. Bargheer, F. Coronado and P. Vieira, *Octagons I: combinatorics and non-planar resummations*, *JHEP* **08** (2019) 162 [arXiv:1904.00965] [INSPIRE].

[51] T. Bargheer, F. Coronado and P. Vieira, *Octagons II: strong coupling*, arXiv:1909.04077 [INSPIRE].

[52] T. Fleury and V. Goncalves, *Decagon at Two Loops*, *JHEP* **07** (2020) 030 [arXiv:2004.10867] [INSPIRE].

[53] F. Aprile and P. Vieira, *Large p explorations. From SUGRA to big STRINGS in Mellin space*, arXiv:2007.09176 [INSPIRE].

[54] H. Prüfer, *Neuer Beweis eines Satzes über Permutationen*, *Arch. Math. Phys.* **27** (1918) 742.

JHEP11(2020)072